Institute of Combustion and Power Plant Technology

Universität Stuttgart

Director: Prof. Dr. techn. G. Scheffknecht
Pfaffenwaldring 23 • 70569 Stuttgart
Phone +49 (0) 711-685 63487 • Fax +49 (0) 711-685 63491

Master Thesis No.

for Mr. cand. Ioannis Polyzois

Matr.-Nr. 2988816

ERASMUS Student

Thermodynamic equilibrium calculation to evaluate influence of alumina-silicate based additives on slagging and fouling tendencies of biomass fuels

Address:	Pfaffenhof 46C, 70569 Stuttgart
Date of issue:	15.12.2015
Date of submission:	15.06.2015
Supervising tutor:	M.Sc. Manoj Paneru

Task Description

Institut für Feuerungs- und Kraftwerkstechnik

Universität Stuttgart ifk

Direktor: Prof. Dr. techn. G. Scheffknecht
Pfaffenwaldring 23 • 70569 Stuttgart
Tel. +49 (0) 711-685 63487 • Fax +49 (0) 711-685 63491

Stuttgart, 15.12.2014
Prof. Sch./Pan.

Master Thesis No. 3341
for Mr. *Ioannis Polyzois*
ERASMUS-Programm
Matr.-Nr. 2988816

Thermodynamic equilibrium calculation to evaluate influence of alumina-silicate based additives on slagging and fouling tendencies of biomass fuels

1. Introduction

Biomass boilers issues regarding slagging, fouling and corrosion are related to alkali species present in fuel. During combustion these alkali species are released as gaseous alkali chlorides, sulfates and/or hydroxides. Alkali chlorides/sulfates later condense on cold boiler surfaces enhancing fouling and corrosion. Subsequent interaction of alkali species with silicon then forms low melting alkali-silicates. This low melting alkali silicates facilitates the formation of compact and strong glassy deposit by dissolving other incoming ash components. Condensing chlorides/sulfates and low melting silicates both reduce boiler performance and its availability. Using aluminosilicate based additive is widely discussed an attractive solution to mitigate both slagging and fouling problems. Additives are expected to reduce formation of molten deposit as well as condensation of alkali chloride/sulfates on cool boiler surfaces. Alumino-silicate based additive are also expected to react with gaseous potassium chloride releasing chlorine as HCl. Releasing chlorine as HCl decreases the risk of condensation of corrosive alkali chlorides.

2. Aim

The aim of this work is to evaluate the influence of aluminium-silicate based on the formation of molten deposit and condensation of alkali salts on cool boiler surfaces. Two biomass fuels (Torrified Straw/Wood pellets) mixed with varying amount of alumina-silicate based additive will be used in Fact Sage simulation. The influence of varying amount of additive will also be

ifk

evaluated experimentally. The experimental work will be focused on evaluating the behaviour of chlorine.

3. Approach

1. Detail literature review (Form of in-organics in biomass, behaviour of in-organics during biomass combustion, Slagging and Fouling issues during biomass combustion, Use of aluminium-silicate additives)
2. Thermodynamic equilibrium calculation using Software FACT Sage (Biomass and Biomass + Varying amount of additives)
3. Experimental test to evaluate the influence of varying amount of additive.

This Master Thesis will be supervised by *Mr. M.Sc. Manoj Paneru*. The IFK-guidelines for student theses have to follow.

Start: 15.12.2014
End: 15.06.2015

(Prof. Dr. techn. G. Scheffknecht) *(M.Sc. Manoj Paneru)*

Student contact: ioanpolyzois@gmail.com

Kurzfassung

In der vorliegenden Studie, wurden die thermodynamischen Gleichgewichtsberechnungen unter Verwendung des thermo Software- und Datenbank 'Factsage 6.3' durchgeführt, um die Neigung zu Verschlackung und Ascheverhalten von Gebraten Stroh und Holzpellets und die Wirkung von Aluminiumoxid-Silikat-basierte Additive zu simulieren. Darüber hinaus, nahmen die Experimente Platz im 20kWth Atmosphärenfallrohrofen der IFK Einrichtung, um die Auswirkungen der unterschiedlichen Menge an Zusatzstoffen in dem Verhalten der Biomasse Cl untersuchen zu können. Die Gleichgewichts Ergebnisse zeigen, dass das Verschlackungverhalten von Biomasse wird vor allem durch sein hohe K-Gehalt geführt. Biomasse Slackeverhältnis sich mit steigenden Temperaturen und niedrige Luft-Kraftstoff Verhältnisse erhöht. Die Steigung ist sehr scharf bei Temperaturen größer als die Fluidtemperatur von Asche. Kaolinit zeigte, dass mit der Bildung von Schlacke gut umgeht und Cl von KCl austragen kann. Die experimentellen Ergebnisse zeigen, dass die Verwendung von variierenden Menge an Aluminiumoxid-Silikat-enthaltenden Additiven eine schnelle Wirkung hat, die durch die schnellen Änderungen von HCl-Konzentrationen im Rauchgas wahrgenommen wird. Als Additiv Fütterung zunimmt, nimmt auch die Menge an Chlor, das aus KCl erhält und damit werden die HCl-Konzentrationen auch erhöht. Zusätzlich, wurde es gezeigt, dass das molare Verhältnis von K / (Al + Si), die Menge an Cl, die in HCl bildet, beeinflusst. Die Verwendung von Additiven, Cl zu KCl zu gehen zurück und folglich wird auch von Asche verhindert. Die Gleichgewichts und die experimentellen Ergebnisse sind vergleichbar, speziell für höhere Additiven Eingang in das System.

Abstract

In the present study, thermodynamic equilibrium calculations were performed using the thermochemical software and database ‘FactSage 6.3’ in order to simulate the slagging tendency and ash behaviour of Torrefied Straw and Wood Pellets and the effect of alumina-silicate based additives. Moreover, experiments took place in the 20kW$_{th}$ atmospheric drop tube furnace of the IFK facility, in order to investigate the impact of varying amount of additives in the behaviour of biomass Cl. The equilibrium results show that the slagging behaviour of biomass is led primarily by its high K content. Biomass slag ratio increases with increasing temperatures and low air to fuel ratios. The increase is very sharp for temperatures over the fluid temperature of biomass ash. Kaolinite was shown to reduce the formation of slag and lead Cl out of KCl. The experimental results show that the use of varying amount of alumina-silicate based additives does have a fast impact which is perceived through the quick changes of HCl concentrations in the flue gas. As the additive feeding increases, so does the amount of chlorine that gets out of KCl and thus the HCl concentrations increase as well. In addition, the molar ratio of K/(Al+Si) is shown to influence the amount of Cl that forms into HCl. The use of additive restrained Cl from going to KCl and consequently was also prevented from ash. The equilibrium and experimental results are close, especially for higher additive input into the system.

Table of Contents

Symbols

Afr	Additive feeding rate	[g/h]
Aw	Additive weight	[g]
A_λ	Measured absorbance of a material at a specific wavelength	[-]
BS (%)	Belt Speed of the disperser	[%]
b	Path length through the sample	[cm]
C	Concentration	[1/m³]
HHV	Higher Heating Value	[MJ/kg]
K_g	Thermal conductivity of gas phase	[W/(m·K)]
k_s	Thermal conductivity of solid phase	[W/(m·K)]
K_λ	Product of multiplication between ελ and b	
LHV	Lower Heating Value	[MJ/kg]
M_i	Molar mass of the element	[g/mol]
ppm	parts per million	[-]
RS	Rotating Speed of the stirring part inside the disperser reservoir	[1-6]
SR	Slag Ratio	[-]
Vol, y_i	Volume share of a component	[%]
Vmol	Molar volume of ideal gas in 1 atm pressure	[L/mol]
wt, γ_i	Mass share of a component	[%]
Δt	Period of time	[s]
ε_λ	absorption coefficient	[cm^(-1)]
η	Dynamic viscosity	[(N*s)/m^2]
λ	Stoichiometric air ratio	[-]
λ	Wavelength	[nm]

List of Abbreviations

ar	As received
dw	Dry weight
A	Aurora additive
Ad	Aurora dry, dried Aurora additive at 105 °C
A*	Referring to Aurora and Aurora dry cases fused
B	bentonite additive
CFA	Chemical Fractionation Analysis
CFB	Circulating Fluidized Bed
CFD	Computational Fluid Dynamics
DTF	Drop Tube Furnace
EDS	Energy Dispersive X-ray Spectroscopy
EDX	Energy Dispersive X-ray Detection
EMPA	Electron Microscopic image Analysis
FTIR	Fourier Transform InfraRed
GHG	Greenhouse gases
FT	Fluid Temperature of ash
g	Gaseous state
HCl	Hydrogen Chloride
HClmax	Maximum theoretical HCl value that can be achieved for the corresponding fuel
HT	Hemispherical temperature of ash
IDT	Initial deformation temperature of ash
l	Liqud state
NDIR	NonDispersive Infrared sensor
OECD	Organization for Economic Co-operation and Development
SEM	Scanning Electron Microscopy
STA	Simultaneous Thermal Analysis
ST	Spherical temperature of ash
s	Solid state
TS	Torrefied Straw
wf	Water free
waf	Water ash free
WP	Wood Pellets
WP+KCl	Wood Pellets enhanced with KCl corresponding to 0.25% of the fuels weight
WP+KCl+B	WP+KCl and addition of Bentonite corresponding to 5.8% of the fuels weight
XRD	X-ray Difraction

List of Figures

List of Tables

1 Introduction

1.1 Background & Motivation

One of the most important greenhouse gases (GHG) is CO_2 which greatly influences mean global surface warming [1]. The biggest part of greenhouse gases comes from the production of energy through the burning of fossil fuels in power plants [2]. Global energy demand is expected to grow by 37% by 2040 [3] which would lead to greater greenhouse emissions and severe impacts for people and ecosystems [1]. However, renewable energy sources with their low-carbon emissions are gaining ground, mostly in OECD countries, while their share in power generation is expected to be the one-third by 2040 [3]. In 2012 the share of traditional Biomass was 9% of the global energy consumption (Figure 1.1), while in the end of 2013 the Bio-power share of global electricity production was 1.8% [4]. Like the modern renewables, bio-power can provide significant shares of total electricity in areas where they are cost competitive and good resources are available [4].

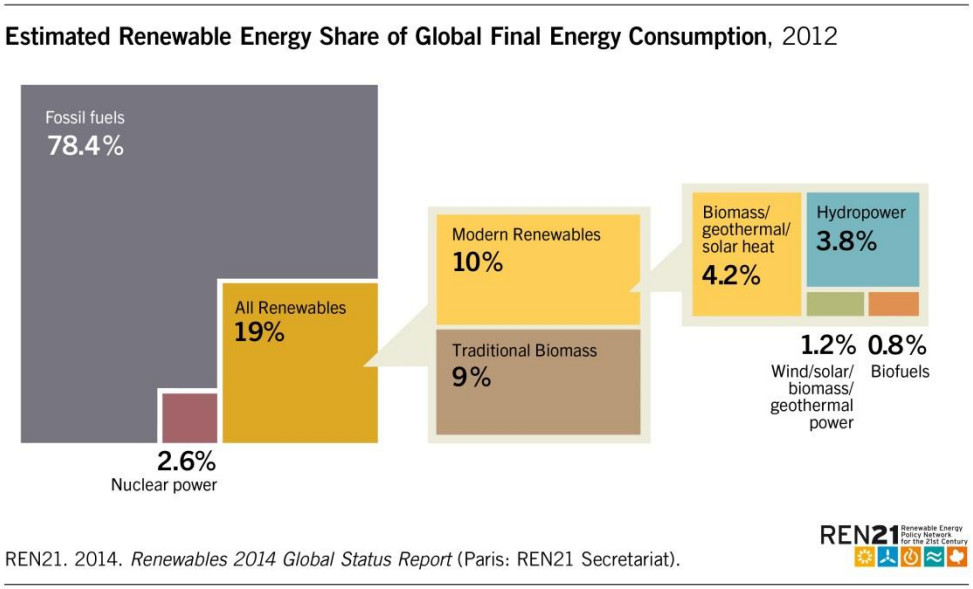

Figure 1.1: Estimated Renewable Energy Share of Global Final Energy Consumption, 2012. Source: Adapted from [4].

However, biomass fuels, that are regarded CO_2 neutral, have different composition from the fossil fuels. They have high amounts of alkali and chlorine which changes the behavior of ash forming elements and thus the deposit characteristics, often causing serious ash related operational problems such as slagging, fouling and high temperature corrosion inside the heat and power production plants [5]. The most important ash-forming elements in biomass are Si, Al, Fe, Ca, Mg, Mn, K, Na, P, S and Cl [6]. Silicon (Si), alkali earth metals (Ca,Mg), Alkali metals (K,Na), sulphur (S) and chlorine (Cl) play a crucial role regarding slagging, fouling and corrosion as concerning woody biomass. In a different path phosphorous (P) in agricultural biomass has a leading role on the ash transformation reactions [6].

Potassium (K) is mainly responsible for the deposit formation inside a furnace. In pulverized fuel boilers where temperatures are high, around 1300°C, potassium is expected to be released in gaseous phase as hydroxides (KOH), chlorides (KCl) and/or sulfates (K_2SO_4). The amount of chlorine inside the fuel limits the creation of KCl and the remaining potassium is transformed into KOH, while K_2SO_4 is more stable in condensed phase (solid, liquid) [7]. Alkali chlorides and sulfates then condense on cool boiler surfaces promoting fouling and corrosion. The following interaction of alkali species with silicon forms low melting alkali-silicates which then facilitates the creation of compact and strong glassy deposit by dissolving other incoming ash components [7]. These condensed chlorides/sulfates along with the low melting alkali-silicates reduce the boiler performance and its availability [7].

An efficient solution to these biomass ash problems is the addition of aluminosilicate minerals (e.g. kalolinite) during the biomass combustion [7]. Previous studies have proven the benefits of aluminosilicate based additives, and their ability to capture gas potassium species [7–9]. The mechanism that takes place is, initially the formation of the amorphous aluminosilicate called meta-kaolin ($Al_2O_3.2SiO_2$) during the thermal decomposition of kaolinite [10]. Meta-kaolin then captures the gaseous alkali species (KOH, KCl and less effectively K2SO4) creating higher melting temperature components [7]. This way formation of molten deposit as well as condensation of alkali chloride/sulfates on cool boiler surfaces are expected to be reduced. Also the additive reacts with gaseous potassium chloride (KCl) releasing chlorine as HCl which, in turn, decreases the risk of condensation of corrosive alkali chlorides.

1.2 Objectives

The objective of this work is to evaluate the influence of aluminium-silicate based additives on the formation of molten deposit and condensation of alkali salts on cool boiler surfaces. This objective will be approached in two different steps. One step is the simulation in Fact Sage of the ash behavior of two biomass fuels (Torrefied Straw/Wood pellets) mixed with

varying amount of aluminosilicate based additive. The other step is the experimental evaluation of the influence of varying amount of additives for Torrefied Straw and Wood Pellets. The experimental work will be focused on evaluating the behavior of chlorine by the measurement of HCl.

2 Literature review

In order to evaluate the combustion performance of biomass, the slagging, fouling and corrosion behavior of biomass and the effect of aluminosilicate additives, it is necessary to have an understanding of the fundamentals of combustion process, the fuel characteristics of biomass, the different ash species formations mechanisms and the aluminosilicate additive intervention procedure. In this chapter procedures that contribute in deposit formation inside boilers are explained, technical issues that come as a consequence and the advantages of aluminosilicate additive use are discussed and also similar case studies that have already taken place and can be taken into consideration are referred.

2.1 Fuel characterization and analytical techniques

Biomass is the fuel that is of interest in this study and more specifically Wood Pellets and Torrefied Straw. In the following sections, the general differences in fuel properties are presented as well as a small description of the techniques used to characterize various properties of biomass fuel.

Fuel Properties

The combustion of biomass has many emission factors that depend on the type and quality of the used fuel, on the combustion technologies and on the operating conditions. In turn the fuel quality hinges upon its own chemical composition, including its water content. Furthermore the ash content varies according to the inorganic species inside the biomass, taking values in general from 0.5 to 3% dry weight (dw) [11]. In these species can be included significant amounts of alkali metals, e.g., potassium and sodium, and alkaline earth metals, e.g., calcium and magnesium. Consequently they are rapidly released into the gas phase and interact with other elements and can result in problems with fouling, slagging and corrosion. Most significantly potassium and sodium tend to be most problematic and they can contribute to the formation of inorganic phases that have lower melting points and lead to the formation of “sticky” molten phases that result in clinkering, fouling, or slagging [12]. Also the potential of chlorine content is high [13].

As regards to wood and also wood pellets, the major constituents are carbon C, oxygen O, hydrogen H and nitrogen N. As for major ash-forming elements in descending order are calcium (Ca), potassium (K), sodium (Na), magnesium (Mg), manganese (Mn), iron (Fe) and aluminium (Al). Minor ash-forming elements include cadmium (Cd), chromium (Cr), copper (Cu), nickel (Ni), zinc (Zn), arsenic (As), mercury (Hg) and lead (Pb) (1). However combustion of wood contaminated for example with lead (Pb) poses potential environmental problems related to particulate emissions and ash disposal. The emissions mainly depend upon

the combustion appliance and condition [10]. Some standards have been established in some European countries and some United States (U.S) for wood pellets [11].

Torrefaction is a thermal method for the conversion of biomass operating in the low temperature range of 200-300 °C. It is carried out under atmospheric conditions in absence of oxygen and used is for energy purposes. The thermal treatment not only destructs the fibrous structure and tenacity of biomass, but is also known to increase the calorific value. Also after torrefaction the biomass has more hydrophobic characteristics that make storage of torrefied biomass more attractive above non-torrefied biomass, because of the rotting behavior. During the process of torrefaction the biomass partly devolatilizes leading to a decrease in mass, but the initial energy content of the torrefied biomass is mainly preserved in the solid product so the energy density of the biomass becomes higher than the original biomass which makes it more attractive for i.e. transportation [14]. During torrefaction biomass loses more oxygen and hydrogen in comparison to carbon which leads to increase of the calorific value [15] .
For torrefied straw the major constituents are carbon C, oxygen O, hydrogen H and nitrogen N [16].

2.1.1 Analytical techniques

In order to analyze the fuel and the ash chemistry and examine their properties various methods exist.

Scanning Electron Microscopy (SEM)

The SEM is one of the most versatile and widely used tools that allow the study of the surface morphology of both biological and non-biological materials. High-resolution images of the topography of a specimen over a wide range of magnifications (as high as 200,000x) and with great depth of field can be obtained. Characterization of fine particulate matter in terms of size, shape may be performed. Biological samples like biomass for scanning electron microscopy analysis are usually coated with a thin layer of electron dense material, such as carbon or atomized gold [17].

Simultaneous Thermal Analysis (STA)

Thermal analysis is used in combustion research for the examination of various properties and behavior of different fuels under a wide range of scenarios. STA is usually the simultaneous measurement of both heat flow, with Differential Scanning Calorimetry and weight changes, with thermogravimetric analysis in order to provide estimation regarding the ash-melting characteristics of various coal and biomass samples [18],[19].

Viscosity measurements

In order to measure the viscosity of biomass ash a high-temperature rotating viscometer can be used. The dynamic viscosity (η) is determined through measurement of the torque or the rotation speed of a rotor immersed in the molten mass which shows Newtonian behavior [20],[21].

Chemical fractionation analysis (CFA)

CFA is an advanced method for characterizing biomass and is based on an element's varying solubility as a result of its existence in a fuel. The procedure consists of 3 steps and each step results in a liquid and a solid residue sample, which are both analyzed for their major and minor elements. The first, water step leaches easily soluble salts, the second, buffer step leaches metal ions and the third, acid step leaches acid-soluble salts and minerals. Insoluble silicates are left in the remaining fraction [12], [22].

2.2 Release of ash species

Biomass fuels contain a significant percentage of potassium and other inorganic elements. The most significant ash-forming elements can be grouped into four types: (1) water soluble salts, (2) elements associated with inorganic materials of the biomass, (3) minerals included in the fuel structure, (4) inorganic material added to biomass from extraneous sources [6]. These mainly are Si, Ca, Mg, K, Na, P, S, Cl, Al, Fe and Mn. A relatively extended study [23–27]exists that has to do with the behavior of the fraction of ash-forming matter in biomass that is volatile during thermochemical energy conversion. For example, several mechanisms are examined for the release of alkali, S,Cl [6]. During combustion ash is formed from these materials through a combination of complex chemical and physical processes and its release leads to different ash related problems. Potassium (K) is the main component that leads to troublesome species which along with high chlorine (Cl) content, as well as with low sulphur (S) concentrations, make the deposition of ash in biomass-fired boilers a severe issue [28]. Some important general conditions have major influence on the ash transformation process: (i) the relative concentrations of the ash –forming elements along with the total amount of ash forming matter, (ii) the relative mutual stability as well as the kinetic properties and the aggregation states of the ash-forming elements, intermediates and final products [6].

Ash transformation takes part in two stages where primary and secondary reactions take place. This is to some extend hypothetical but serves the practical purpose of organizing the properties of the ash-forming elements into a conceptual model [6]. Primary reactions are mainly used to define and denote the affinity between the ash-forming elements and oxygen in relation to the oxygen affinity of the carbon-hydrogen matrix of the fuel, isolated from any further reaction [6]. Because of this relation mainly component oxides are formed, except for

alkali metals and chlorine that form less stable oxides and will initially readily react with the present water vapor to more stable and relatively volatile hydroxides for alkali and HCl for chlorine [6]. In order to move to the secondary reaction stage, the primary products of these ash-forming elements from the initial stages of combustion could be divided into two categories, basic and acidic compounds (Table 2-1).

Table 2-1: Basic and acidic components of primary products of ash forming elements. Source: Adapted from [6].

Basic compounds	Acidic compounds
KOH (l,g), (K2O)	P2O5 (g)
NaOH (l,g), (Na2O)	SO2 (g)/SO3 (g)
CaO (s)	SiO2 (s)
MgO (s)	HCl (g), (Cl2)
H2O (g)	CO2 (g)
	H2O (g)

The compounds are arranged according to their reactivity which descends as we move from top downwards the list. This order is not absolute and might be different for example, for varying temperatures. It is based on thermodynamic considerations regarding pure equilibrium condition and is a helpful tool for organizing these complex ash transformation reactions [6].
In a normal scenario K-species are expected to be successively formed in the order of phosphates, sulfates, chlorides, silicates and carbonates depending on the relative concentration of the ash elements.
Initially, phosphates are molten and rather volatile. When encountered with alkali earth oxides, solid ternary phosphates are formed [6]. The sulfates are condensed under lower temperatures (l,s), when at higher temperatures are volatized (g) and released in the flue gas [6]. Chlorides are released in the flue gas and precipitated at lower temperatures [6]. Preferably molten K-silicate particles are formed due to high KOH availability leading to high K-silicate particle density [6]. The presence of Ca and Mg in the melt drives out K, with evaporation of K as a result and also increases the melting temperature, which is possible to reduce the slagging tendency [6]. Furthermore, in case that woody biomass is contaminated with sand and/or clay (that often contain Al) a chance for formation of alkali aluminosilicates (e.g. $KAlSi_2O_6$ leucite, $KAlSiO_4$ Kalsilite) exists. These compounds have high temperature stability and high melting temperatures and as a result contribute to lower slagging tendencies [6]. Carbonates will more rarely form if there is a surplus of basic oxides over the acidic compo-

nents [6]. All the above give us an overview over the main secondary ash-forming reactions taking place in the combustion of biomass, which can schematically be seen below (Table 2-2) [6].

Table 2-2: Survey of Major Secondary Ash-Forming Reactions (Schematic). Source: Adapted from [6].

reaction		comments
$P_2O_5(g) + 2KOH(g) \leftrightarrow 2KPO_3(l,g) + H_2O(g)$	(2-1)	fast reaction,[a] product molten and partially volatile in residual ash[b]
$SO_3(g) + 2KOH(g) \leftrightarrow K_2SO_4(l,g) + H_2O(g)$	(2-2)	fast reaction, product molten or not
$HCl(g) + KOH(g) \leftrightarrow HCl(l,g) + H_2O(g)$	(2-3)	fast reaction, product not stable in residual ash
$SiO_2(s) + 2KOH(g) \leftrightarrow K_2SiO_3(l) + H_2O(g)$	(2-4)	medium fast reaction, product stable and molten in residual ash
$CO_2(g) + 2KOH(g) \leftrightarrow K_2CO_3(l,g) + H_2O(g)$	(2-5)	fast reaction, product not stable in residual ash
$P_2O_5(g) + 3CaO(s) \leftrightarrow Ca_3P_2O_8(s)$	(2-6)	medium fast reaction, product stable and solid in residual ash
$SO_3(g) + CaO(s) \leftrightarrow CaSO_4(s,l)$	(2-7)	medium fast reaction, product (not) stable and solid in residual ash
$2HCl(g) + CaO(s) \leftrightarrow CaCl_2(g,l) + H_2O(g)$	(2-8)	medium fast reaction, product not stable in residual ash
$SiO_2(s) + CaO(s) \leftrightarrow CaSiO_3(s)$	(2-9)	slow reaction,[c] product stable and solid in residual ash
$CO_2(g) + CaO(s) \leftrightarrow CaSO_3(s)$	(2-10)	medium fast reaction, product not stable in residual ash[b]
$K_2SiO_3(l) + CaO(s) \leftrightarrow K - Ca - silicate(l)$	(2-11)	rather slow reaction,[c] product stable and molten in residual ash

[a] The reaction rates are classified into four categories on an arbitrarily scale. [b] The stability in residual ash varies according to the thermal condition of the specific appliance. [c] These reaction rates are also highly dependent upon the dispersion of fuel and reactant particles.

For potassium the combination of all mechanisms results in a fractionation inside the boiler. K might be converted in volatile compounds, mostly KOH and KCl at temperatures greater than 800 °C or non-volatile ash compounds, mainly solid slilicates, that remain inside the boiler and on surfaces depending on the temperature and chemical composition of the particles [28]. As the temperatures decreases, and along with the presence of SO_2 in the flue gas, the chloride may convert to sulphate by the following sulfation mechanisms [5],[28,29]:

$$2KCl + SO_2 + {}^1/_2\, O_2 + H_2O \rightarrow K_2SO_4 + 2HCl \quad (2\text{-}12)$$

$$2KCl + SO_2 + O_2 \rightarrow K_2SO_4 + Cl_2 \quad (2\text{-}13)$$

Equilibrium conversion to K_2SO_4 is not always possible and only a part of K(g) is converted to K_2SO_4, when the rest is converted to KCl or K_2CO_3. Also with the passing of time solid KCl and K_2CO_3 might react with SO_2(g) and produce K2SO4(s) [28].

2.3 Formation of residual ash and aerosols in thermal fuel conversion systems

As we stated before, ash after going under different physical processes, including fragmentation, shedding and coalescence during char burnout, the external inorganic materials are converted either in volatile or non-volatile compounds [28].

The non-volatile ash compounds remaining in the char may melt and coalesce inside and on the surface of the char, depending on the composition of the particles and the temperature. These results in the formation of residual ash, with a wide range of compositions, shapes and sizes of the particles, related to the parent mineral particles' characteristics. Depending on factors as the density and size of the residual ash particles, the combustion technology and the flue gas velocity, a part of the residual ash will be constrained and joined with the flue gas to form the coarse part of fly ash, while the other part will stay at the lower zone and form bottom ash. In comparison to the fine-mode fly-ash particles from volatized ash compounds, coarse fly-ash particles are larger, usually exceeding 5μm [30].

Upon cooling of the flue gas in the convective heat exchanger section, vapors of volatized compounds condense or react on the surface of pre-existing ash particles in the flue gas. Because of the much larger specific surface of the fine-mode particles compared to the coarse fly-ash particles, the concentrations of condensing or reacting ash-forming elements increase with decreasing particle size [30].

If the concentration of inorganic vapors in the flue gas and the cooling rate in the heat exchanger are both high, super saturation of these vapors takes place, leading to formation of new particles by nucleation [30]. Nucleation and condensation are two competing processes, and if enough surfaces for condensation are available, then nucleation partly or totally gets suppressed. In other case, very small aerosol particles, in the size range below 1μm, are formed [28]. When these particles are formed, they start to coagulate with other aerosols or with coarse fly ashes [31].

Due to different formation pathways of coarse fly ashes and aerosols as well as due to different chemical composition and behavior, these two fly ash fractions must always be treated separately [32]. Nevertheless, since the presence of coarse fly ashes influences the formation and behavior of aerosols, the interactions between these two have to be taken into account. The different mechanism for particle formation are shown schematically below (Figure 2.1) [32].

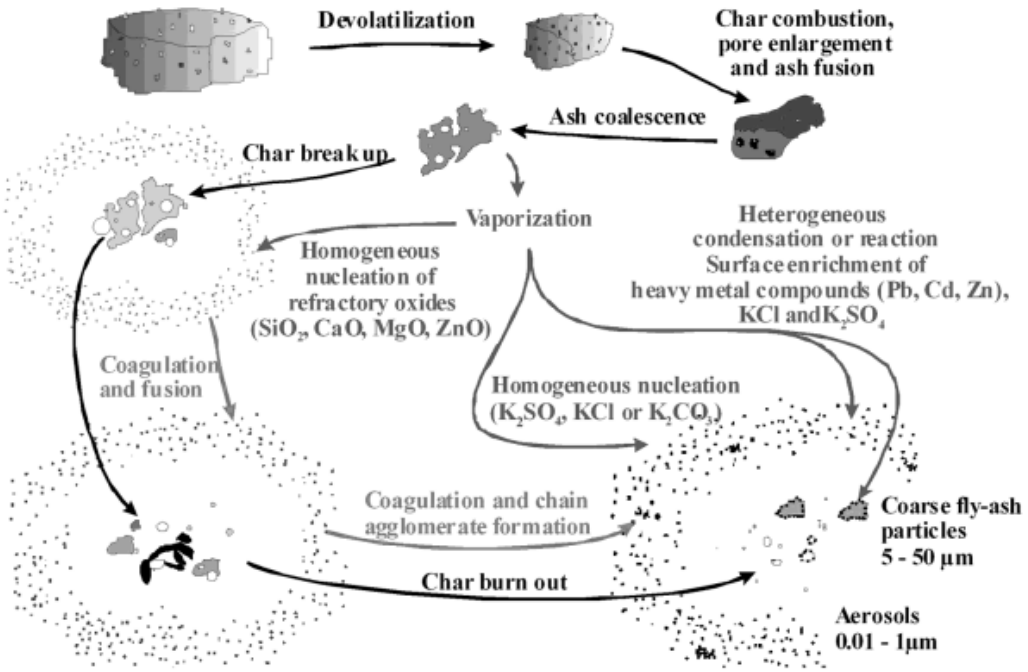

Figure 2.1: Mechanisms involved in ash formation in biomass combustion. Source: Adapted from [23].

2.4 Transport of ash species (including quantification of ash transport and adhesion of ash species)

In general there are various mechanisms for ash deposition on heat transfer surfaces. The main mechanisms are, diffusion, condensation of vaporized inorganic compounds , inertial impaction, thermophoresis and chemical reactions [28,33,34].

2.4.1 Diffusion and Condensation

Diffusion is the transport of particles and gas molecules from an area with high concentration to the surrounding areas with lower concentrations by Brownian motion. The concentration of the depositing and condensing particles is decreased near an obstacle, such as a heat exchanger, which is acting like a sink. Condensation of volatile inorganic species is the primary mechanism for the formation of convective pass fouling, for example on heat transfer surfaces, especially when biomass fuels contain high levels of volatile species [28,34,35].

2.4.2 Inertial Impaction

Inertial impaction starts with gas flowing towards a surface. As the flow of the gas changes direction in order to bypass the obstacle, coarse particles that are considerably large, are not able to follow the flow because of their inertia, so they might continue their course towards

the surface. Also in turbulent eddy impaction, the particles are driven towards surfaces by turbulent eddies and to become deposited they need to have enough inertia in order to penetrate through the laminar boundary layer surrounding the target. So the impaction on the heat exchangers in the flue gas ducts is a combination of these two mechanisms [28,33].

2.4.3 Thermophoresis

An aerosol particle experiences collisions with gas molecules. A net forced is applied on a particle which is positioned inside a temperature gradient. This happens due to the fact that the gas molecules on the hot side of the particle have averagely higher kinetic energy than those on the cold side. This way they push the particle towards the cold region when the molecules on the cold side cannot withstand. This process is called thermophoresis and its effect is higher on clean tube surfaces where the temperature gradient between the surface and the flue gas is then the steepest. On the contrary, while the thermal insulating deposit layer gets thicker, then the outer-surface temperature increases and so the temperature gradient decreases [28,35].

2.4.4 Chemical reactions

Chemical reactions like oxidation, sulfation and chlorination processes can occur within the deposit layer and between gaseous and solid compounds under the combustion conditions. For example, silica along with alkali and alkaline earth minerals, especially with the readily volatized forms of potassium in biomass, can lead to the formation of low melting point compounds which readily slag and foul at normal biomass boiler temperatures (800-900 °C) [28]. The produced alkali silicates and/or mixed alkali and /or calcium chlorides/sulphates tend to deposit on the reactor wall or the heat-exchanger surface causing fouling/corrosion at low fusion temperature (typically <700 °C) [28].

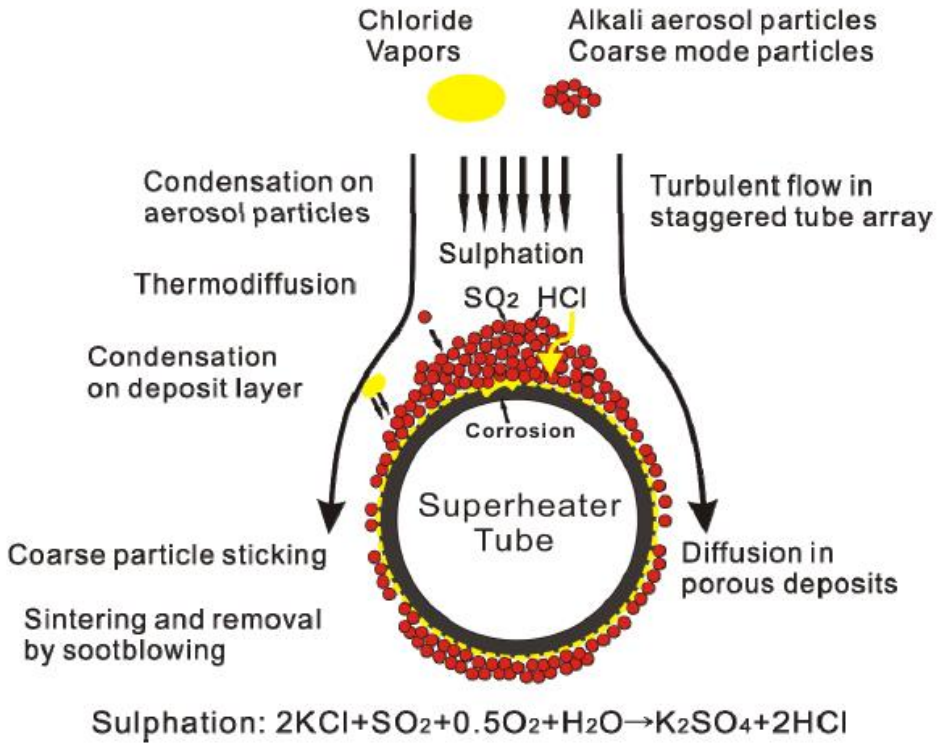

Figure 2.2: Schematic of mechanisms of ash formation and deposition on a superheater tube surface. Source: Adapted from [22].

2.5 Deposit build-up, consolidation, and shedding (including heat transfer in deposits, sintering of deposits)

2.5.1 Slagging

Slagging is dominant in the radiant heat transfer area and the initial layers of slagging consist greatly of small, lightly sintered particles and less from fewer larger, impacted and deformed upon impact, particles [36]. The composition of these layers for biomass combustion is mostly alkali oxides together with glassy silicate phases, but this depends from the fuel composition [36].

As the deposit grows, the temperature of the outside surface gets rises and at some point gets higher than the melting temperature of the deposited low melting material, at least as regarding the outer layers. While the deposit surface becomes molten, the majority of the arriving particles tend to stick on it and so, the composition of the outer layer becomes very much alike to the chemical composition of the bulk fly ash [35]. Furthermore, low excess air and inappropriate air/fuel ratio might lead to the continuous increase of slagging deposits and

reducing conditions, and the excessive slagging may lead to the extension of the flame in the convective part of the boiler, possibly causing slagging there also [35,36].

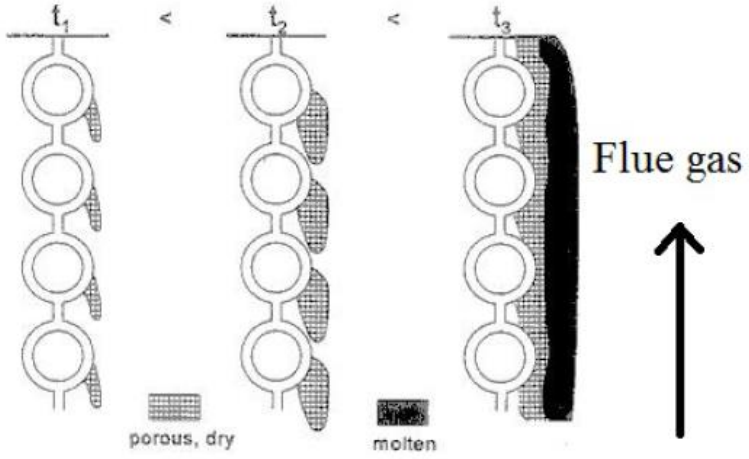

Figure 2.3: Slagging in the high temperature region. Source: Adapted from [28].

2.5.2 Fouling

Fouling deposits are formed in the convective parts of the boiler and are made up of fly ash particles and condensed volatile species not so strongly bonded as the slags. At the beginning the outer layer of the fouling deposit is porous but subsequently sintering strength develops in the deposit, depending on time and temperature [35]. High temperature fouling takes place in sections where temperature overcomes the stability of the sulfates/chlorides and consists of fly ash particles that are mainly bonded with alkaline silicate liquids [35]. Low temperature fouling takes place in the colder sections of the convective pass where the temperature ranges from 650 to about 975 °C and the sulfate phase dominates the bonding mechanism between the particles [28,35]. There is a variety of common problems related to the exaggerated formation of ash fouling deposits in the convective sections of the boilers, which apply to all boilers fired with biomass fuels. Generation of higher flue gas velocities in the open gas channels results in increased gas-side erosion wear of the tube surfaces. Additionaly, high convective pass fouling which leads in the blockage of a significant number of flue gas passes in the tube banks, has as a result the increase of the tube temperature in the flues gas passes that remain open [35]. Consequently metal wastage due to gas side corrosion takes place [35].

Ash related problems inevitably prevent with the smooth operation of the boiler. They interfere with the biomass combustion processes, reduce energy conversion efficiencies and significantly deflect the further application of biomass materials as fuel for heat and electricity production [9].

2.5.3 Deposit Build-up

High deposit strengths create the problem of deposit removal from heat exchange surfaces [35]. The main reason for strengthening of the deposits is the increase in the area of contact between the particles of the deposit, which happens because of sintering and chemical reactions [37]. Furthermore, passage of time is followed by hardening of the deposits and it becomes more difficult to remove. In addition high gas temperatures and straws with high potassium content lead to the same effect, cause of partial melting of the deposit or its generation to a high degree by direct condensation on a surface [38].
Ash deposits on heat transfer surfaces cause harsh problems for efficient heat transfer and excessive ash deposition might even lead to plugging of the flue channels [35].

2.5.4 Shedding of deposits

In order to decrease the effect of the problems caused by ash deposits different techniques are put into use, e.g. use of additives that can convert the inorganic species into less harmful forms, which is going to be the main goal of this study, pretreatment of fuels by leaching out alkali, co-firing with clean fuels, inhibition of sintering and the use of different deposit shedding methods [35].
Effective deposit shedding techniques are considered cost efficient for the matter of deposit removal from the heat transfer surfaces [35], while these processes can be caused naturally, without any operational or mechanical influence, or artificially as a part of the boiler operation [35,39]. The important methods of ash shedding are presented below.

Erosion

Erosion takes place when rather large and sharp edged fly ash particles, often rich in SiO_2, collide with non-gluey areas on the surface of the deposit, deforming and cutting the present material. The rate of erosion is related to the shape of the incoming particles. Hard, pointy SiO_2 grains cause erosion creating cuts, while glass spheres first create a surface deformation [35]. Furthermore the size of the particles that impact the surface influences erosion. Smaller particles get carried around the object with the gas flow because of their small inertial momentum, while the erosion rate increases along with the increase of the size of the particles, until it reaches a constant value for large particles (45µm) [35,39].

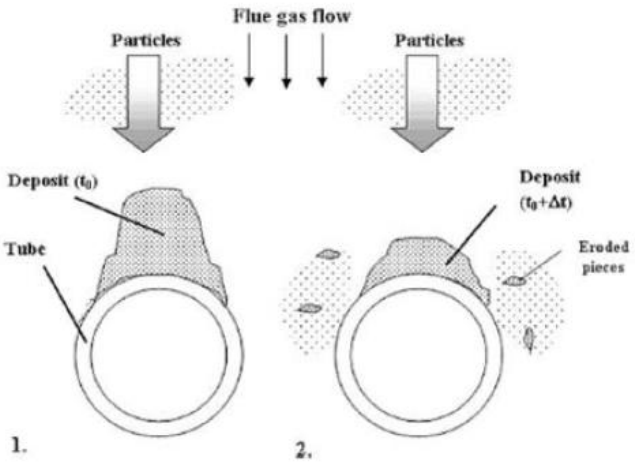

Figure 2.4: Deposit erosion mechanism, a) Initial deposits on the tube, b) deposits after shedding through erosion. Source: Adapted from [32].

Gravity shedding

Gravity shedding is the process of deposit removal when the gravity force of the deposit exceeds the tube adhesion strength and also the deposit shedding through surface melting is included. The first kind is possible when the gravity upon the deposit becomes larger than the strength of which the deposit is attached on the tube or the internal strength of the deposit. An attachment is initiated when the stresses forced by the soot blower are greater than the tube-deposit adhesive bond at some point on the tube deposit surface. On the other hand, the gravity shedding by melting can take place, especially in the furnace region. In this case, molten deposits may flow down the boiler walls when the combustion conditions are suitable for low viscosity slag deposits. The temperature gradient through such a deposit, will lead the slag coating close to the wall surface to be solid, when the outer deposit coating will be molten [35,39].

Thermal shock induced shedding

Thermal changes and differences in the thermal expansion coefficients of the tube and deposit can also cause shedding. Furthermore soot blowing or load variations/fluctuations might cause local temperature changes. The mechanism behind this thermal shock induced shedding is that a sudden temperature gradient may cause an uneven expansion of the deposit and the tube, or between separated , bordering layers, leading to deposit fractures. All and all the sudden temperature gradients are caused either by flue gas or steam temperature fluctuations or artificially, by changing the thermal load. Finally ash deposits can be removed from heat transfer surfaces by applying mechanical or thermal stress inside them by using high pressure steam, air and water [35,39].

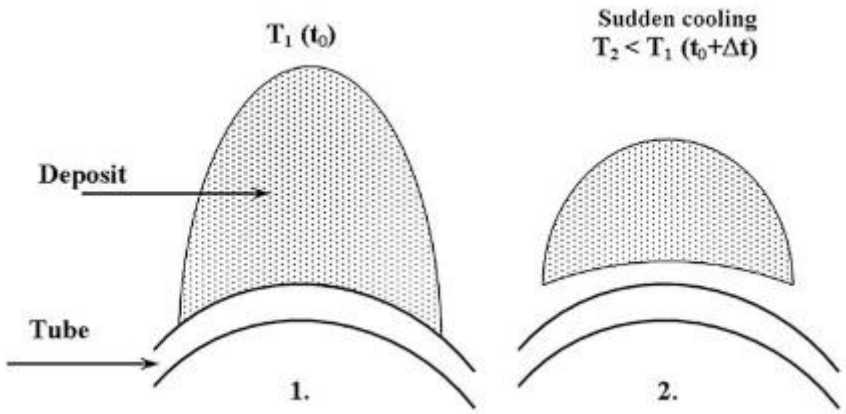

Figure 2.5: Mechanism of thermal shock a) deposit placed on a tube, b) shrinkage of the deposit, due to sudden cooling. Source: Adapted from [32].

Mechanically induced shedding

Mechanically induced tension in the deposit usually caused by vibrations or momentum transfer from sootblowing. Sootblowing is currently the most typical deposit shedding technique used in coal, biomass and Kraft recovery boilers [39]. Removal of deposit from the heat transfer surfaces occurs indirectly, because of mechanical and thermal stresses applied by water, high pressure air or steam, that are forced through nozzles in the deposit. Different sootblowing mediums are used for dealing with different deposits. For example, water is the most effective medium for removing heavily sintered or slagged deposits. During sootblowing process, a high pressure steam (jet) form the sootblower hits the deposit ash presented below in Figure 2.6. When the jet impacts the deposit two main forces are applied on it. A longtidutial (drag) force and a lateral (lift) force. For more information on the properties influencing sootblowing, consult [39].

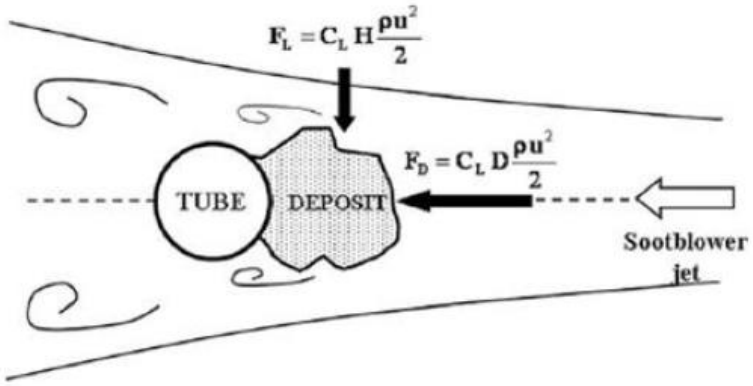

Figure 2.6: Longitudinal and lateral component of a force, caused by the interaction between a sootblower jet and a deposit. Source: Adapted form [32].

2.5.5 Heat transfer in deposits

The thermal properties of the deposit, i.e. its thermal conductivity and the surface emissivity, define the heat transfer between the flue gas and the steam inside the heat exchanger tubes. Deposit's physical structure which means the particle size distribution, the porosity and the sintering conditions influence these thermal properties significantly. While the radiative properties depend on the surface conditions, the conductivity properties depend on the properties inside the deposit [39].

The effective thermal conductivity of porous ash deposits depends on the thermal conductivity of solid phase k_s, the thermal conductivity of gas phase k_g, the porosity, the size distribution of pores or particles and the deposit sintering state. The properties k_s and k_g are influenced by temperature and the chemical composition. Because the thermal conductivity of solid phase is two or three orders of magnitude higher than that of the gas phase, heat conduction through the deposit will mainly take place through the solid phase. The overall thermal conductivity is thus strongly dependent on the material porosity. The emissivity is affected by the deposit surface conditions (i.e. whether it is fused or particulate), the particle size and the chemical composition [39].

Figure 2.7: Effect of temperature on the thermal conductivity of a coal ash shample (the arrows indicate heating and cooling of the sample) [39].

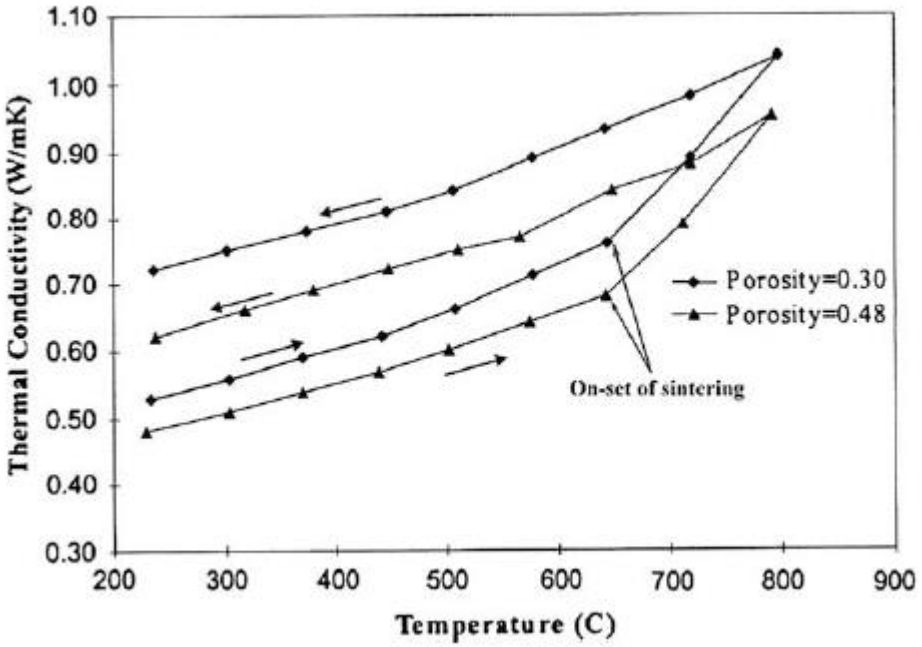

In general as the temperature rises, the thermal conductivity of deposits increases. Above in Figure 2.7 the experimental data for the temperature dependency of a coal ash deposit on thermal conductivity is shown. Below the sintering point the thermal conductivity is not strongly influenced by the temperature change. The thermal conductivity of the deposit in this case follows the change in the thermal conductivity of the gas phase. Also it is shown that the thermal conductivity of an ash deposit during cooling is higher that the case of heating, where also the trend does not follow the same path. This is because irreversible changes have taken place in the physical structure and the porosity of the samples. In a similar way, the emissivity is affected by the temperature increase due to surface structural changes, i.e. through a particle size due to sintering. Furthermore, below the sintering temperature, for increase of temperature the emissivity of coal ash decreases, while at higher temperatures as sintering and fusion of ash takes place, it increases strongly.

In conclusion, the effective thermal conductivity varies significantly with the type of the deposit. A fused deposit (consisting of a continuous solid phase, with discontinuous gas voids) has a higher thermal conductivity than a particulate structured deposit (consisting of a continuous gas phase, with discontinuous solid particles). The first stages of sintering are followed by an increase in the deposit thermal conductivity. Successive sintering increases the density of the deposit, but does not change considerably the deposit thermal conductivity.

Finally, a slag structure has a significantly higher thermal conductivity than of a particulate structure, especially in the porosity range 0.2-0.8 [39].

2.5.6 Deposit sintering

Sintering is the process of compacting and forming a solid mass from the particles without melting it to the point of liquefaction. The force that is driving particles to sintering is their surface energy. The energy change due to densification is connected with a decrease in surface area and a decrease of the surface energy by elimination of solid-vapor interfaces and creation of new lower energy solid-solid interfaces. Sintering can take place by many mechanisms as shown schematically in Figure 2.8. Viscous flow sintering is a liquid state sintering involving a viscous liquid [35]. When a reaction between the particles leads to the formation of a third component, then chemical sintering takes place. Especially in the low temperature part of the flue gas channel, chemical sintering can be important for fouling [35]. Solid state sintering takes place because of diffusion along the particle surface, through the interior of the particles and through the surrounding gas by vaporization and successive condensation [35]. Liquid or viscous phase appears mainly to be the dominant sintering mechanism [35].

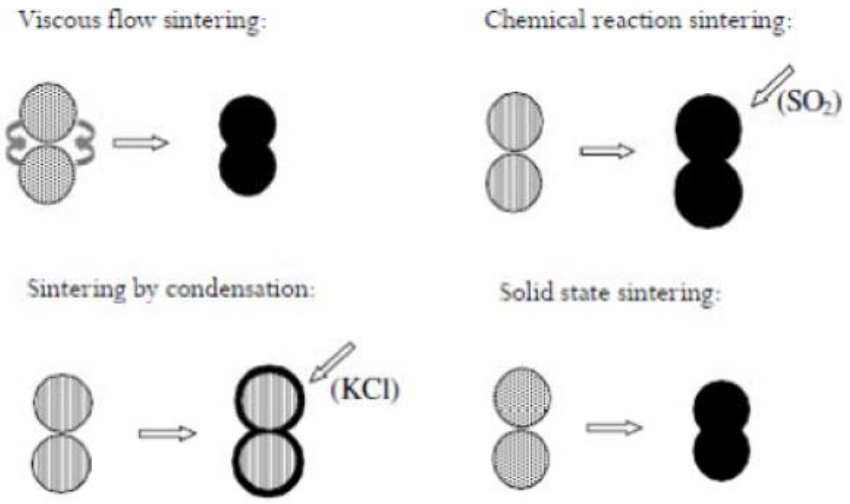

Figure 2.8: Graphical representation of different types of deposit sintering. Source: Adapted from [28].

2.6 Use of additives to minimize deposit formation and corrosion

In order to deal with and minimize the different operational problems that are mentioned above there is a variety of techniques can be used. One of these techniques is the use of

additives [40]. Additives refer to a group of minerals or chemicals that have the ability to change the ash chemistry, decrease the concentration of problematic species and raise ashes melting temperatures. The feeding of additive into the furnace can be done (i) either with pelletization of the substance together with the fuel or some other way of premixing them and then entering the furnace, or (ii) spraying the additive as powder or solution apart of the fuel and entering the furnace separately. The second method is better in the case we want to change the additive/fuel ratio while the burning process is still running, almost instantly [9].

Different additive mechanics to deal with biomass ash related problems have been introduced: Chemical reaction, where the low melting temperature elements in biomass fuels can be converted into high temperature melting ones. Physical absorption, in which case porous additive particles with large surface areas capture condensable vapours, melted ashes as fine particles, i.e. aerosols and transport them out of the combustion system. Enhancement of ash melting temperatures by the introduction of more inert materials and elements (i.e. SiO_2 and Al_2O_3) into ash residues. Dilution of ash and thus restriction of ash melt formation and accumulation [9].

Furthermore the effectiveness of an additive depends on certain factors: (i) Additive particle size distribution, which means that, the smaller the additive's particle size is, the more surface area is available for reaction. (ii) Reaction temperature and time. (iii) Composition (active compounds in the additive). (iv) Stoichiometry (i.e. sufficient amounts of additive) [40].

The chemical binding of an additive is a desired attribute in order to lighten ash related problems during combustion. The most problematic specie formed during biomass combustion is $KCl_{(g),(l)}$ and can initiate and boost various operational problems [9], among them, high temperature corrosion [5]. For this reason most of additives are used in order to capture and transform KCl into high temperature melting species through a series of solid/gas or solid/liquid, chemical reactions, after it has normally volatized from fuel particles as vapor. Complementary, some additives may also react with melted potassium silicates and phosphates and change their ash chemistry in order to create other chemicals and reduce the amount of ash melts [9].

Considering their reactive components, additives can be categorized into: (1) Aluminium silicate based additives, (2) Sulphur based additives, (3) Calcium based additives, (4) Phosphorus rich additives [9].

Aluminium silicate based additives

Aluminium silicate based additives, when reacting with potassium chloride produce potassium aluminum silicates. The related reactions are shown below in Table 2-3. One representative of aluminum silicate additive is kaolin, which is rich in kaolinite with the chemical formula $Al_2Si_2O_5(OH)_4$. Kalcilite ($KAlSiO_4$) and leucite ($KAlSi_2O_6$) are two main products identified

from the reaction between kaolinite and $KCl_{(g)}$ and have comparatively high melting temperatures, 1500 and 1600 °C respectively [7,9,41]. Also other aluminium additives, i.e. bentonite, when used, they capture KCl and give more complex potassium aluminium silicates, such as $KAlS_3O_8$. Furthermore, SiO_2 and Al_2O_3 can react with KCl on high temperatures, but with not the same efficiency and capacity compared to kaolinite [9]. During the reaction of aluminosilicate with KCl, gaseous HCl is formed [29]. For temperatures at 900°C or below, the capture efficiency of kaolinite is similar for KCl and KOH, but less effective for K_2SO_4 [7].

Table 2-3: Key reactions involved between aluminium silicate based additives and potassium chloride. Source: Adapted from [9].

$Al_2O_3.xSiO_2 + 2KCl + H_2O \rightarrow K_2O.Al_2O_3.xSiO_2 + 2HCl(g)$	(2-14)
$2KCl + H_2O(g) + Al_2O_3 \rightarrow 2KAlO_2 + HCl(g)$	(2-15)
$2KCl + SiO_2 + H_2O \rightarrow K_2O.SiO_2 + 2HCl(g)$	(2-16)

Sulfation

Gas phase sulfation

The reduction of sticky and corrosive chlorides in flue gas can take place also by sulfation. Gaseous alkali chlorides are converted into less harmful alkali sulfates by the sulfur existing inside the fuel or different sulfur containing additives. The reactions taking place are (2-12) and (2-13) [5,28]. Sulfation of KCl(g) in the gas phase is usually fast and the oxidation of SO_2 to SO_3 in the reaction mechanism is rate limiting for the sulfation reaction [29].

The availability of sulfur for reactions of sulfation is important for deposition and corrosion rates. Experiences from combustion of biomass and coal in industrial scale, conclude to the fact that with S/Cl>4 in the fuel, chlorine-related corrosion problems were rare, while with S/Cl<2 the problems occurred often [29].

Solid phase sulfation

At lower temperatures where chlorides as solids are found, the oxidation reactions of SO_2 are considered as too slow for efficient sulfation. Solid phase KCl sulfation is not fast enough to play its role into creation of sulfates in fly ashes. Nevertheless, solid state sulfation is important in deposits, over longer periods of time. It is considered as one of the mechanisms involved in the aging of deposits [5].

The challenge when it comes to the use of additive, is to choose the most optimal for the scenario that it is needed. That means that the additive should be effective, cheap and not give rise to materials handling or environmental problems. There is no additive with all these qualities so the selection of additive is a compromise between performance and price [40].

2.7 Case studies (use of additives)

Several studies [7,8,41,42] through the last decades have been conducted for researching how additives can reduce biomass ash related problems.

In the experimental work [41] Steenari et.al. investigated the effect of kaolin and limestone powder, on the ash deposition behavior of various types of biomass. This work showed that slag formation and ash fouling can be restricted. Almost all of the biomass fuels had ash sintering and melting temperatures lower than 1000 °C, due to potassium salts in combination with silica and phosphates with high K/Ca ratio. However with the use of the additives in amounts corresponding to 2-10% of the weight fuel, calcium/magnesium phosphates and potassium aluminium silicates with higher melting points where formed.

In a former study of 2004 [8], Ivarsson et.al. studied the effect of kaolin and limestone on the slagging behavior of two different kind of wood pellets. One problem-free and one severely slagging. The results of this study come in agreement with the one's previously mentioned. The results show that for the use of limestone in a solution, the severe slagging tendency of the problematic wood-pellets could be totally eliminated. This is achieved because the composition of the slag changes from relatively low temperature melting silicates to higher temperature melting silicates and oxides. Adding a kaolin suspension to the problematic material has as a result a minor decrease in slagging tendency of the material, because the additive eliminates the Ca-Mg silicates in favor of K-Al silicates which also have relatively low temperatures. On the other hand, when adding kaolin to the problem free wood-pellets, there is an increase in the slagging tendency of the material, because high-temperature melting Ca-Mg oxides react to form more low-temperature melting Ca-Al-K silicates.

In another case [43], Wu et.al. used spent bleaching earth (SBE) and kaolinite as additives during straw dust-firing inside an entrained flow reactor (EFR), which was designed to simulate the combustion conditions of a suspension fired boiler. For the straw, the Cl was almost totally present in the fly ash. Also about 70% of the K in fly ash was water-soluble and KCl was estimated to contain more than 40% of the water-soluble K. The deposition and corrosion potential of fly ash from straw dust-firing was found to be high. The results showed that SBE could react with gaseous alkali, reducing the Cl retention in fly ash and so decreasing alkali chloride greatly. At the same time SO_2 emissions increased and formation of water soluble salts decreased. Furthermore, through dilution and chemical reactions the Cl content in the deposit was reduced as well. With similar molar ratio of K/(Al+Si) in the fuel mixture, the effect of kaolinite on alkali chloride formation was slightly higher. Overall the corrosion potential in the super heaters could be greatly decreased by the use of additives in straw dust-firing.

Xiong et.al. [42] examined the effect of kaolinite on ash related problems of corn stover pellets. The study took place in 2007, in a small-scale under-fed burner (Eco Tec 50kW). While combusting corn stover raw material with the addition of 3% kaolin, the severe slagging tendency of fuel was considerably reduced. The reduction of slagging can be attributed to the change from relatively low melting temperature silicates to higher melting temperature silicates [42]. For the fuel without additive co-firing, the low melting fractions of the slag consisted mainly of potassium calcium silicate. When kaolin was added, because of extensive formation of leucite ($KAlSi_2O_6$), a reduction of potassium was observed and the glass became dominated by calcium, aluminium and silicon. Furthermore, the process was followed by significant reduction of glass amount [42].

In the experimental study [7], Paneru et.al. studied the influence of aluminosilicate base additives on deposit formation of wood pellets combustion. The study took place inside an atmospheric drop tube furnace (BTS). Potassium in wood pellets together with silica are responsible for formation of deposit, where potassium silicates play a leading role. When using aluminosilicate additives, K-Al-silicates are formed instead which have a very high melting point, and also aluminosilicates react with $KCl_{(g)}$ releasing $HCl_{(g)}$. This way high temperature deposit growth (slagging) and condensation of potassium salts (K_2SO_4 and KCl) (fouling) is decreased. Sulfation also in lower temperatures (<950°C) plays its role to reduce the risk of KCl condensation. The additive amount necessary to minimize deposition problems depends on the composition and form of the additive, the composition of the fuel and the temperature of the application.

The conclusion made from these studies is that, aluminium silicate based additives, indeed deal effectively with the ash related problems of biomass by decreasing their slagging tendency and their corrosion potential. Nevertheless, the choice of an additive for a real industrial application is not simple. Its technical as well as its economical characteristics must be taken into consideration.

2.8 Modelling of deposit formation (FactSage, Others)

There are various tools available to model the various aspect of deposit formation and to have better understanding of the ash chemistry. Some of them are discussed below.

FactSage

FactSage is a thermochemical simulation software and database that made its appearance in 2001 as the combination of two distinguished software packages in the area of computational thermochemistry: F*A*C*T/FACT-Win and ChemSage[44,45].

The FACT databases are a very large set of evaluated and optimized thermodynamic databases for inorganic systems. There are two types of thermochemical databases that FactSage can access: compound (pure substances) databases and solution databases. The former contain the properties of stoichiometric compounds, either obtained from phase diagram optimizations or taken from standard compilations. The latter contain the optimized parameters for solution phases[44,45].

The user can work with the software and databases in different manners and calculate and display thermochemical equilibria and phase diagrams in a plentiness of formats. The Equilib module is the Gibbs energy minimization tool of FactSage. For a given set of constrains (temperature, total pressure, total mass of each element etc.) the software calculates the equilibrium conditions by minimizing the total Gibbs energy of the system. This is mathematically equivalent to solving all the equilibrium constant equations simultaneously. All the needed data is automatically extracted from the databases[44,45].

The main limitation attributed to thermodynamic modelling of the combustion process is the lack of consistent and accurate databases. This makes difficult a proper assessment of all possible formed phases in an ash system [46].

The FacSage software has been used in order to predict the ash behavior and ash fusion temperature at high temperature under reducing atmosphere conditions. Also for the same study, the ash transformation results by FactSage come to agreement with the XRD results [47]. In another case the thermal analysis via FactSage modeling confirmed the determination of the detailed mineral composition of 4 different biomass ashes [48]. Furthermore there have been several studies in which the phase equilibrium calculations were used to investigate the ash deposition tendencies in solid fuel combustion systems[49–51].

2.9 Experiences on deposit probe measurements in full-scale boilers

In order to examine ash formation mechanisms and ash related problems in pilot-scale but also in full-scale boilers, often deposition probes are used. These probes may be cooled by water or air, or non-cooled, may consist of different materials and are planted at places inside the boiler that are considered to have high deposition potential.

Munksund and Umea, Sweden

In the study [5] sampling processes using various probes in different facilities in Munksund and Umea, Sweden are described [29,52–54]. Measurements is full scale industrial boiler were performed in order to understand and decrease chlorine related high temperature cor-

rosion problems in biomass fired boilers. Corrosion problems were evaluated with the help of corrosion probes with different alloys. SEM/EDS analysis gave information for the corrosion products and deposits. A laboratory study [54] was performed inside an electrically heated tube furnace to increase the fundamental understanding of deposit formation, which focused on the resulting phase composition when mixtures of potassium and sodium chlorides were condensed. WRD was used to determine the phase composition of the deposited salts.
In chlorinating environments no positive effect on corrosion resistance was seen from non- or low- alloy steels. High alloy, austenitic steels containing also nickel, corroded much less.
Condensation on NaCl and KCl on cooled surface, showed that even though the two salts were mixed in the gas phase, most of the deposited salt was present as separate phases.

Denmark

Several measuring campaigns with focus on deposition behaviour have taken place at full-scale power plants firing biomass in Denmark. The study [55] includes a summary of the applied experimental probe techniques and an overview of the data collected, when biomass alone was combusted in suspension and grate fired boilers. The probe deposits examined, were focused on the rate of deposit formation, chemistry of ash and deposits and in a few cases corrosion studies and shedding observations. The probes used where simple air-cooled, as well as more advanced for in-situ deposit measurements.
A general conclusion is that temperature of flue gas influences the deposit behaviour of biomass fired boilers, meaning that the increased flue gas temperature leads to increase in deposition rates and altered chemical composition of the deposits formed. For the two combustion technologies, grate- and suspension-firing, the rates of deposit formation were found comparable, while the chemical composition of the fly ashes are quite different, even for the same type of fuel. The chemistry of deposits also varied with variation of firing technology and fuel type. However, the deposits structure and chemistry had some general features. Furthermore the temperatures of probe surface and flue gas and the deposits chemistry influenced the shedding behavior.

3 Experimental Set-up & Method

The experimental set-up, methods, combustion parameters and equipment that were used are described in the following sections.

3.1 Experimental facility

All the experimental procedure took place in the atmospheric drop tube furnace (BTS-VR), with 20kW thermal power, of the IFK facility. The combustion reactor has an electrically heated ceramic tube of 2500 mm length and 200 mm diameter. In the tube a certain temperature profile can be achieved, by heating in five different locations (2 × 12 and 3 × 8 SiC – heating elements). The residence time of the particles inside the chamber is 5-6 s. Fuels were inserted in a conical silo above the furnace and from there fed by a screw conveyor inside a tube that led to the top of the furnace. The additive feeder was located next to the fuel feeder. The detailed decription of the additive feeder and the modification made in the fuel feeding line, in order to accommodate the additive online feeding, is briefly discussed in section 3.1.2. Carrier air passed through the additive feeder and entered the same tube as the fuel. In this way fuel, carrier air and additive (when used) entered the chamber together (Figure 3.7) .Combustion air (both primary and secondary air was fed directly to the burner. At the end of the furnace, at 2.5m from the burner, the emissions of the flue gas were measured. NO [ppm] and NOx [ppm] were measured with the help of a Chemiluminescence analyser, O_2 vol.-% with the help of a paramagnetic analyser SO_2, CO_2 vol.-% CO vol.-% by NDIR (Nondispersive infrared analyser) and O_2 [ppm] and SO2 [ppm] were measured by NDIR. HCl [ppm] was measured by an FTIR Analyzer (Fourier Transform InfraRed) with the sampling taking place in the gas pipe, before the filter (205~365°C). As HCl measurement was the focus measurement during this work the principle of FTIR measurements and the device will be briefly discussed below.

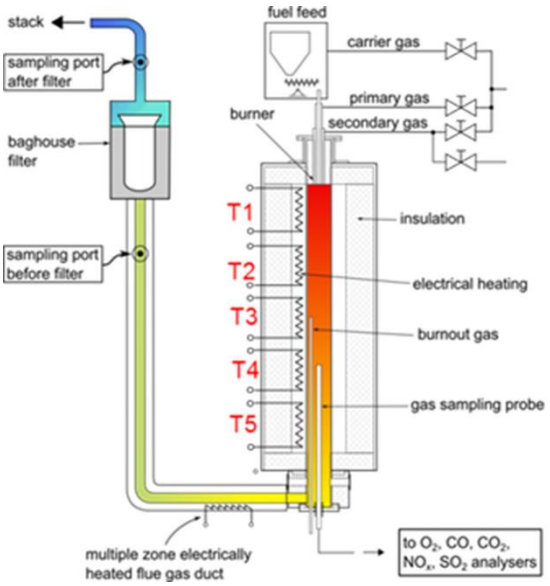

Figure 3.1: Atmospheric drop tube furnace (BTS)

3.1.1 Gasmet™ FTIR

FTIR are the initials of Fourier Transform Infrared Spectroscopy. An FTIR analyzer has the ability to detect gaseous compounds by their absorbance of infrared radiation. Each compound produces a unique infrared spectrum because each molecular structure has a unique combination of atoms, something that enables the identification (Qualitative analysis) and analysis (Quantitative measurement) of gaseous compounds. The FTIR analyzer can detect virtually all gas-phase species (both organic and inorganic) and thus at the same time measure multiple analytes in a complex gas matrix [56].

The device used in this study is a Gasmet DX4000 portable FTIR gas analyzer. The whole set of components consists of the measuring device Gasmet DX4000, a portable sampling system, a portable sampling probe, heated lines and a laptop equipped with the Calcmet software [56].

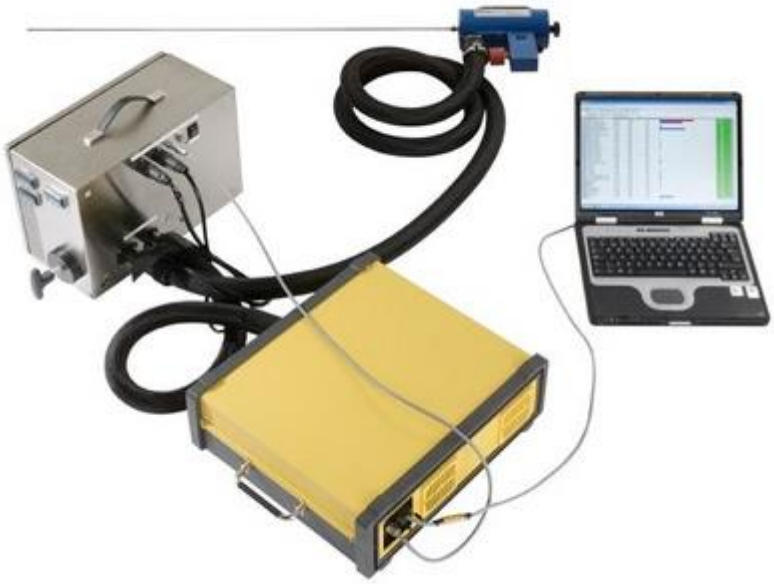

Figure 3.2: FTIR system parts. Source: Adapted from [48].

Fourier Transform Infrared (FT-IR) spectrometry was developed in order to overcome the limitations that dispersive instruments came upon. A simple optical device called interferometer was deployed as a solution to slow scanning processes and can measure all of the infrared frequencies simultaneously. This results in a signal measurement in order of seconds.

Most interferometers employ a beamsplitter which takes the incoming infrared beam and divides it into two optical beams. One reflects off of a flat mirrored fixed in place and the other reflects off of a mirror which is on a mechanism that enable the mirror to move slightly. The two beams meet again at the beamsplitter and recombine and because the path of the

first beam has fixed length, while the path of the second one changes together with the second mirror, the two beams “interfere” with each other. Thus the resulting signal is the interferogram (Figure 3.3).

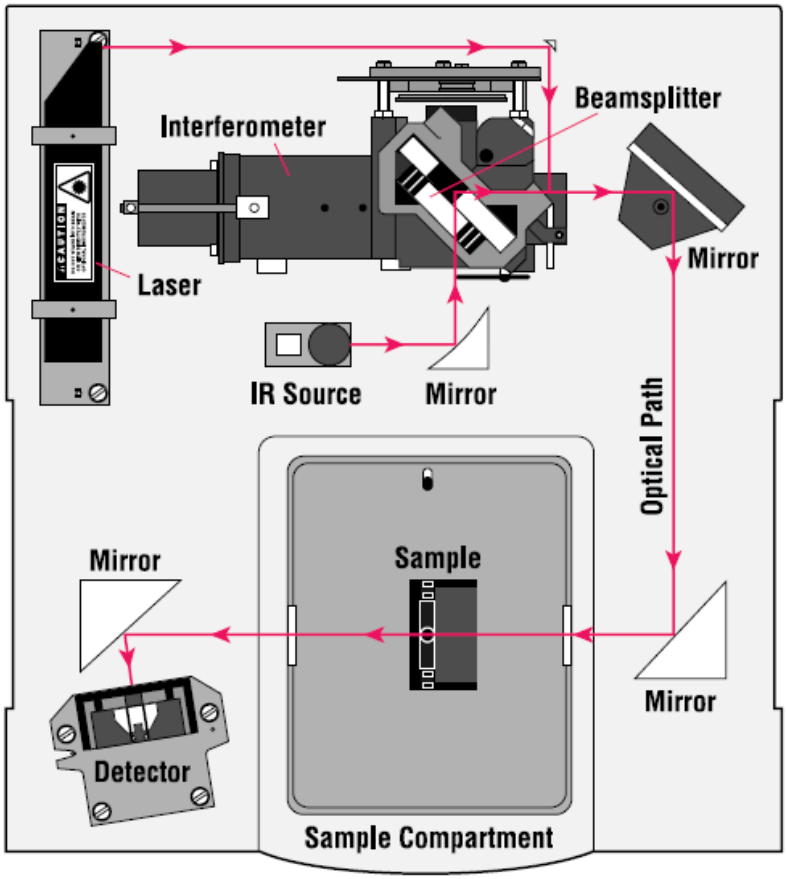

Figure 3.3: Simple spectrometer layout. Source. Adapted from [49].

The normal instrumental process starts with infrared energy emitted, in the form of a beam, from a glowing black-body energy source and passes through an aperture which controls the amount of energy presented to the sample (and finally to the detector). Then the beam enters the interferometer where the “spectral encoding” takes place and consecutively the produced interferogram signal exits the interferometer. After that, the beam enters the sample compartment where it is transmitted through or reflected off of a surface of the sample, depending on the type of analysis taking place. This is where specific frequencies of energy, which are unique every sample species, are absorbed. Finally, the beam passes to the detector for the last measurement. The detectors are specifically designed to measure the special interferogram signal. The measured signal after digitization is sent to the computer where the Fourier transformation takes place and the final infrared spectrum is then presented to

the user for interpretation and any further manipulation [57]. The process is displayed in Figure 3.4.

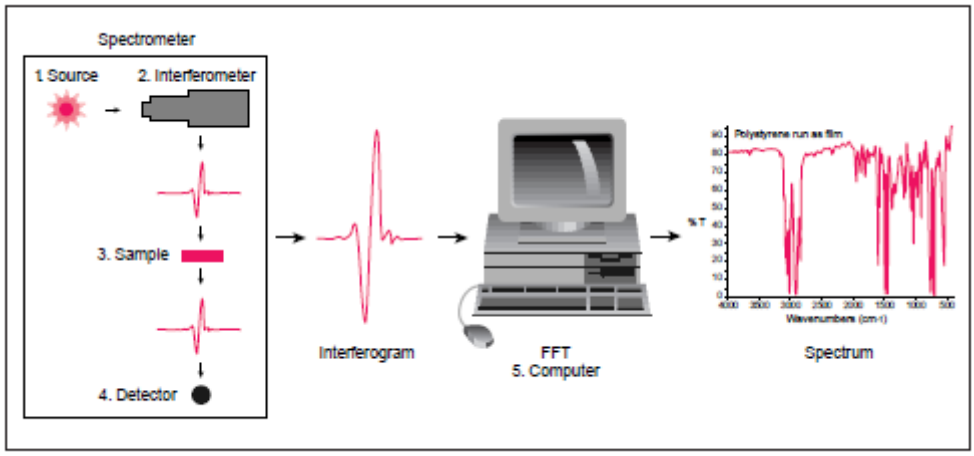

Figure 3.4 : Sample analysis process. Source: Adapted from [49].

Beer-Lambert's absorption law (Gases concentration calculation)

When the infrared radiation passes through a material, some intensity passes through without interacting with the molecules, while the rest is beig absorbed by them. The proportion of absorbed intensity that enters the material is in direct relation to the concentration of absorbing molecules [58].

The principle of Beer-Lambert's lawis descripted by the following equation:

$$A_\lambda = \varepsilon_\lambda \times b \times C \qquad (3\text{-}1)$$

Where:

A_λ	is the measured absorbance of a material at a specific wavelength (λ)
ε_λ	is the absorption coefficient of the material at that wavelength
b	is the path length through the sample
C	Is the concentration of the absorbing material

In the case of constant path length b in a particular application and for the constant absorption coefficient ε_λ of a given material at a particular wavelength, these two variables combine into a single constant K_λ. And thus he have:

$$A_\lambda = C \times K_\lambda \qquad (3\text{-}2)$$

By measuring the absorbance of an unknown sample at the appropriate wavelength, the concentration of the sample is predicted by:

$$C = \frac{A_\lambda}{K_\lambda} \qquad \textbf{(3-3)}$$

Reliability of the results and analysis

Measurements can be made continuously and results are shown and updated on the screen after each measurement.

To correctly analyze the sample, a good quality background must be measured, an analysis library must be specified and set and the sample itself must be measured. When all these three operations are from the beginning correctly done, reliable analysis results can be obtained.

The application library has to be supplied with reference spectra for all gas components that the gas contains and all these components must be used in the analysis in order to gain optimal accuracy. For each gas component, at least one reference spectrum must be included. However, in the case that the concentration-absorbance curve of some reference is not linear and the measurement of a wide range of concentrations is needed, it might be necessary to include more reference spectra of different concentrations. The Calcmet software picks the references closest to the calculated concentration for the analysis automatically. Consequently the results will be unreliable if the gas contains an important amount of any gas component that is not in the analysis library.

In order to optimize the performance, it is necessary to use different spectral ranges for different components and each range can consist of one to three spectral areas. In each of these ranges, modifications that follow certain rules should be made, i.e. leave out range parts with absorbance peaks or limit the absorbance taken into consideration so that only parts with linearity are available. This way the concentration of a component is avoided to be calculated very high. Furthermore, between all these ranges from the different components some interfere with each other. So for an analyte the other components that happen to interfere with it have to be defined as interfering components.

The reliability of the analysis can be verified with the use of the Residual spectrum, which is the residual between the measured spectrum and the calculated spectrum when using the analysis settings made before. If the residual is very small, a linear combination spectrum using the reference spectra and the current analysis settings was successfully formed. On the other hand, when residual between the two spectrums is clearly high, it indicates that either the measurement was bad, or the current analysis library is not suitable to analyse the sample accurately [59].

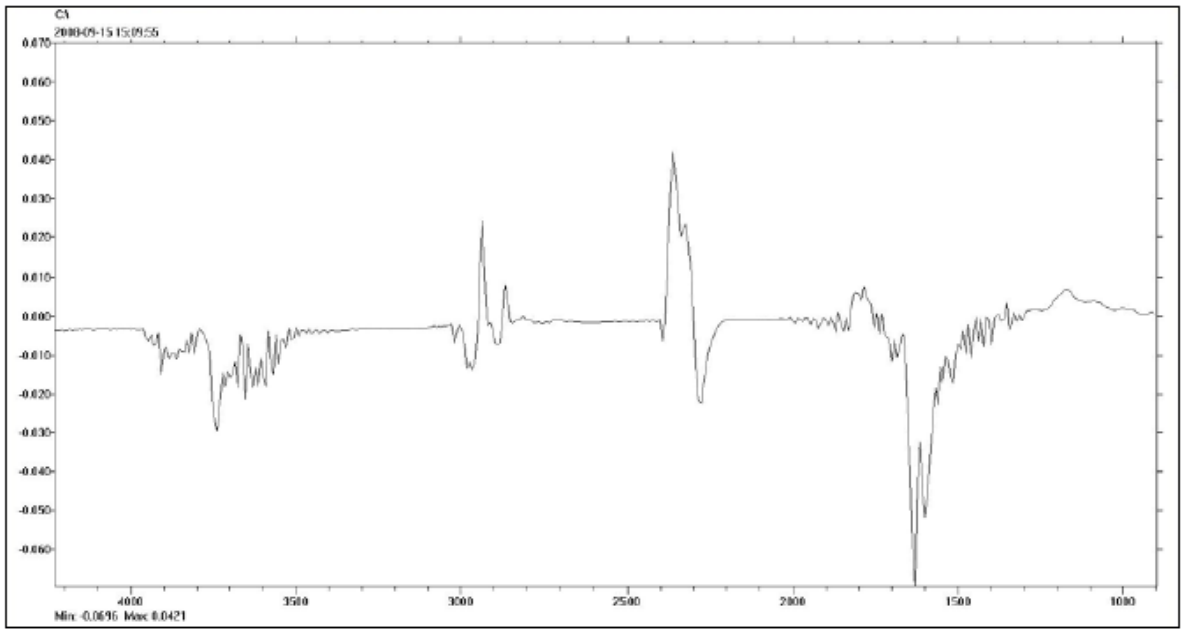

Figure 3.5: Residual spectrum that shows an unsuccessful analysis. Source: Adapted from [51].

The major advantages of FT-IR consist of speed (most measurements in are made in a matter of seconds), sensitivity (detectors are much more sensitive, optical throughput is much higher resulting in lower measurement noise levels), mechanical simplicity (moving mirror the only moving part in the instrument and internal calibration (no calibration by the user needed). Along with several other benefits, these advantages make measurements made with FT-IR extremely reliable for positive identification of virtually any sample, an invaluable tool for quality control and increase the practical use of infrared for quantitative analysis [57].

3.1.2 Additive feeder TOPAS SAG 410

The device used for supplying the additive into our system is a dust disperser (SAG-Solid Aerosol Generator) with the help of a control unit Figure 3.6. The procedure for the dispersion of dry dust and powder comprises of two steps, the supply of material to the disperser and the dispersal of the material as aerosol [60].

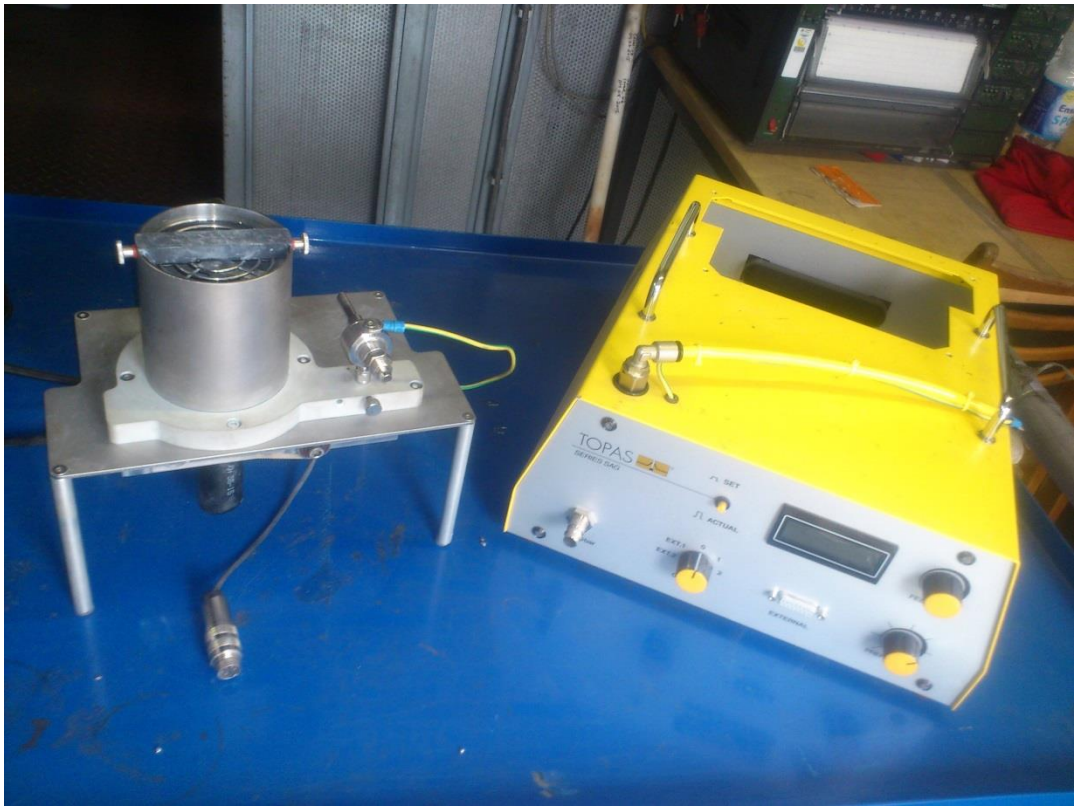

Figure 3.6: Disperser and control unit.

More analytical the feeding technique and the equipment function are as follows. First the additive is inserted inside the cylindrical reservoir on the top of the disperser. This reservoir is equipped with a rotating stirring part, moved with the help of a small motor. This way the material inside tends to be distributed evenly and doesn't stay still on the sides. Then from a small hole at the bottom of the container, the additive falls on the moving toothed belt under the main base surface of the feeder, which is moved through drive wheels with the help of another small motor. The well-defined spaces between the teeth make the constant and reproducible supply of powder possible. Then the small amount of powder inside each teeth gap is sucked and removed from the belt by an ejector nozzle. From there on the additive is finally transported in the form of aerosol by the carrier air, which passes through the nozzle, inside the tube that leads to the furnace [60]. While entering the tube, the carrier air, the additive and the fuel are met and enter the furnace from the top together (Figure 3.7).

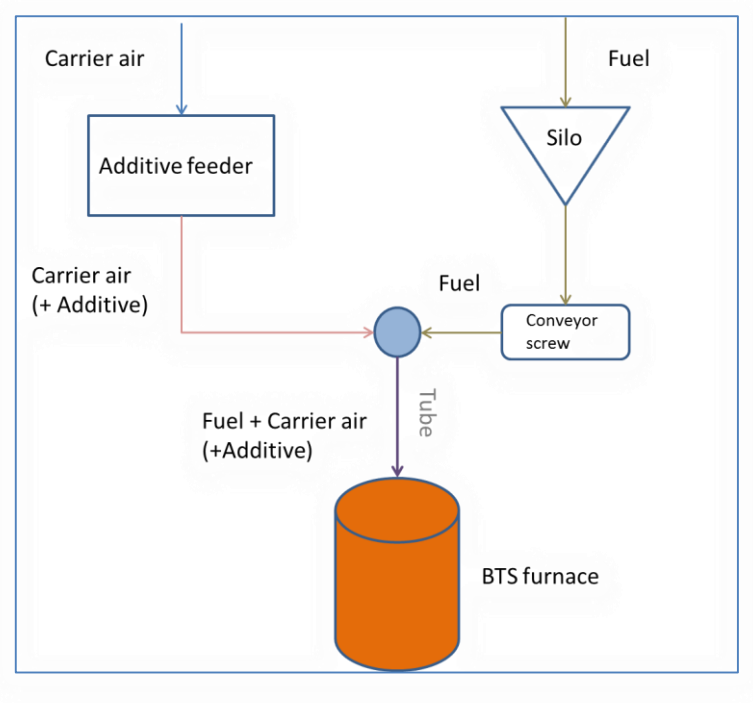

Figure 3.7: Flow chart of fuel, carrier air and additive.

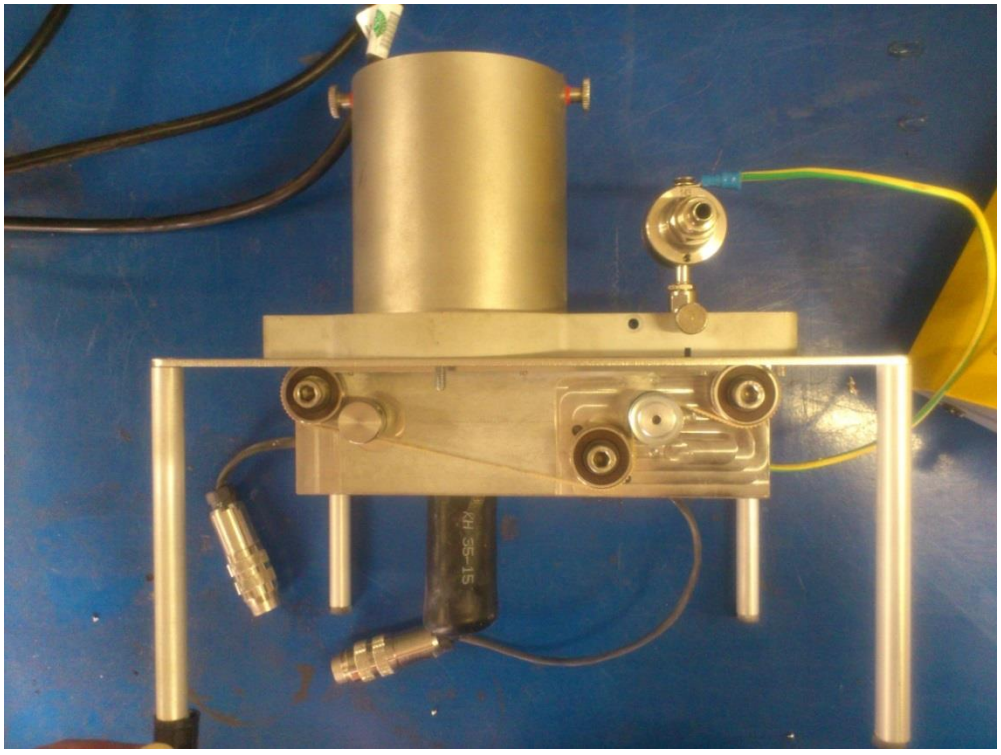

Figure 3.8: Disperser-Side view.

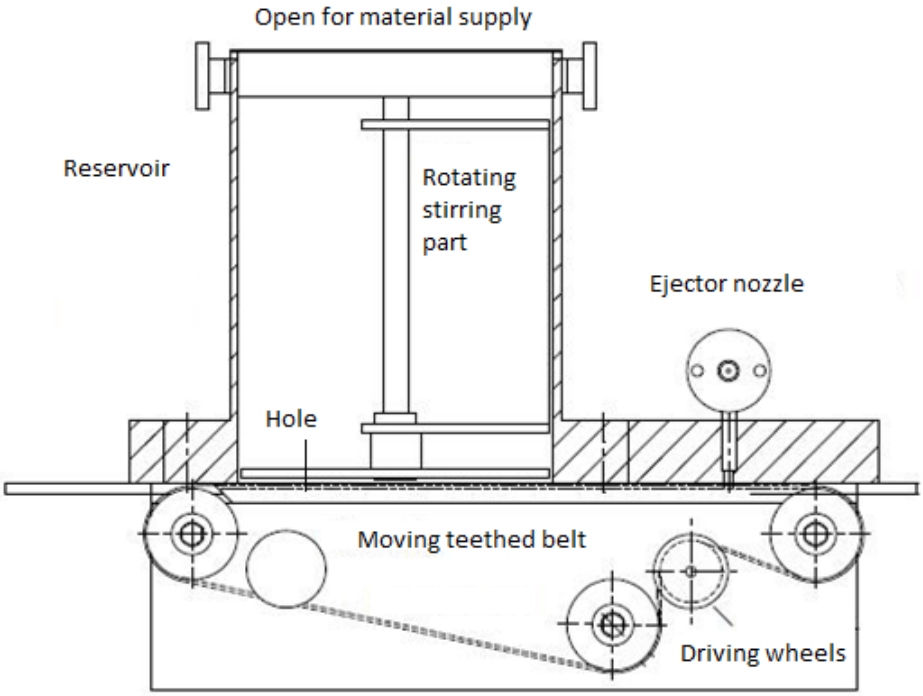

Figure 3.9: Disperser-Side section. Source: Modified from [53].

The device has easy control and operation. With the help of the switches on the front surface of the yellow box, the user is able to change the 1) moving speed of the belt (0-100%) and 2) the rotating speed of the stirring part (0-6 scales) in the reservoir (so the reason we have two motors is to change the belt the stirring speeds separately). Primarily by adjusting the speed of the belt, the operator can change the feeding rate in a wide range, because also the powder amount transferred to the nozzle changes. Secondly, the stirring part's rotating speed influences the feeding rate, because the better the distribution inside the reservoir, the more additive falls on the belt. Another small detail that plays an important part on the feeding rate is the right adjustment of the nozzle. The nozzle can be adjusted higher or lower above the belt, so that it captures the material properly. So depending on the belt speed as well as the particle size, the optimal adjustment of the nozzle position has to be made, in order to have higher suction efficiency. Additionally another important factor that influences the additive feeding rates is the powder nature, i.e. the particle size, moisture, volume. For example bentonite that has bigger volume than aurora reached lower feeding rates from the two, calculated in g/h. On the other hand, dry aurora because of its higher density reached the highest feeding rates observed. Finally, the disperser needs to be dismantled after some operating time (depending on the used additive) so that agglomerated material can be removed and cleaned from tight spots, in order to have a smooth function.

Scaling and isolation

Through the whole experimental process the additive feeder was placed inside a heavy cubic metallic construction and when inside, on top of an electronic scale.

The scale was reset every time a change was made to the feeder's operation, or additive was supplied inside the feeder, and used to measure the loss of the feeder's weight through the passing of time, from zero to negative values. Its precession was in amounts of 5 centigrams. This way it was possible to calculate the feeding rates of every smaller additive feeding session using the simple equation:

$$Afr = (Aw_1 - Aw_2) * 3600/\Delta t \quad (3\text{-}4)$$

Where:

Afr	is the calculated feeding rate for a certain operation setting
$Aw_1 - Aw_2$	is the difference between the initial and the final additive weight for a period of time Δt
Δt	a period of time in s

The values of every measurement where saved automatically to the computer at which the scale was connected.

The aim of the metal cube was to isolate the feeder and the scaling process from external forces and noise and also provided higher stability.

3.1.3 Fuels & Additives

The fuels and additives used in this study are listed in Table 3-1. The proximate, the elemental and the oxide analysis of the fuels are presented in Table 3-2, Table 3-3 and **Table 3-5** accordingly. The ash fusion temperatures of the fuels are presented in Table 3-4: Ash fusion temperatures of biomass fuels.. Notable information is that TS has about the double Cl content compared to WP. For the fuel WP+KCl two samples were taken and the lab analysis was similar for both of them. For this reason the components presented here as results are averages of the components of the two samples. The idea and preparation procedure for the WP+KCl fuel is presented in section 3.2.2. Additionally, the achieved Cl content of WP+KCl was 5.3 times the initial Cl content of WP. The initial try was to increase it at levels as high as

6 times the initial wood pellets chloride content. Furthermore we see that the K content in TS is about ten times the K content of WP (

Table 3-5), which is really important to remember when it is known that potassium is the most troublemaking species as for deposition problems. Important ash forming elements of the fuels are presented also in Figure 3.10. The additive oxide analysis as received from the lab in presented in Table 3-6: Additive oxide analysis.

Table 3-1: Fuels and Additives.

Fuels	**Additives**
Torrefied Straw	Aurora
Wood Pellets	Bentonite
Wood Pellets + 0.25%KCl	

Table 3-2 : Fuel proximate analysis

	Proximate analysis [wt%]			
Fuel	Moisture (ar)	Volatile (waf)	Ash (wf)	Fix C (waf)
TS	7.89	76.2	4.4	23.84
WP	7.95	79.5	1.38	20.49
WP+KCl	7.35	79.1	1.52	20.82

Table 3-3: Fuel elemental analysis

	Elemental analysis [wt%] [waf]					[MJ/kg]
Fuel	C	H	N	S	Cl	LHV (ar)
TS	53.13	4.90	0.52	0.085	0.057	17.49
WP	51.11	4.79	0.63	0.066	0.026	17.42
WP+KCl	51.67	5.11	0.64	0.083	0.141	17.42

Table 3-4: Ash fusion temperatures of biomass fuels.

	Sintering (°C)	DT (°C)	ST (°C)	HT (°C)	FL (°C)
TS	720	840	1130	1150	1160
WP	960	1170	1175	1180	1190
WP+KCl	950	1180	1185	1190	1230

Table 3-5: Fuel oxide analysis

	[wt%] (wf)		
Fuel Ash Oxides	TS	WP	WP+0.25%KCl
Al2O3	1.65	5.61	5.46
CaO	19.52	19.56	17.86
Fe2O3	3.26	12.76	10.45
K2O	24.90	7.59	18.15
MgO	2.94	5.83	5.11
Na2O	0.45	1.24	1.44
P2O5	2.65	2.50	2.42
SiO2	39.59	37.53	31.67
SO3	4.26	4.90	5.36
TiO2	0.14	1.49	1.21

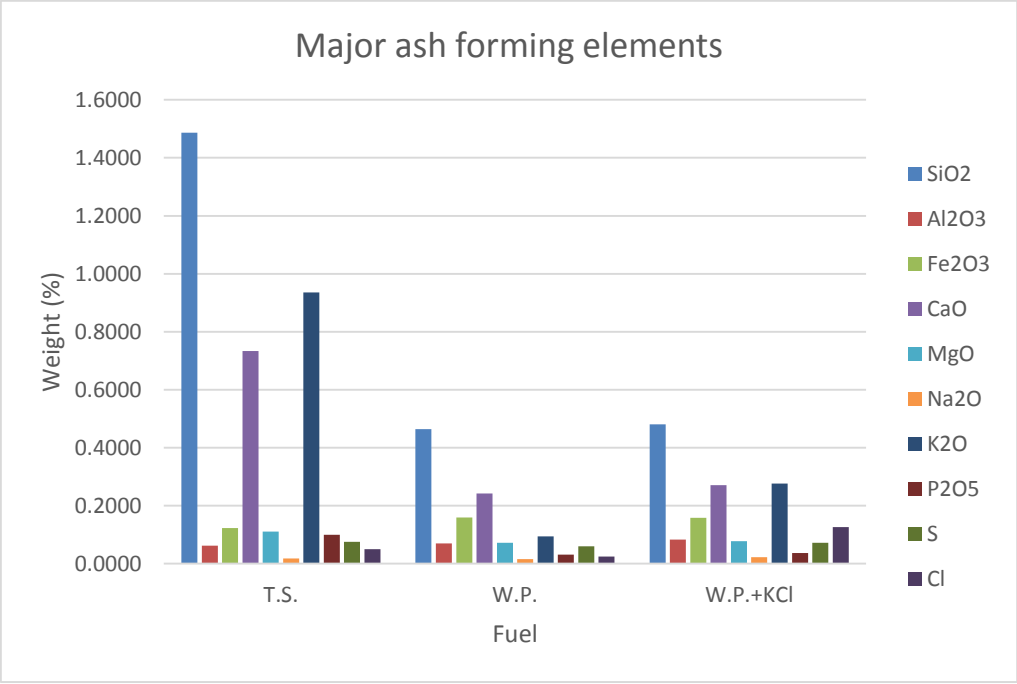

Figure 3.10 : Important ash forming elements of the different fuels.

Table 3-6: Additive oxide analysis

	[wt%] (ar)	
Additive oxides	Aurora	Bentonite
Al2O3 (wt%)	24.5	27.6
BaO (wt%)	0.021	0.017
CaO (wt%)	0.064	0.155
Fe2O3 (wt%)	0.992	0.733
K2O (wt%)	1.73	1.06
MgO (wt%)	0.21	0.213
MnO2 (wt%)	0.008	0.004
Na2O (wt%)	0.044	0.037
P2O5 (wt%)	0.1	0.035
SO3 (wt%)	0.024	0.142
SiO2 (wt%)	37.2	49.3
SrO (wt%)	0.017	0.01
TiO2 (wt%)	0.074	0.37
Moist 105°C (wt%)	12.56	0.85
Combine water 950°C (wt%)	10.28	11.44

3.2 Experimental method

In this section the experimental method followed is described in detail. The general purpose of this study is to investigate the effects of aluminosilicate additives on chlorine chemistry. Aluminosilicates react with the main troublemaking element of biomass, which is potassium (K), forming K-Al-silicates. One way to observe that is the production and increase of gaseous HCl, because Cl from KCl is released after the K capture.

3.2.1 Conditions

The combustion conditions were constant with temperature of 1300°C at the top of the furnace, 1200°C at the middle and 1100°C at the bottom, while the pressure inside was 1atm. The feeding rate of the fuels was kept around 1.5 kg/h and the excess oxygen at the end of the furnace around 3% in order to achieve a stoichiometric air ratio λ=1.15. Also the CO_2 levels were kept around 16.5%. O_2 and CO levels were taken into account and changes were made in the feeding rate of the fuel or the amounts of air inserted inside the furnace when disturbances in their values were observed. The total flue gas volume was 11.5 Nm^3/h.

3.2.2 Experimental procedure

The experimental campaign was carried out over the duration of two weeks. The first week Torrefied Straw (TS) was used as fuel. While the second week the fuels were Wood Pellets (WP) and WP+0.25%KCl (WP+KCl). The aim was to examine how the HCl levels were changing with the use of additive, so separate experimental sessions were conducted for each fuel with varying amount of different additives. A list with the experimental sessions that took place is presented inTable 3-7. The table has one column for the fuel used in each session, one column for the variation of additive in g/h and one column for the kind of measurements that took place.

Table 3-7: List of experimental sessions.

Fuel	Additive	Measurement
TS	Aurora varied (0-167 g/h)	HCl in the flue gas
TS	Bentonite varied (0-92 g/h)	HCl in the flue gas
WP	Bentonite varied (0-76 g/h)	HCl in the flue gas
WP+KCl	Aurora varied (0-120 g/h)	HCl in the flue gas
WP+KCl	Bentonite varied (0-61 g/h)	HCl in the flue gas
WP+KCl	Aurora dry varied (0-223 g/h)	HCl in the flue gas
WP+KCl	No additive	HCl, Deposit and Ash
WP+KCl	Bentonite fixed (87 g/h)	HCl, Deposit and Ash

The measurements from the measuring equipment were continuously made every 10 or 20 s, depending on the equipment settings, and mainly the amounts of HCl in ppm, but also CO in ppm and O_2 in % were observed. Each session started with pure fuel combustion. When HCl concentrations increased and then stabilized for pure fuel, additive started to get inserted into the system. Increases of the belt speed by 5, 10, or 20% (depending on how big the change from the previous measurement was) were made successively every time HCl values were observed to start rising from the previous values and then stabilized again. The rotating speed of the stirring part was kept at scale (3). If an increase in belt speed was followed by no change or a decrease in HCl, which meant that the additive feeding rate went down, then the rotating speed of the stirring part was increased over (3). If again there was no increase in HCl then that meant that it couldn't get managed to feed more additive into the system, or that maximum HCl levels were achieved. Then the feeding of the additive was stopped and the rate of how fast HCl numbers decreased was observed, for a period of time from 5 to 10 minutes.

As said above, when the feeding of the additive was increased, it took time for the HCl values to increase and then finally stabilize (about 3-4 minutes from new disperser setting to HCl stabilization). The same happened when the additive feeding was stopped. This phenomenon might be because of the memorial behaviour of the measuring instruments or/and because of the remaining effect of the additive inside the furnace after some time.

Finally, there were times that the function of the system was not smooth so the experimental session had to be stopped and that the problems that appeared could be dealt with, i.e. changes in the facility, cleaning of certain crucial parts, fuel/ additive feeding, reset of the additive disperser. When the issues were dealt with the procedure continued or started over.

Ash sampling

One of the objectives of this study was to examine the fly ash behavior and chlorine chemistry. For this reason two experimental sessions at stable conditions were conducted. In the first one WP+0.25%KCl was burned and in the second one WP+0.25%KCl+5.8%Bentonite was burned. For both cases probe sampling took place for about 2 and 1 hour respectively. The ceramic sampling probes were weighted before the session and then placed on top of the vertically adjustable ceramic tube at the centerline of the furnace, at 1.5 m from the bottom. After the sampling period ended, the probes were carefully extracted, let to cool and weighted again. The difference between the final and the initial weight of the ceramic probes in respect to the sampling time, gave the deposition rate. For the first case, after the ash deposition, ash sampling took place also through the vertically adjustable tube for 1.5 and 2.5 m form the bottom, each for a period of half an hour. The wet ash sample was gathered at the lowest part of the tube, which is one floor lower than the facility and collected for analysis. Moreover filter ash samples for both cases were collected for analysis.

The idea of WP + KCl fuel

In the case of torrefied straw, because of its high Cl content, the minimum (when combusting pure fuel) and the maximum HCl values were high enough for examining and also their difference was great, for both aurora and bentonite as additives. On the other hand, in the case of wood pellets, because of its lower Cl content, both minimum and maximum HCl values were low, so the effect of additive couldn't be examined properly. This led to the idea of mixing WP with KCl and increasing its Cl content as high as 6 times the initial one. This way the highest HCl levels among all the experimental sessions were expected and finally achieved. The mixing procedure is described below. Enough batches of 2 or 2.5 kg WP+KCl were made in order to last the experimental needs. For each batch the necessary amount of KCl was calculated, and then KCl in fine salt form was diluted inside distilled water. The water amount was also calculated so that the solution created was not saturated and then the solu-

tion was put into a spray bottle. Next, an amount of WP was laid on a surface, spayed with a share of the solution and then mixed sufficiently. The same procedure was repeated until the fuel on the surface had the weight of 2 or 2.5 kg plus the weight of calculated water + KCl solution. When every batch was ready, a sample was taken in order to get analyzed later. The mean Cl_{WP+KCl}/Cl_{WP} ratios achieved from the two samples can be seen in Table 3-3. The ratios are not 6 as it was planned to be, and this might be because some of the solution evaporated during the process. But it is shown that the mixing was good enough for the experimental needs, that were to greatly increase the Cl content for WP.

The idea of Aurora dry

For both Aurora and Bentonite the feeding rates did not increase after 60-80% belt speed of the disperser. This is partly because of the moisture and thus the high volume of the additive particles that limits their transfer potential. For this reason the thought of drying and this way condensing the Aurora additive came up, which also had much more moisture than Bentonite (Table 3-6) and could be evaporated with low temperature drying (105°C). The product was an Aurora additive with much more condensed, less agglomerating behavior inside the feeder and of course greater feeding potential.

Thermochemical simulation

Part of this study is also the theoretical examination of the effect of additives by the means of thermochemical simulation and to see how these results match the experimental ones. For this reason thermochemical software and database 'FactSage software 6.3' was used in order to process calculations for equilibrium conditions in the temperature range that prevail in the combustion chamber.

FactPS, FToxide, FTsalt and FTpulp databases were chosen for gas, liquid and solid pure components. FT Oxide-SLAGA and FT salt-SALTF has been chosen to define the liquid solution phase. The first solution represents the silicate slag system while the second represents the salt eutectics. The temperatures set for the calculation were in the range of 500 to 1500 °C, when pressure was 1 atm and the amount of combustion air was set for 1.15 air ratio. The fuel components inserted as input were H_2O (moisture), C, H, N, S, Cl, O, air (O_2 and N_2) and the oxides SiO_2, Al_2O_3, Fe_2O_3, CaO, MgO, Na_2O, K_2O and P_2O_5, all in grams. After the calculations were complete, data were extracted to excel software, properly formed and corresponding diagrams showing results of our interest were created.

Same kind of simulation took place also for the case of additive use, in order to see if the HCl values measured by FTIR came in agreement with the thermochemical calculations. The same component species were used with the difference that the common fuel and additive input components were a sum from both.

4 Results and Discussion

In this section of the thesis the results from the experimental as well the simulation part of the study are presented separately and in the order they were conducted. Description, discussion and comments are included in order to give the best explanation and have an understanding of what is shown.

4.1 Equilibrium results

Calculations were made for a wide range of temperatures from 500 to 1500 °C and mainly for the temperatures inside the furnace (1100-1300°C). Also other parameters were varied in a range of interest in order to examine their effect on ash species and deposit formation.

4.1.1 Slag Ratio

The slag ratio here is defined as:

$$SR = \frac{liquids}{liquids + solids} \quad (4\text{-}1)$$

Where liquids are the sum of all liquid components and solids the sum of all the solid components produced in these temperatures. All the components are measured in grams. The slag ratio is used to examine the slagging tendency of the two biomass fuels and see at which temperatures it is more critical. A first calculation and comparison between the slag ratios of the two fuels, for λ=1.15 and a wide temperature range (500-1500°C) is shown below (Figure 4.1, Figure 4.2).

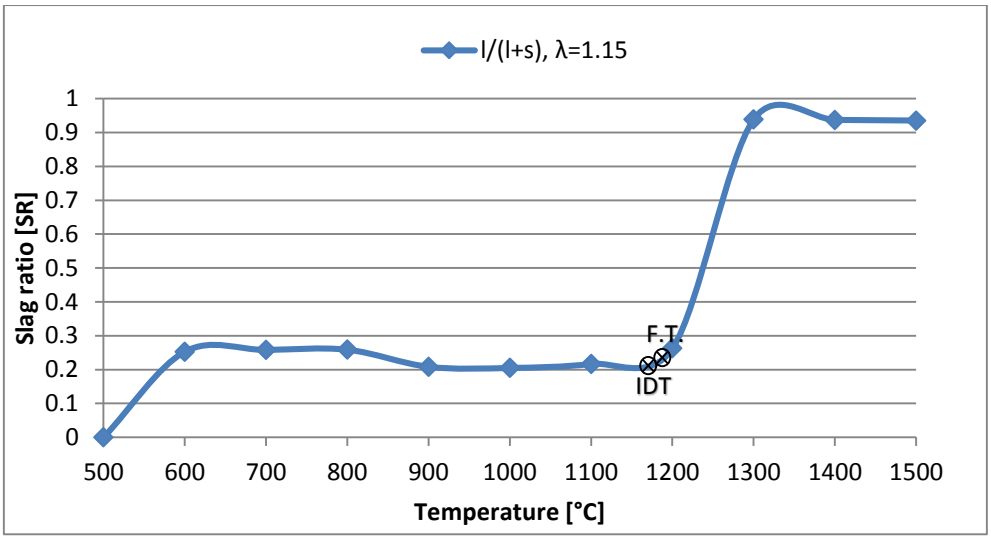

Figure 4.1: Slag ratio of Wood Pellets for varying temperature and λ=1.15.

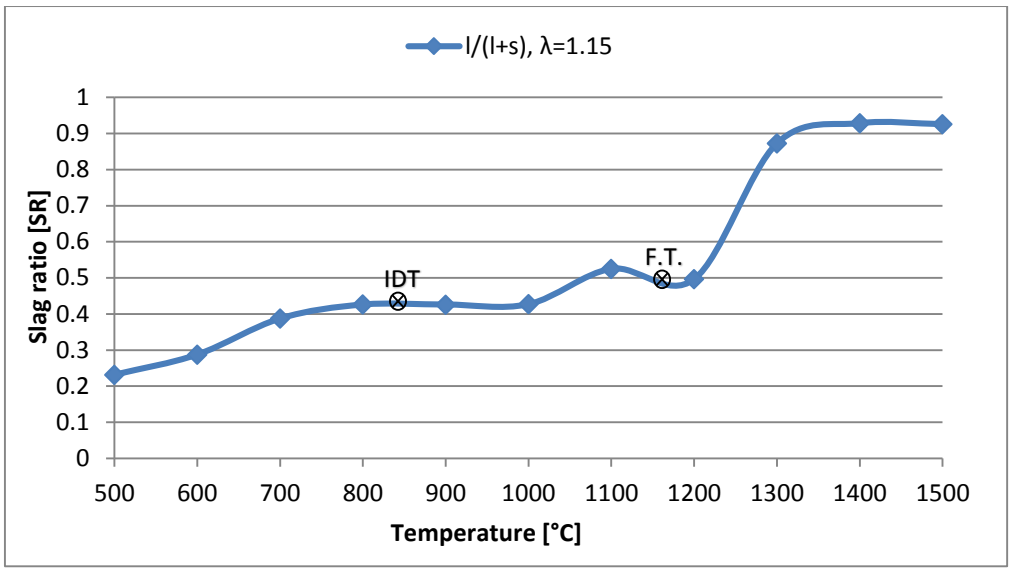

Figure 4.2: Slag ratio of Torrefied Straw for varying temperature and λ=1.15.

Initially the above equilibrium results show that as the temperature increases so do the slag ratios. This happens because with the increase of temperature the solid components decrease while the slag components increase. The comparison between the two biomass cases shows that TS has higher slag ratios in the biggest part of the examined temperature range. This happens because the ash initial deformation temperature for TS is at 840 °C, which is much lower that the ash initial deformation temperature of WP, which is at 1170 °C (Table 3-4). So the ash components of TS start melting earlier than those of WP. However in both diagrams (Figure 4.1, Figure 4.2) it can be seen that the ash fluid temperatures of TS and WP are very close, at 1160 °C and 1190 °C respectively. After these crucial temperatures, almost all the ash components go into liquid phase. So the slag ratios increase sharply over 1200 °C and at 1400 °C the slag ratios for both fuels are already over 0.9. This translates to very high risks of deposition and corrosion inside the combustion chamber because these temperatures are found there. The simulation of biomass ash behavior with the help of FactSage has been examined by various authors [61,62]. The increase of slag amount with the increase of temperature is a common finding.

The slag ratio was also calculated for different lambda (air to fuel ratio) values. Calculations for the temperature range 500-1500 °C and also for the range of air-fuel ratios λ=0.7-1.15 were made, and the results are shown below.

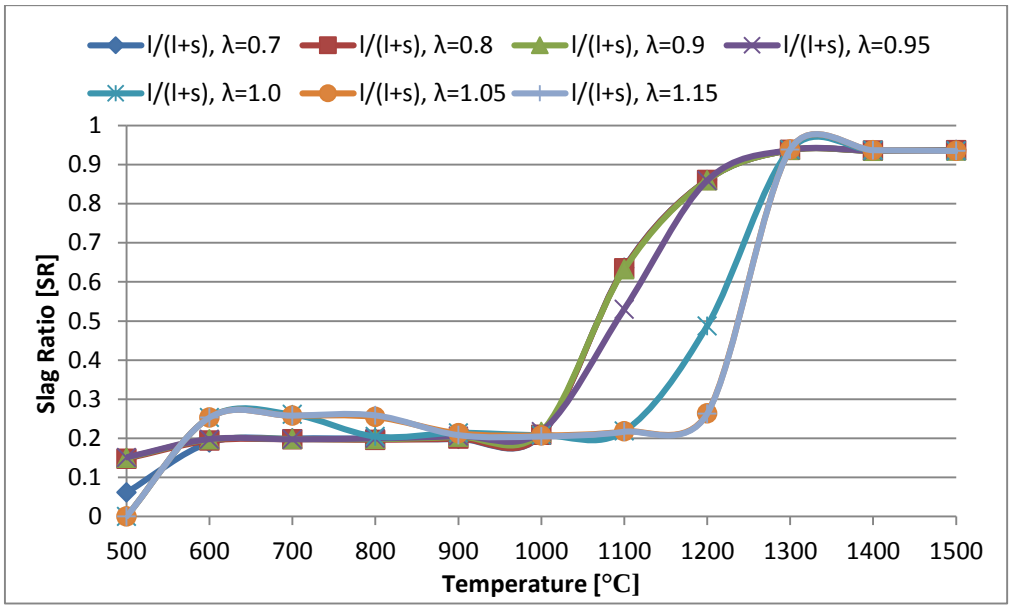

Figure 4.3: Slag ratio of Wood Pellets for varying temperature and lambda.

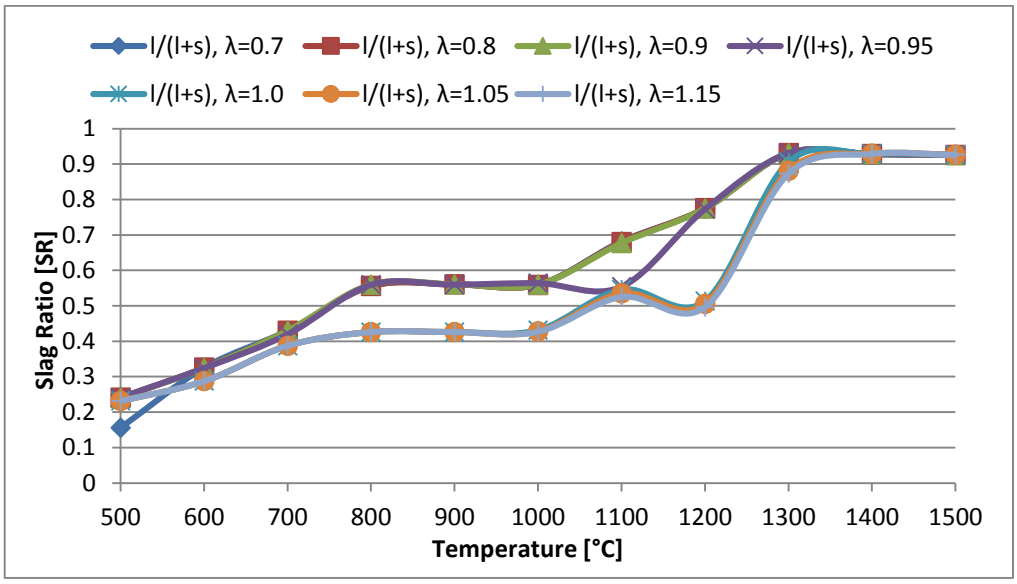

Figure 4.4: Slag ratio of Torrefied straw for varying temperature and lambda.

A first look shows that the lambda is a factor that influences the slag ratios. In the case of WP (Figure 4.3), two temperature zones where the slag formation behavior changes can be distinguished. For lower temperatures (600-900°C), as the λ increases, the slag ratio also increases. But for higher temperatures (1000-1300°C), as the λ increases, the slag ratio decreases. Also this behavior can be separated in respect to λ into 3 groups. One for lower than stoichiometric air to fuel ratio (λ<1), one for stoichiometric (λ=1) and one for higher than stoichiometric (λ>1).

In the case of TS (Figure 4.4), everywhere between 700 and 1300 °C the slag ratio behavior is similar, i.e. as the λ increases then the slag ratio decreases. In respect to λ we can separate this behavior into 2 groups. One for λ<1 add one for λ≥1.

Consequently, in high temperatures where combustion takes place, like inside our furnace, it is preferred to have higher air to fuel ratios than 1 so that the slag ratio is significantly decreased, as shown in Figure 4.3 and Figure 4.4.

4.1.2 Component production in respect to λ

As shown above the slag ratio tends to go down as the air-fuel ratio increases in high temperatures. The changes in the produced species for the temperature of 1200 °C and the variation of λ are shown here in detail and the slag ratio behavior is explained. This temperature was selected as representative for the conditions in the middle of the furnace.

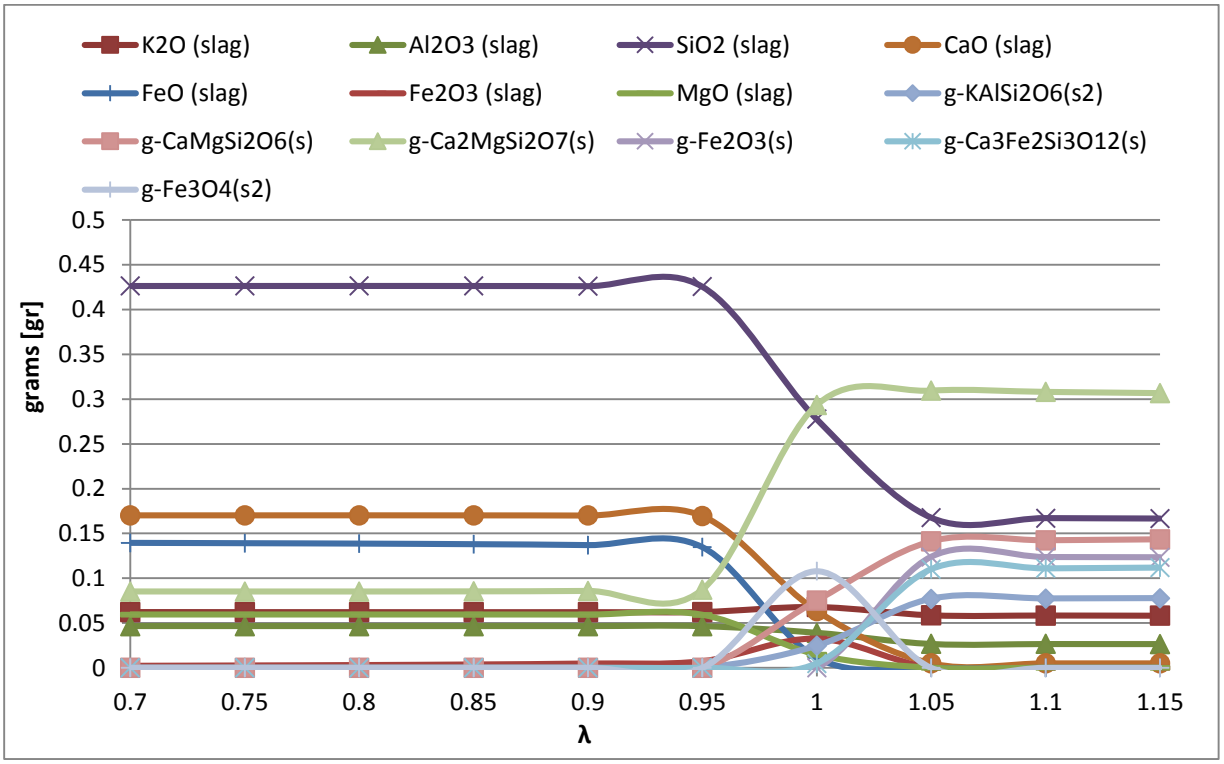

Figure 4.5: Combustion products' fluctuation of Wood Pellets for λ variation, 1200 °C.

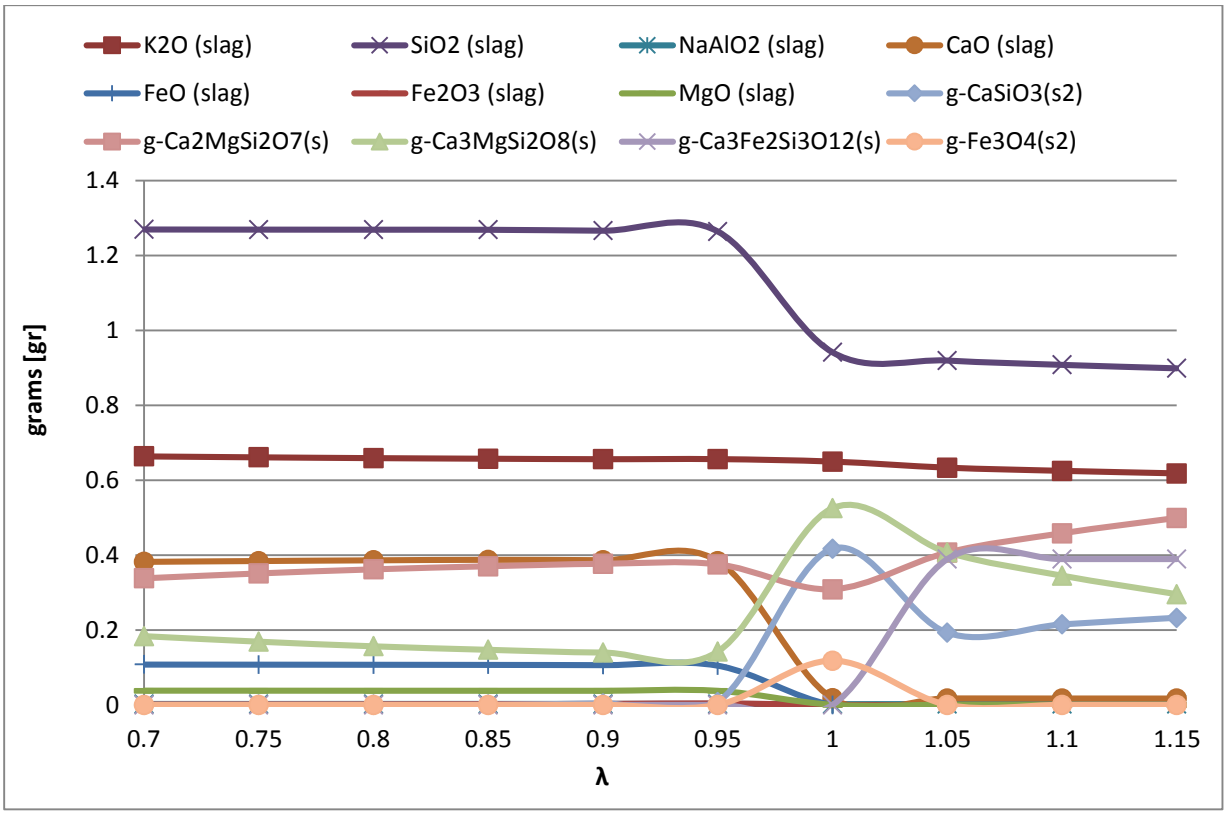

Figure 4.6: Combustion products' fluctuation of Torrefied Straw for λ variation, 1200 °C.

For both WP (Figure 4.5) and TS (Figure 4.6) the behavior of the produced species is similar. For lower λ values (0.7-0.95) slag components are mostly formed, while solid components are lower or don't exist at all. For 0.95≤λ≤1.05 there is an area where phases and amounts of components change. So while λ increases in this area, slag decreases when solids increase. Finally for higher λ (1.05-1.15) slag components are lower, while solid components are higher or start to form. In general 0.95≤λ≤1.05 is a transition range but for λ<0.95 and λ>1.05, components tend to be more stable.

For example, it can be seen in Figure 4.6 that for lower λ, Ca is found mostly as CaO in slag. But while λ increases and we move into the transition range 0.95≤λ≤1.05, CaO (slag) decreases and Ca-Mg-silicates in solid form increase or start to get formed. Near λ=1.15 the CaO in slag is really small while Ca exists only in solids.

Here needs to be mentioned the difference in amount (g) of products that can be seen between the two fuels (Figure 4.5, Figure 4.6). In the case of TS, especially for K found inside the slag, the amount of products formed is 3 times higher than in the WP case. This is primarily due to the much higher K but also the Si content of TS.

4.1.3 Potassium in WP and TS products in respect to temperature

The high slag ratios observed in 4.1.1 are caused mainly by the different potassium species. Therefore this part of equilibrium results is focused on the K behavior of the combustion products. In Figure 4.7 and Figure 4.8 it is shown how the potassium (K) moves between different products depending on a wide range of temperatures, for air-fuel ratio of 1.15.

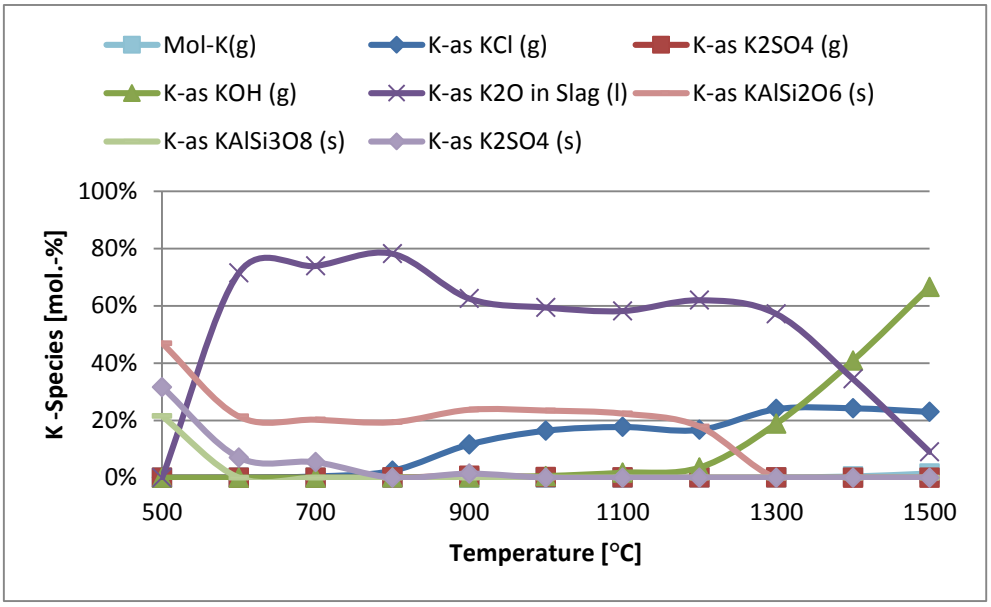

Figure 4.7: Molar ratio of potassium inside different K products of Wood Pellets, λ=1.15.

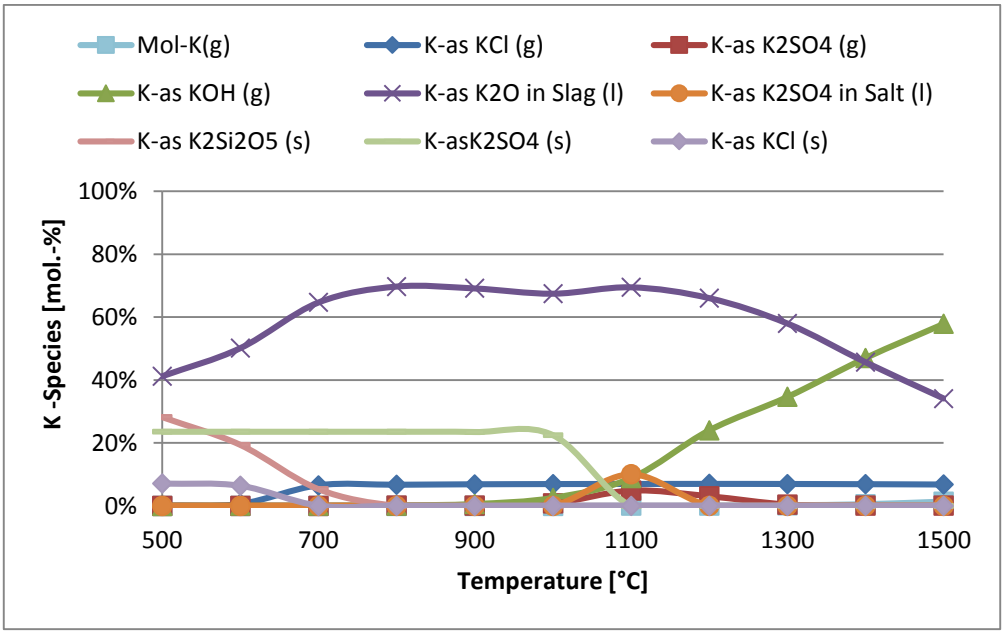

Figure 4.8: Molar ratio of potassium inside different K products of Torrefied Straw, λ=1.15.

For both fuels it is shown that there is a general tendency of potassium to exist, in the biggest part of this temperature range, primarily inside slag. The potassium in slag is represented as K2O in the FACT Sage solution database.

Starting form the highest temperature, it can be seen that K exists mainly as gaseous compounds, i.e. KOH(g) and KCl(g) (plus a small percentage of K(g)) and less in slag. As the temperature decreases, the percentage of K inside the slag increases while the great availability of KOH leads towards the formation of K-silicates and K-Al-silicates [6]. Furthermore the presence of SO_2 combined with the existing chlorides and hydroxides leads to the production of sulfates. Still, because K2SO4 has a very low vapor pressure, thermodynamically it is more stable in condensed phase (solid or liquid) [7]. Additionally it can be seen that for TS the same percentage of KCl(g) converts directly to KCl(s). This means that the amount of KCl depends exclusively on the Cl content of the fuel.. Also, as temperature decreases, this potassium molar amount does not go through liquid phase because if it was captured in slag then, Cl would get released as HCl which is an irreversible reaction and then KCl(s) wouldn't form again. However for WP, as time proceeds, the gaseous KCl reacts again with SO_2 and K_2SO_4(s) is produced, as seen in [28]. Liquid K_2SO_4 is seen only in the TS case, for 1100 °C, in salt. These findings are close to the studies of Nutalapati et al. (2007) [49], Shao (2011) [63] and Paneru et al. (2014) [7].

Another important observation is that in the TS case, K in slag stays in high levels, even at the highest and the lowest temperature of our range, because the K content of the fuel is so high that not all of it can be captured by other helpful components, i.e. Si, Al or SO_4 (sulfation).

Both cases help towards understanding that, because slag appears already at the lower temperature range, means to raise the melting temperature of potassium ash species need to be used, in order to reduce deposition problems at the operational temperatures relevant to pulverized fuel combustion.

4.1.4 Kaolinite Variation

At this point, the simulation of Kaolinite addition and its influence on the potassium species behavior is presented in Figure 4.9. The choice of Kaolinite was made because this is the main component of the alumunium silicate based additives, which are able to raise the melting temperatures of ash species. It was varied from 0 to 6.17 grams or 0 to 100% respectively and this amount was chosen after a plentiness of calculations in order to have best results, in terms of K in slag avoidance. Air to fuel ratio was set to 1.15 and temperature to 1200 °C,

because it can be found inside the combustion chamber and because, as seen in 4.1.1, after this temperature the slag ratios increase sharply.

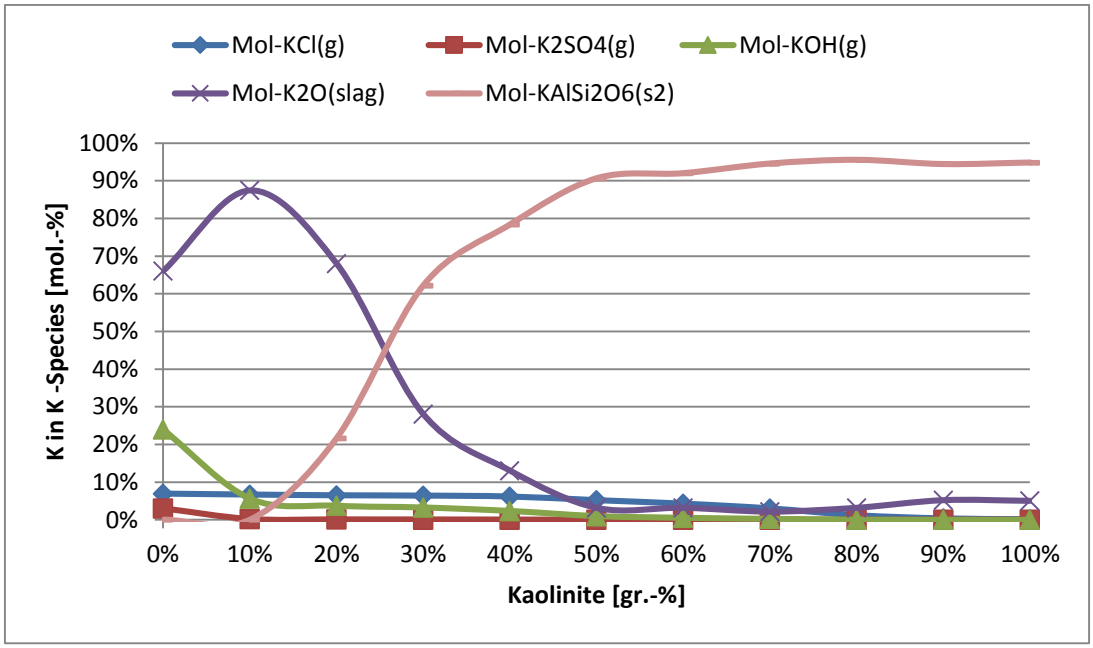

Figure 4.9: Influence of Kaolinite variation on potassium distribution. Torrefied Straw 1200 °C, λ=1.15.

For 0-10% variation, as the additive increases, Kaolinite reacts with the rest of K in gas (KOH, K_2SO_4) and almost all of potassium goes into slag. With even more insertion of kaolinite into the system, it reacts with what is left from the rest of K in gas, with KCl and mostly with K in slag and as a result potassium aluminosilicates start to form and increase accordingly [7]. Finallly for 80-100% variation, most of K exists inside potassium aluminosilicates. It is important to be observed that KCl reacts slightly for low Kaolinite variation and its reaction starts to become significant around 50% variation, after the additive has reacted with almost all of K in slag. So it seems that the reaction of aluminosilicates with KCl is not prioritized.

Next step is to examine how Cl behaves when additive is fed into the system. The simulation took place under the same temperature, air to fuel ratio and Kaolinite variation range. The results are presented in

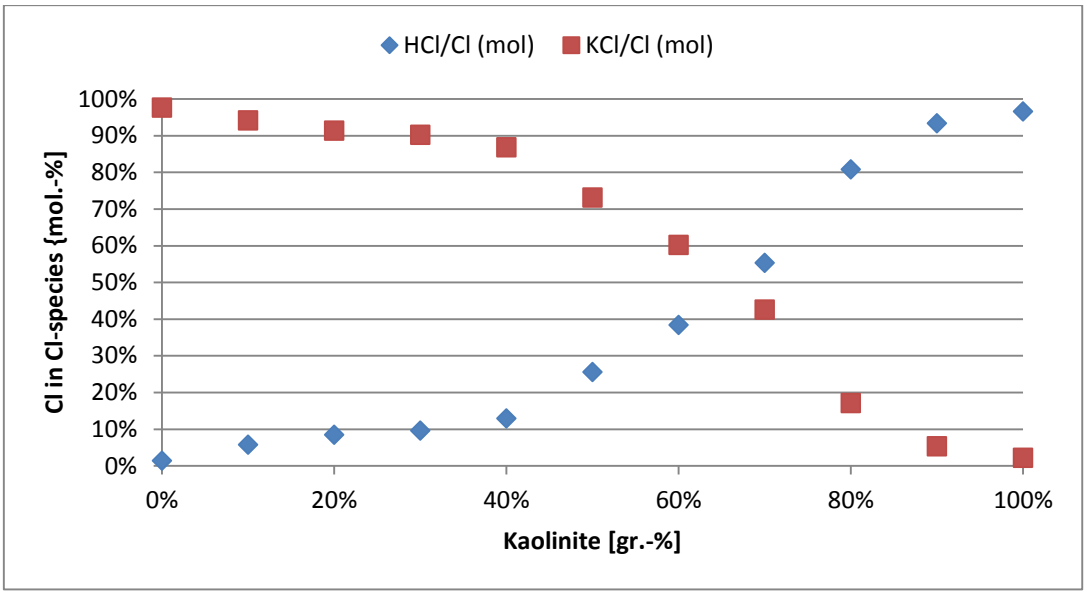

Figure 4.10: Influence of Kaolinite variation on potassium distribution. Torrefied Straw 1200 °C, λ=1.15

A first look shows that Cl exists entirely inside two components, KCl and HCl. Their behavior is opposite as the additive insertion into the system increases, because the reactions (2-14),(2-15) and (2-16) take place. For low Kaolinite variation, as said before, the reaction with KCl is very small (because the additive reacts first with the other K components), which also leads to small increase of HCl. With more input of Kaolinite the reaction rate with KCl increases because the additive starts reacting more with KCl, thus the HCl formation rate also increases. Especially after about 50% of variation, Kaolinite reacts mostly with KCl, and for maximum Kaolinite insertion into the system KCl amounts are insignificant and all the Cl content exists as gaseous HCl.

At this point, an important observation is made from both Figure 4.9 and Figure 4.10. When HCl is high, it means that the additive has reacted with KCl, but before it has reacted with K in slag so it is low. Thus high HCl concentrations might imply that potassium in slag has been deal with.

4.2 Experimental results

Combustion performance

For all experimental sessions, the exit excess O_2 and the CO_2 in flue gas were maintained around 3 vol.-% and 16.5 vol.-% respectively. Furthermore, the CO concentration is an indicator for the efficiency of the combustion process, because higher CO levels indicate incomplete combustion while high CO fluctuations can reveal some combustion instability. In our cases CO values were relatively low, mostly below 20 ppm. The emission measurements

were made in flue gas at the end of the furnace (bottom) or later in the gas pipe with the FTIR.

In Figure 4.11, the case of WP+KCl as fuel is given as an example, showing the obtained emission measurements before and after the use of additive. It is clear that for the long combustion time of only the fuel, all the different emission components are inside limits and fluctuations are not important. Also when additive is inserted into the system, the range of the emission of the different components is not changing. This means that not only each individual session was stable, but also the act of feeding additive did not influence the combustion behavior. All the other cases show a similar stability and combustion quality.

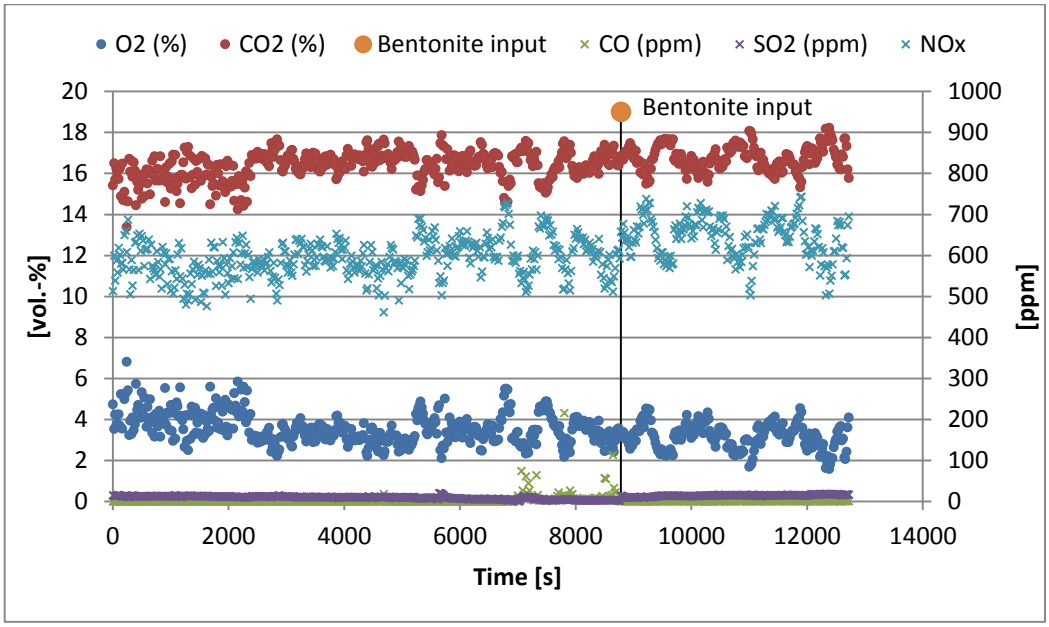

Figure 4.11: Combustion emissions for the case of WP+0.25%KCl with and without Bentonite addition.

4.2.1 Impact of additive feeding on HCl emission

The maximum theoretical HCl concentration in emission that could be achieved if all of the Cl content of the fuel reacted towards the formation of HCl is calculated with the help of the formula:

$$C_{HCl_{max}} = \frac{\frac{\gamma_{Cl}}{M_{Cl}} * \frac{M_{HCl}}{V_{mol}} * 10^6}{(\frac{\gamma_S}{M_S} + \frac{\gamma_C}{M_C} + \frac{\gamma_N}{2M_N} + \frac{0.79}{0.21}\left(\frac{\gamma_S}{M_S} + \frac{\gamma_C}{M_C} + \frac{\gamma_H}{4M_H} - \frac{\gamma_O}{2M_O}\right)) \frac{21}{21 - y_{O_2}}} \quad (4\text{-}2)$$

Where:

$C_{HCl_{max}}$ is the maximum theoretical HCl concentration in emission that could be achieved if all of the Cl content of the fuel reacted towards the formation of HCl, in mg/m^3

γ_i is the mass share of the element i in the fuel in (%)

M_i is the molar mass of the element in g/mol

V_{mol} is the molar volume of ideal gas in 1 atm pressure, 22.414 L/mol

y_{O_2} is the volume share of excess oxygen in flues gas in %

In order to compare this value with our measurements, (4-2) is converted so that the results are in ppm, in the new formula:

$$HClmax = C_{HCl_{max}} * \frac{V_{mol}}{M_{HCl}} \quad (4\text{-}3)$$

Whole experimental sessions

The whole experimental sessions for TS and WP+KCl and the additives used are displayed in Figure 4.12, Figure 4.13, Figure 4.14, Figure 4.15 and Figure 4.16. In each diagram, the effect of the additive used, on the corresponding fuel's behavior is presented, as every single HCl concentration measurement is shown through the course of time. The numbers above the diagram indicate the feeding rates of the additive in g/h, which were adjusted in the session at that time point. Also the theoretical maximum HCl concentration value is displayed as the upper limit for each fuel.

From here one when referring to HCl concentration values, the word concentration might be skipped for ease.

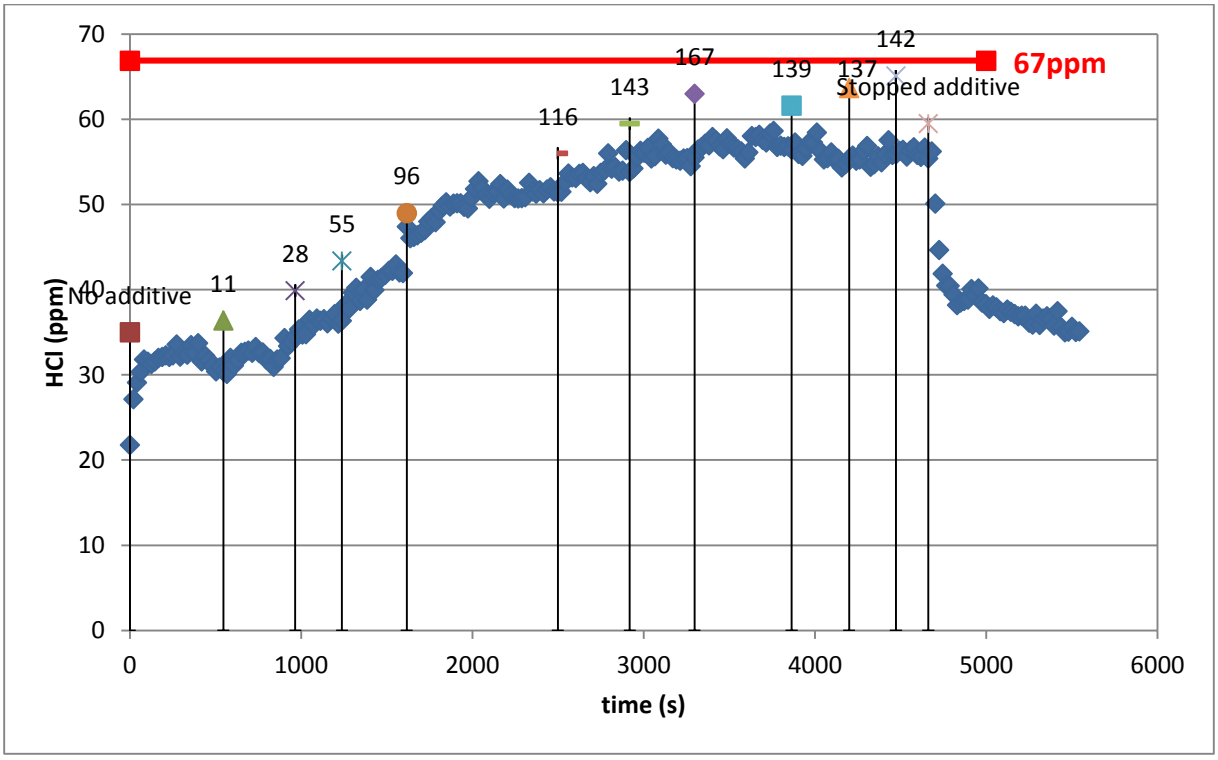

Figure 4.12: Whole Torrefied Straw Aurora session.

In Figure 4.12, the whole experimental session of TS combustion with Aurora addition in displayed. The maximum theoretical HCl value for Torrefied Straw is calculated to 67 ppm. An overall view of this image shows that the HCl emissions of pure TS begin with low values and they go up as the feeding of Aurora begins and then increases. It starts from 32.34 ppm which means that for pure fuel, 48% of Cl exists in HCl(g). Then the additive is fed into the system following the consecutive process described in 3.2.2. Finally the HCl reaches maximum values around 57.15 ppm which is close to the theoretical maximum one (66.88 ppm), when also the maximum Aurora feeding at 166.5 g/h is achieved. At this point about 85% of chlorine is released as gaseous HCl.

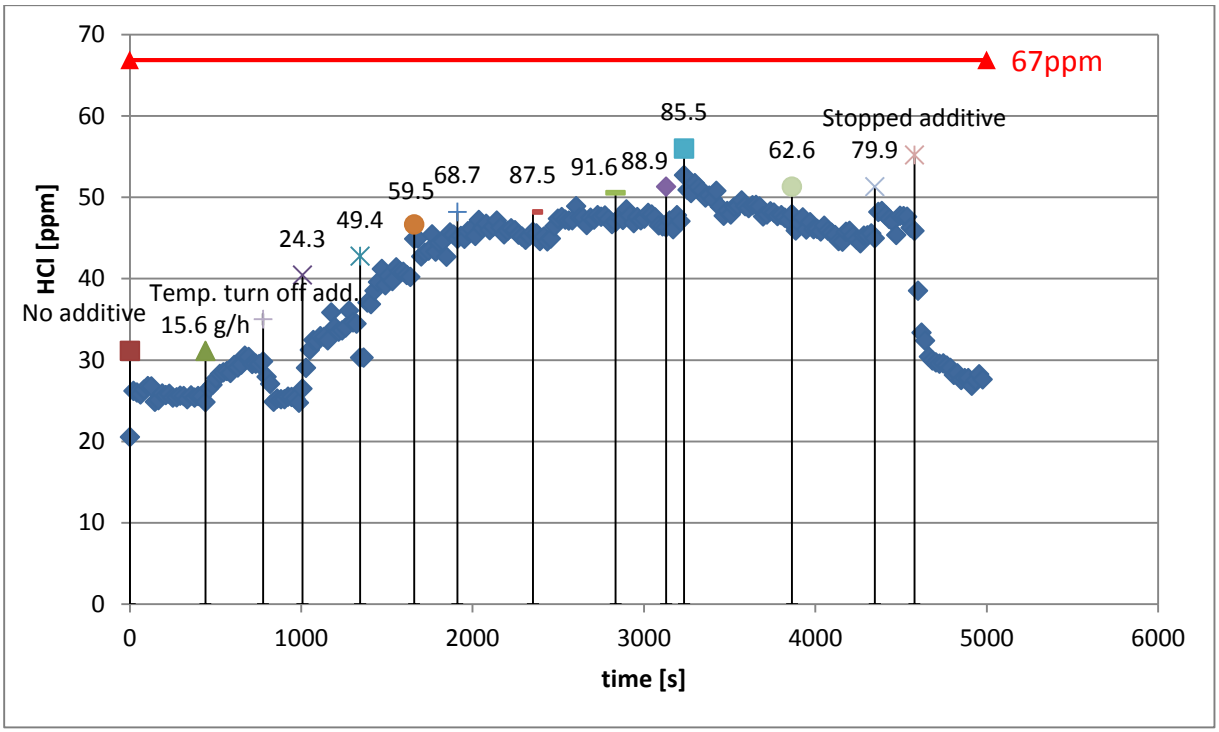

Figure 4.13: Whole Torrefied Straw Bentonite session.

In Figure 4.13, the whole experimental session of TS combustion with Bentonite addition in displayed. Similarly to the aurora case, the general impression that this images gives is that for pure fuel the HCl emissions are low and they increase with the insertion of Bentonite into the system. In this session the initial HCl levels for pure fuel where about 25.7 ppm (~38% of Cl as HCl for pure fuel). The highest measured HCl values were close to 47.5 ppm (~71% of Cl as HCl), when also having the highest Bentonite feeding rate, at 91.6 g/h. These values are close enough to the theoretical maximum HCl value of TS, but not so close as when using Aurora. This big difference will be discussed below (Figure 4.18).

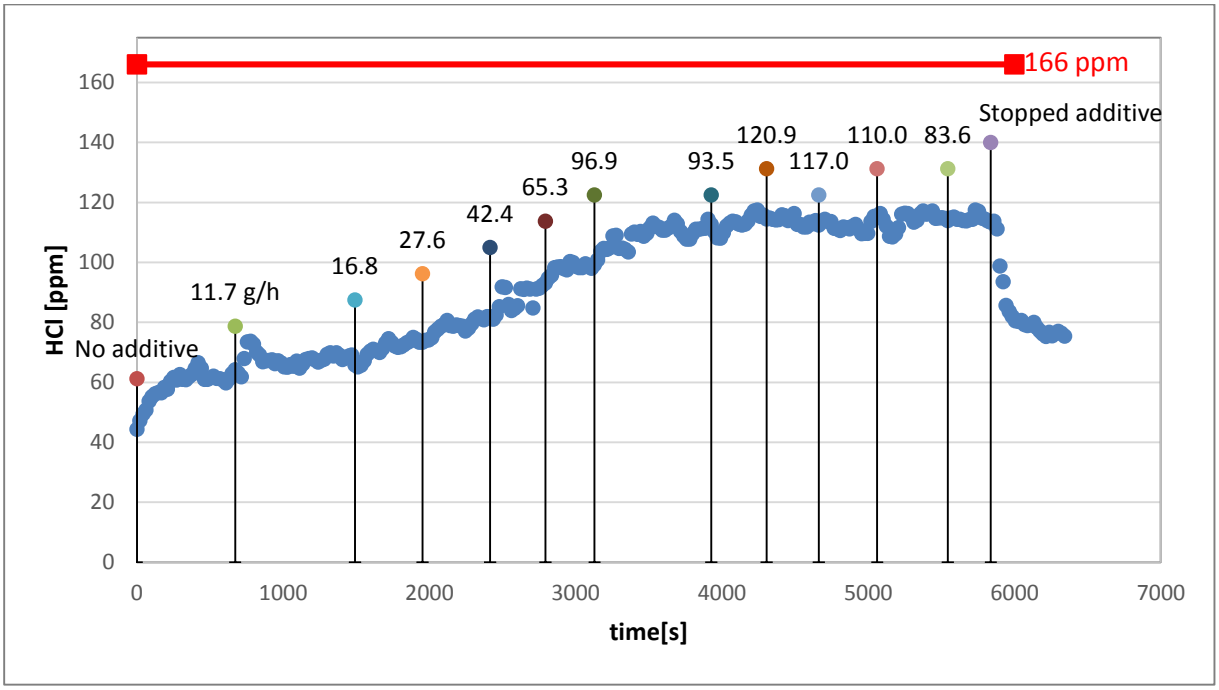

Figure 4.14: Whole Wood Pellets+KCl Aurora session.

In Figure 4.14, the whole experimental session of WP+0.25%KCl combustion with Aurora addition in displayed. Similar to the previous cases, it is clear that as the additive feeding rates change, so do also the HCl emissions. The HCl concentrations for pure fuel were around 62 ppm (~37% of Cl into HCl) and the highest HCl values were about 116.3 ppm (~70% of Cl in HCl) for 93.5 g/h aurora feeding. The highest HCl values are not close to the theoretical maximum HCl value for WP+0.25%KCl, which is 166.04 ppm.

In general the behaviour of WP+KCl with the co-feeding of Aurora case seems similar to the TS-Aurora case. Nevertheless the highest HCl values are not close to the theoretical maximum HCl value for WP+0.25%KCl, which is 166.04 ppm.

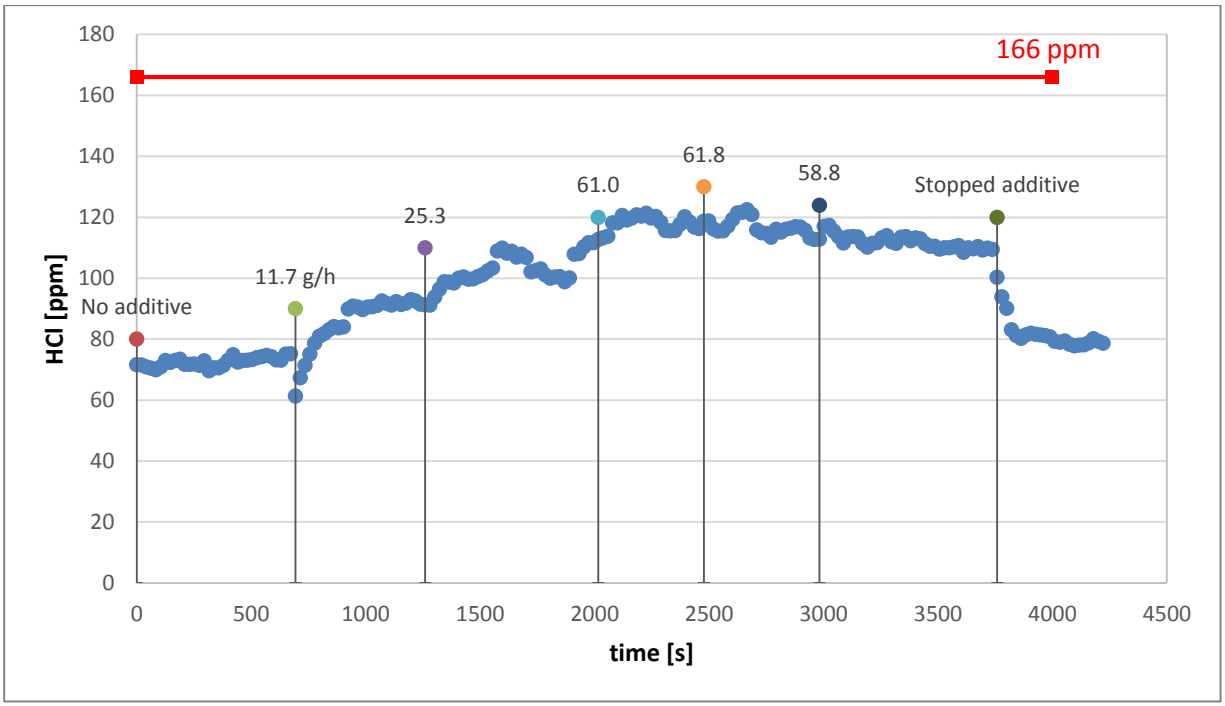

Figure 4.15: Whole Wood Pellets+KCl Bentonite session.

In Figure 4.15 the whole session of WP+KCl with Bentonite as additive is shown. A first look shows that in general the fuel responded to the use of additive and the HCl levels increased accordingly. The HCl values for pure fuel were around 75.2 ppm (~44% of Cl content in HCl). The highest HCl values were measured to be around 118.5 ppm (~71% of Cl content in HCl), for the bentonite feeding of 61 g/h. The results show that the highest HCl values measured were not very close to the theoretical maximum HCl value, which is 166.04 ppm for WP+0.25%KCl.

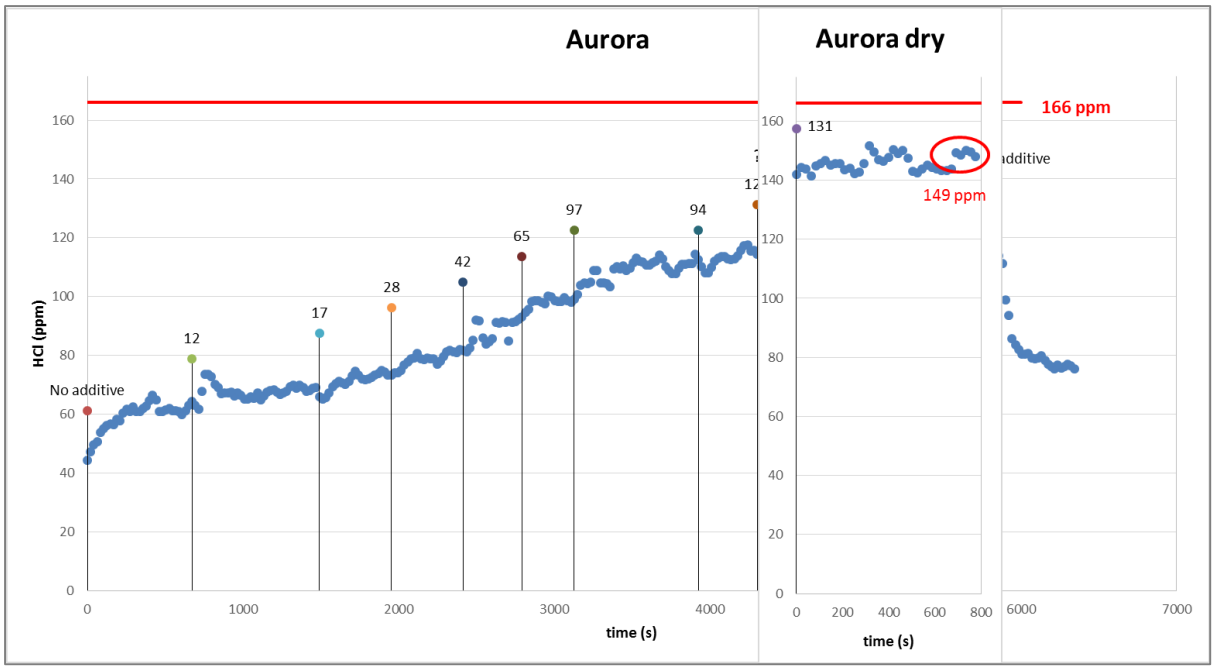

Figure 4.16: Whole Wood Pellets+KCl Aurora dry addition

Additionally, in order to feed more additive into the system and achieve higher HCl concentrations from the WP+KCl fuel combustion, the procedure described in 3.2.2 for drying Aurora took place and the attempt was succesful. As seen in Figure 4.16, as soon as it was dried, Aurora had a great impact in the system. The additive achieved higher feeding rates, and had a faster response, maybe because of its fine and dry nature which leads to larger specific surface area and less transport limitations [43], [40]. The highest HCl values observed were around 148.77 ppm (~90% of Cl content in HCl) for the additive feeding of 131.4 g/h. These values are close to the theoretical maximum HCl value for WP+0.25%KCl (166.04 ppm) and also are the highest HCl concentrations observed between all sessions.

Furthermore the experimental session for pure Wood Pellets combustion with the addition of Bentonite took place. The maximum theoretical HCl value for WP is 33 ppm. For pure fuel HCl was measured at 12.28 ppm (~37% of Cl content in HCl), while with the maximum addition of Bentonite at 77.48g/h, the increase in HCl concentrations was small. The highest value observed was around 17.5 ppm (~53% of Cl content in HCl). The whole experimental session of WP can be seen in Figure 7.26.

As we would expect, Wood Pellets flue gases seem to have lower HCl concentrations in general compared to Torrefied Straw, because of their lower Cl content, something also shown by Nordgren et al. (2010) [64]. The same way, the flue gases of Wood Pellets+KCl have the highest HCl levels between all cases, because of their much higher Cl content.

In some of the above cases, it was not possible to increase the feeding of the additive after a certain point, so the possibility of achieving higher HCl values with these fuels and additives exists. In some other cases, the measured HCl concentrations did not increase, even after the additive feeding rates seemed to keep increasing. This might mean that the additive's effect is limited after some rate of insertion into the system, or that the residence time of the particles inside the chamber (5-6 s) is not enough for the reaction to happen for the entire amount of KCl(g) [40], or that some additive feedings measured in high belt speeds were not very precise. The matter could be further investigated.

After the all the cases were presented, it can be stated that the course of the sessions went as expected. No important fluctuations were observed and both Aurora's and Bentonite's response were fast, when thinking about long hours combustion sessions. Furthermore, it was possible to show that the use of additives, when combusting biomass, has an impact on HCl concentrations. The effect of additives was high, since for both TS and WP+KCl the highest measured HCl values reached close to the maximum theoretical one for each fuel. This happened normally when the highest additive feeding rate was achieved.

The high HCl concentrations translate into dealing with potassium in slag and also prevention of Cl from going into ash. These experimental data come in agreement with the equilibrium calculation presented before since the input of additive into the system increases the HCl concentrations. Also these findings come to verify the assumptions concluded in the previous studies of Jensen et al. (2013) [35], Wu et al. (2011) [43] and Aho (2001) [65], which say that Cl must have been released as gaseous HCl, because after the addition of aluminosilicates, the Cl content found in biomass ashes was found much lower compared to no addition.

HCl mean values for the corresponding dry additive feeding rates

In Figure 4.17 the results from four different sessions are presented. Torrefied Straw and Wood Pelltes+0.25%KCl with the addition of Aurora (A) and Bentonite (B) each. This image is a summary of their whole experimental sessions. The HCl concentration values (ppm) are grouped here together in HCl mean concentration values (ppm). The HCl mean values (ppm) is an average of a range of data. This range was selected manually for HCl values (ppm) that seem to have stabilized after an additive feeding rate was set (g/h), and before it was changed to a new additive feeding rate (g/h). Every HCl mean concentration value (ppm) corresponds to the former additive feeding rate (g/h). The additive feeding rate values are presented here after being dried from their initial values. So the comparison between the additives is without moisture and only their useful part is taken under consideration. HCl

mean values until the highest one calculated are presented only. Also the theoretical maximum HCl value is displayed as the upper limit for each fuel.

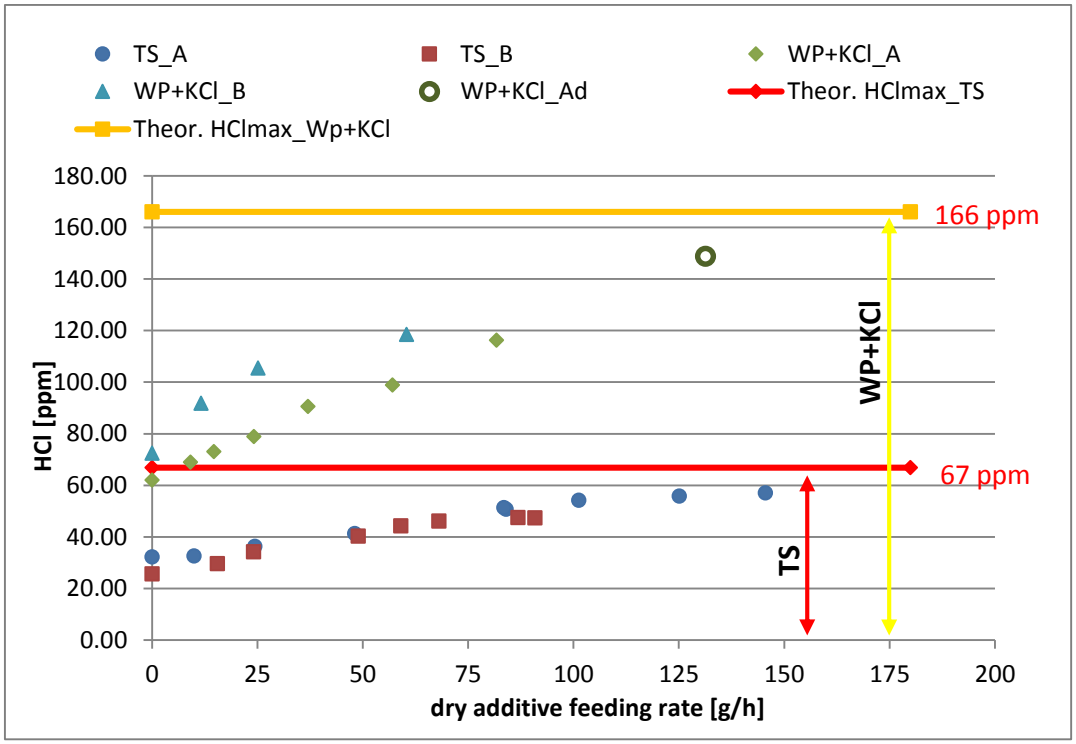

Figure 4.17: HCl mean values for their corresponding additive feeding rates – TS and WP+KCl cases.

This image makes easier to see how the variation of additives influences the HCl concentrations. As the additive feeding rates are increased successively, so do the HCl concentrations, in all cases. So different results can be achieved with different input of additive into the system.

Furthermore, it can be seen that the areas with HCl values for the two fuels (and their A, B cases) do not meet. The initial HCl values, for pure fuel (additive 0 g/h) and the highest HCl values, between the two fuels have big differences. This is of course because of the different Cl content of the fuels (chlorine in WP+0.25%KCl is more than 2 times higher than in TS).

Both additives' effect seems to be similar on both fuels regarding HCl. However there are some small differences. Initially it is shown that Aurora was managed to be fed until higher feeding rates than Bentonite (Ad stands for dried Aurora and is the extension of the WP+KCl_A case). The feeding of higher additive amounts gave an advantage and led into higher effect and HCl values. In the TS case, the two series of HCl values seem to follow the same line. But in the WP+KCl case, for the same additive feeding rates, the HCl increase seems to be happening more sharply with Bentonite than with Aurora. These differences

between the additives's effect might be linked to their physical characteristics and the surface reaction kinetics, as suggested by Wu et al. (2011) [43].

However, it seems that there is a fluctuation in the measurements of FTIR. The measurements for pure fuels, between the two additive sessions for each fuel, do not give the same mean HCl values. One the one hand, in the case of TS, the HCl value of pure fuel is higher in the session for Aurora. On the other hand, in the WP+KCl cases, the first measurements, for pure fuel give different mean HCl values as well, but this time, they are higher for the dried Aurora case (which is not presented above but in the annex). The fluctuation range of measurements observed for FTIR is presented in Figure 4.18. The mixing of WP with KCl might be responsible for the bigger differences in the cases of WP+KCl, since the homogeneity of it is not known. It is considered possible that this difference range in HCl values for pure fuel might be the same also for the next HCl values, between the two additive cases, for the same additive feeding rates. The fact that these measurement ranges exist is important and they will be used later on.

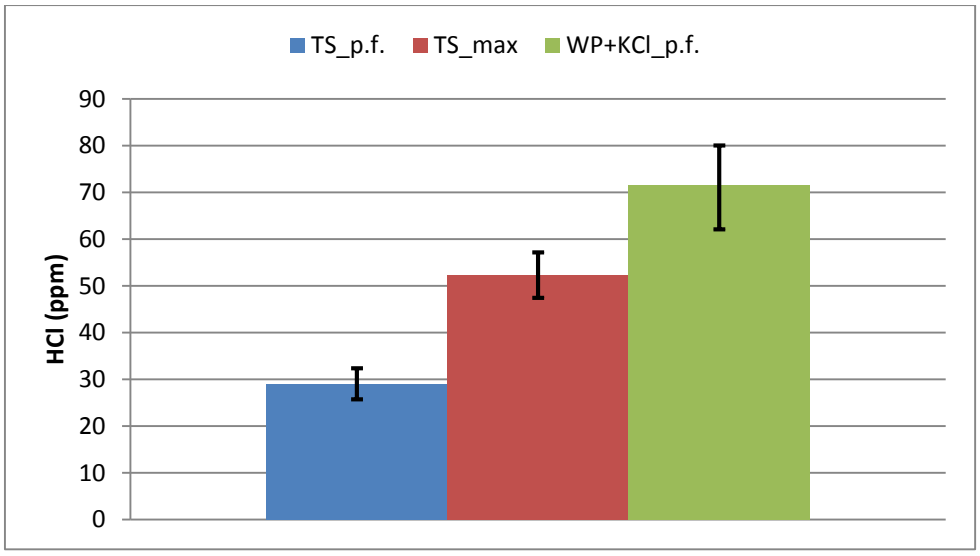

Figure 4.18: Fluctuation range for FTIR measurements.

4.2.2 Chlorine as HCl in respect to K/(Si+Al)

The components that react with the potassium of the fuel and lead to the release of HCl, are silicon and aluminum, which exist in the incoming additive, but also to a certain amount inside the fuel. For this reason the molar ratio of potassium into the fuel to the aluminum and silicate inside both the fuel and the additive is of great interest. The K/(Si+Al) molar ratios for the dried components mentioned above were calculated for dry additive feeding rates (dried at 105°C) and are presented in Figure 4.19 (the * symbol in WP+KCl_A* means that both Aurora and dried Aurora data were fused for the results presented). This image exists in order to show how the ratio behaves for different additive amounts, but also for the comparison of the two additives.

It is shown that as the additive feeding increases, the K/(Si+Al) molar ratio is decreasing. Furthermore, it is clear that for each different fuel case, Aurora and Bentonite have the same K/(Si+Al) molar ratios for the same rates of additive feeding, which is due to their similar dried composition. This could mean that the potassium related problems of the fuel may be dealt similarly by Aurora and Bentonite.

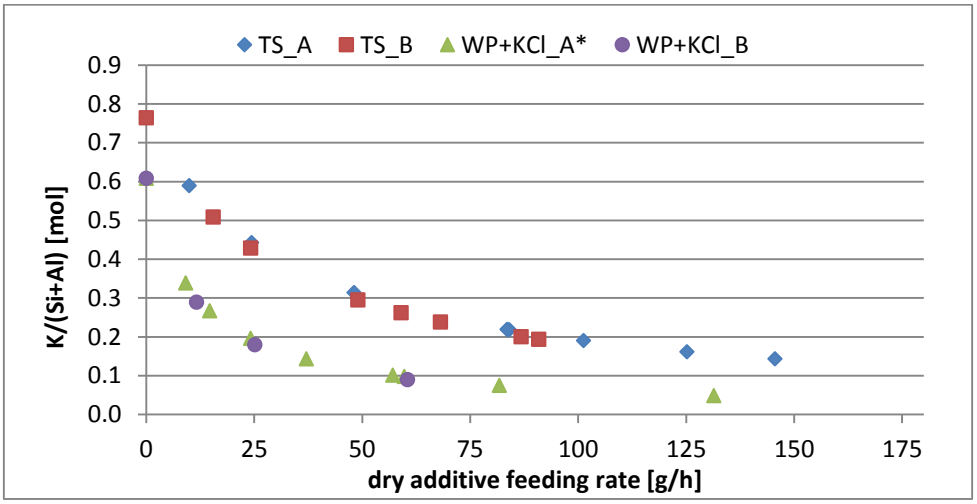

Figure 4.19: K/(Si+Al) ratios for different additive feeding rates. TS and WP+KCl cases.

It is of interest to examine what part of the total fuel chlorine content goes to the formation of HCl when additives are fed. This can also be translated to, the ratio of actual HCl formed to the theoretical maximum HCl value than can be achieved.

Torrefied Straw

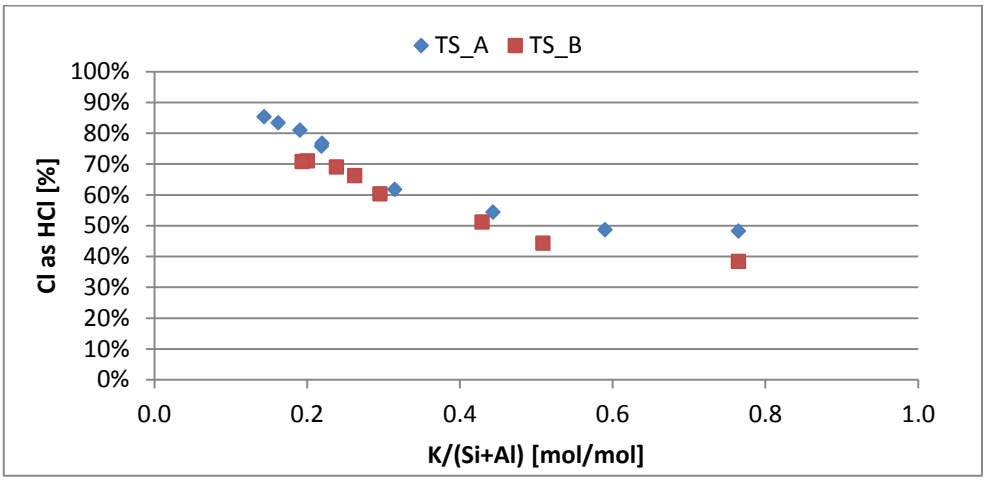

Figure 4.20: Percentage of fuel Cl that transforms into HCl in respect to K/(Si+Al) ratios, for TS.

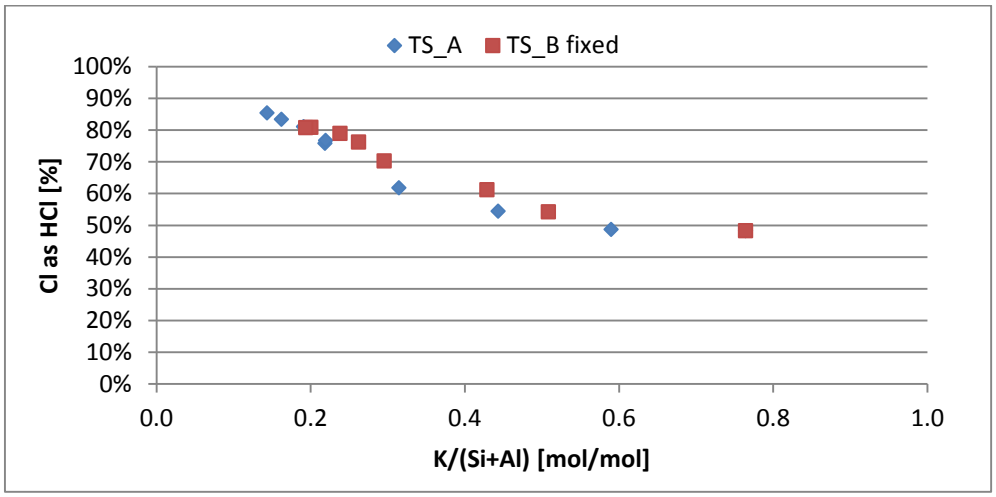

Figure 4.21: Fixed percentage of fuel Cl that transforms into HCl in respect to K/(Si+Al) ratios, for TS.

For the TS cases the HCl/HClmax (Cl as HCl) ratios were calculated for the corresponding K/(Si+Al) molar ratios presented in Figure 4.19 and the results are displayed in Figure 4.20. It is reminded that for TS the HClmax is 66.88 ppm. It is shown that for the same K/(Si+Al) ratios the existence of Cl in HCl is similar for both additives. But this comparison cannot be completely accurate since the initial pure fuel HCl levels for the two cases, as seen inFigure 4.18, are different.

For this reason, also Figure 4.21 was created, which displays the same diagrams as the previous one, but this time in the Bentonite case all the calculated HCl are increased by the dif-

ference range of pure fuel displayed in Figure 4.18 (referred as fixed). This way, the comparison between the two additives starts from the same base.

WP+KCl

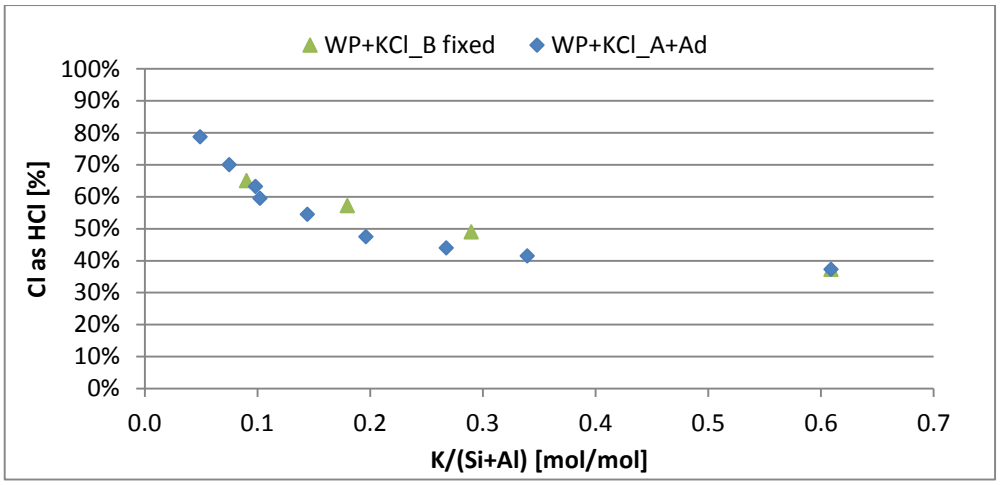

Figure 4.22: Fixed percentage of fuel Cl that transforms into HCl in respect to K/(Si+Al) ratios, for Wood Pellets+KCl.

For the WP+KCl cases the HCl/HClmax ratios were calculated for the corresponding K/(Si+Al) ratios presented in and the results are displayed in Figure 7.29. The comparison from this image cannot be completely accurate since the initial pure fuel HCl levels for the two cases are different, as shown inFigure 4.18.

Thus, for WP+KCl cases altered diagrams were created also, presented in Figure 4.22. This time the data of the Bentonite and dried Aurora sessions were changed so that all their calculated HCl values were decreased by the difference range of pure fuel displayed in Figure 4.18 (referred as fixed). Also the data of both Aurora cases were fused together, since the result representation here is for dry fuels.

After taking into consideration the FTIR measurement fluctuations and observing Figure 4.21 and Figure 4.22, the comparison between Aurora and Bentonite becomes easier. From these images it is observed that for both fuels, the effect of the two additives end their differences are similar. The use of Bentonite, leads more Cl content towards the formation of HCl than the use of Aurora, for the biggest part of K/(Si+Al) range that Aurora and Bentonite share in common. However, because Aurora was managed to be fed more, for the lowest potassium to aluminosilicate ratios, Aurora manages to lead more chlorine towards the formation of HCl. This is because the Bentonite-cases points seem to follow a more straight line, when the Aurora-cases follow a curved line (seen better in Figure 7.30, Figure 7.31). Differences in the

effect of additives and also their comparison in respect to K/(Si+Al) molar ratios, were also examined by WU et al. (2011) [43].

.

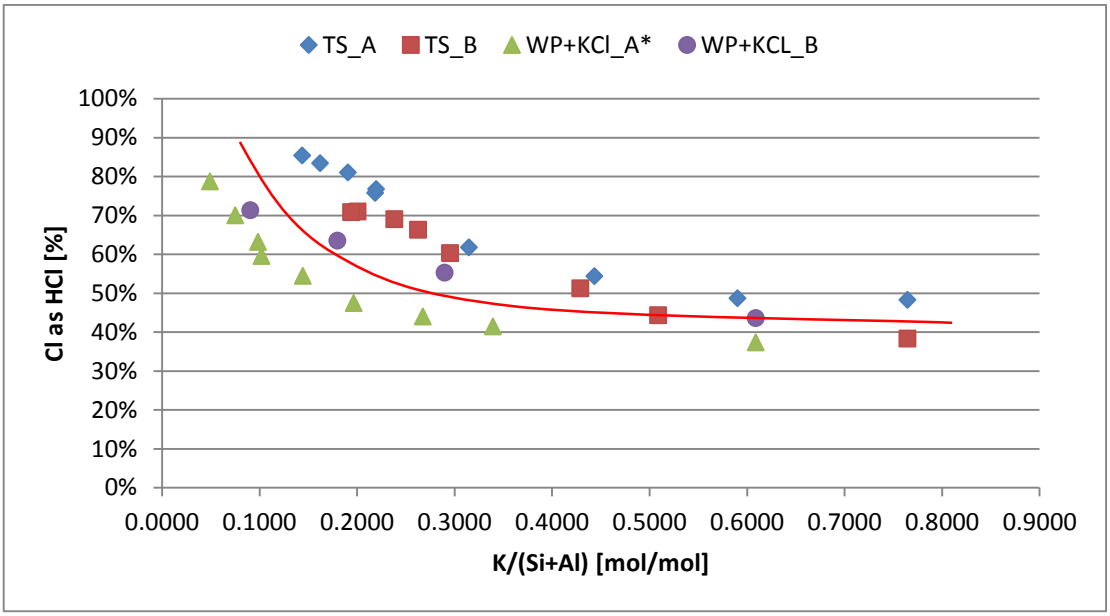

Figure 4.23: Percentage of fuel Cl that transforms into HCl in respect to K/(Si+Al) ratios, for TS and WP+KCl.

In Figure 4.23 are presented the results of Cl as HCl in relation to K/(Si+Al) molar ratios for all TS and WP+KCl cases. It is obvious that overall as K/(Si+Al) decreases, the Cl as HCl increases. This means that the more additive enters the system, the more Cl goes towards the formation of HCl and for the lowest K/(Si+Al) molar ratios, most of Cl is released as gaseous HCl.

Furthermore, when overlooking the small differences, the additives seem to have a similar effect which follows a general trend. This trend is displayed here with a line going through the result points.

From literature as mentioned before, the reaction that takes place between aluminosilicates and KCl in order to release HCl is: $2\mathrm{KCl(g)} + \mathrm{Al_2Si_2O_7} + \mathrm{H_2O} = 2\mathrm{KAlSiO_4(s)} + 2\mathrm{HCl}$ [7]. This means that for the reaction to take place, the molar ratio K/(Si+Al) has to be less than 0.5 [40]. When looking in Figure 4.23, for K/(Si+Al) just below 0.5, the increase in HCl/HClmax (Cl as HCl) is very small. This is probably because, as seen in the equilibrium calculations in 4.1.4, the additive is not available to react with KCl, but first seems to react with the rest of K in gas and K in slag. The reaction with KCl at lower than 0.5 is very small and after all the K in slag has been dealt with, then the reaction with KCl becomes dominant. The increase of Cl to HCl becomes sharper, around the K/(Si+Al) ratio of 0.3 and is dominant around the ratio of 0.2. So it could be said that, for K/(Si+Al) molar ratios greater than 0.5, the additive reacts

mostly with the rest of K in gas (KOH, K_2SO_4), for ratios between 0.5 and 0.3 it reacts mostly with K in slag and for ratios lower than 0.3 it reacts mostly with KCl(g).

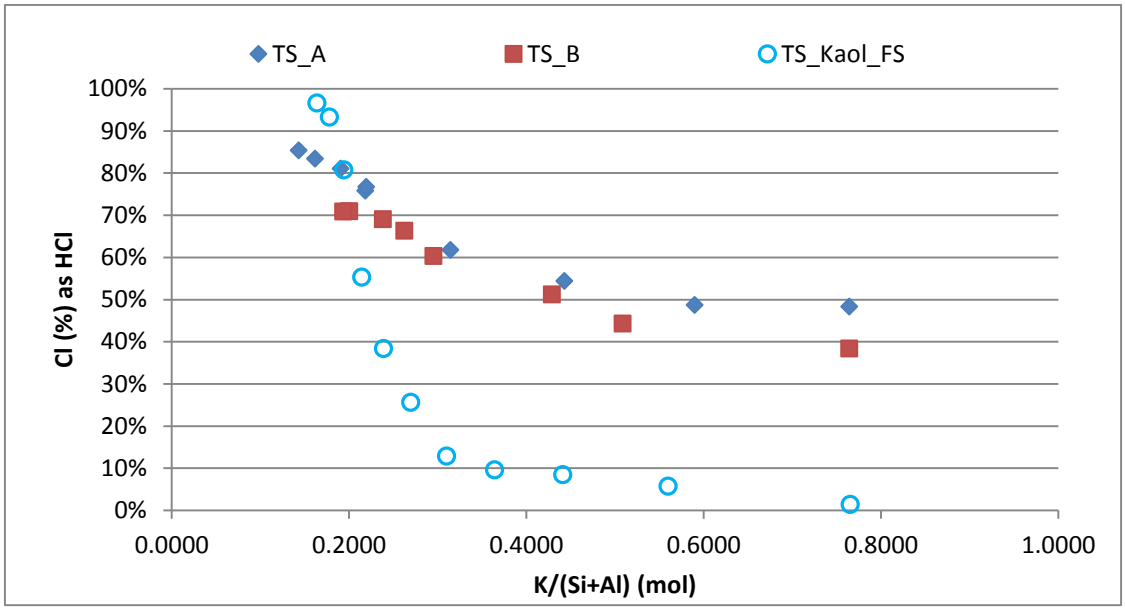

Figure 4.24: Percentage of fuel Cl that transforms into HCl in respect to K/(Si+Al) ratios, comparison of TS experimental and FactSage results for 1200°C

The Figure 4.24 presents the comparison of Cl as HCl [%] for the experimental results of TS and the equilibrium calculation of TS. It should be noted that the measurements took place at 200 °C temperature, when the FactSage results are equilibrium output at 1200 °C. For high K/(Si+Al) molar ratios, the trends are comparable but still the differences between experimental and equilibrium results are big. This happens probably because as the temperature of measurement location is 200 °C, the impact of sulfation mechanism on HCl (2-12) is accounted. On the other hand, the equilibrium calculation at 1200 °C does not take this mechanism under consideration, since it is happening at lower temperatures (2.6). However, the interaction between the alkali species and the aluminosilicates is expected to take place in temperatures as inside the combustion chamber. So 1200 °C for the equilibrium calculations is used. At K/(Si+Al) molar ratios lower than 0.3, much more additive is entering the system and it starts reacting more with KCl as stated before. So Cl as HCl [%] increases. At this area, the measured and equilibrium results come closer, probably because the increase in HCl is mostly influenced by the additive increase.

4.2.3 Chlorine content in ash

The filter ash samples obtained from the sampling experimental sessions for pure WP+KCl and WP+KCl+Bentonite, were given to the lab for analysis. In Figure 4.25 are shown, the Cl content of the filter ash samples presented from the analysis, as well as the maximum theoretical Cl content, that would exist in ash if all of the chlorine of the fuel stayed there.

In the case, that no additive was fed into the system, it can be seen that 88% of the total Cl content ends up in ash, while only the rest 12% is missing. This absent part of chlorine is most probably going towards the formation of HCl. On the other hand, in the case of bentonite feeding, the chlorine content in ash is decreased to only 9% of the total Cl content expected in the pure WP+KCl case. This means that the biggest part of Cl was released as HCl, something proposed in various studies [29,35,65]. To talk in other terms, the Cl content of ash in the case without additive is as high as 10 times the chlorine content in the case with additive. The obvious conclusion made from this comparison is that additive use is very effective into leading chlorine towards the formation of HCl, through the reaction of aluminosilicates with KCl. This way the chlorine content of ash gets vastly reduced and the risk of alkali related corrosion is decreased.

However, the mean HCl value of the whole pure WP+0.25%KCl session was 57.59 ppm and the theoretical maximum HCl value for WP+0.25%KCl is 166.04ppm. This translates into that, 35% of Cl appears to react into HCl, much more than it was expected from the filter ash sample analysis. One possible explanation for this big deviation is that, the HCl measurements took place before the filter, which might give as a result higher HCl values. Another reason is maybe because some other components, that were expected to be found in ash, left the furnace in gaseous form. So this increases the Cl content. Furthermore, another possible reason is that, some Cl species might tend to stay inside the filter and so filter ash has increased Cl content. Further investigation on the matter is advised.

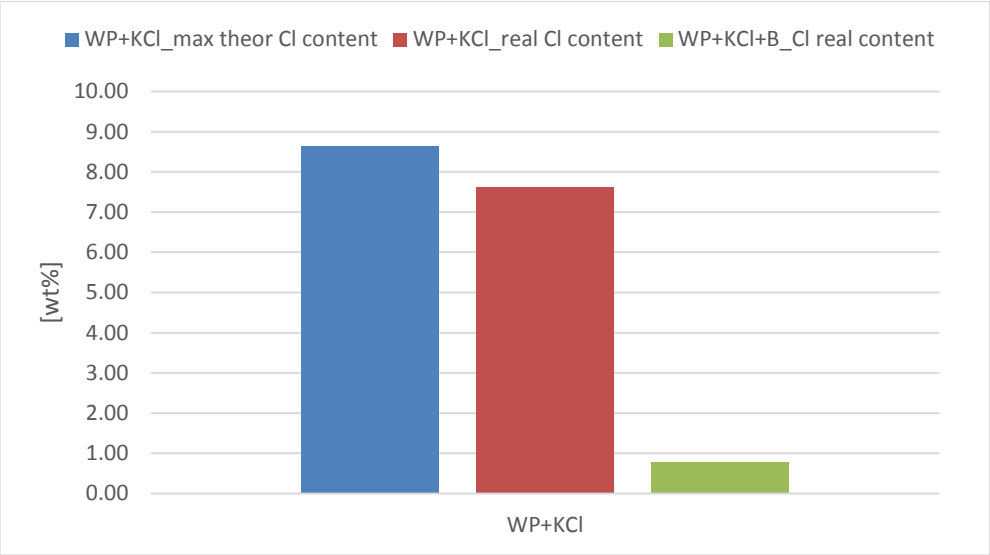

Figure 4.25: Cl content found in filter ash in comparison with maximum theoretical content that could exist, for Wood Pellets+KCl.

4.2.4 Ash deposition rates

The ash deposition tests on the ceramic probes took place for WP+0.25%KCl, with and without the feeding of Bentonite additive and lasted 70 and 123 minutes respectively. The ash deposition rates were calculated as the weight difference of the probes, after and before the tests, divided by the period of time that the deposition lasted. The rates are presented in Figure 4.26.

The deposition rate in the case additive was used is higher than the case without additive. With a first look, these results do not meet with the theory which says that, alumino-silicate additives increase the ash melting temperatures and lead towards the formation of less sticky ash components (K-Al-silicates instead of K-silicates) and thus decrease the slagging and deposition tendency. However, in the case of additive use, the input of additional ash components in big amounts has to be taken into serious consideration. Compared to the pure fuel case, much more ash creation potential exists during combustion. This is the reason of the higher ash deposition rate in the plus additive session. Similar findings were shown by Tobiasen et al. (2007) [40] and Wu et al. (2011) [43].

Analysis of the deposit needs to be done in order to examine its nature and properties. In any case, this was an experimental session of secondary importance, so the details can be further investigated later. The aim was to see how the combustion under stable conditions behaves, with and without additive and also to confirm the deposit tendency of the biomass.

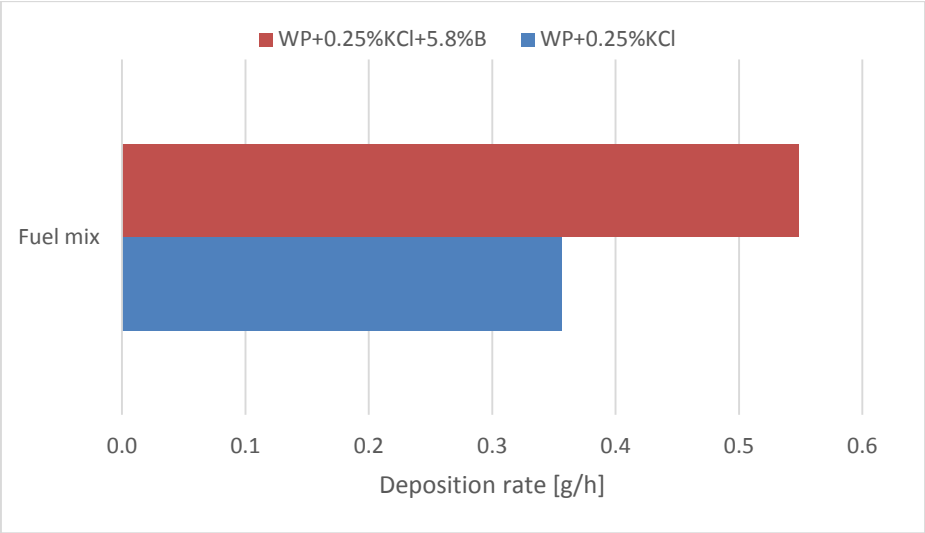

Figure 4.26: Ash deposition rates for Wood Pellets+KCl, with and without bentonite feeding.

5 Conclusion

The aim of this study was to evaluate the influence of aluminium-silicate based additives on the formation of molten deposit and condensation of alkali salts on cool boiler surfaces. The ash behaviour of two biomass fuels (Torrefied Straw and Wood pellets) was simulated in the thermochemical software and database 'FactSage 6.3', with and without the variation of additive. Combustion experiments were carried out in 20kW$_{th}$ atmospheric drop tube furnace BTS of the IFK facility, with the combustion of Torrefied Straw, Wood Pellets and chlorine enriched Wood Pellets (by premixing KCl) and the variation of Aurora and Bentonite as additives. The experiments were focused on evaluating the behaviour of chlorine.

Equilibrium calculation results show that for both biomass fuels slag ratio increases with the increase in temperature. This increase is very sharp for temperatures over the fluid temperature of ash, as obtained from ash fusion tests. Additionally, the slag ratio is also influenced by the air to fuel ratio. In general as λ increases the slag ratios decrease. Moreover, the results showed that biomass slag formation is led primarily by its high potassium content. Potassium exists in gaseous species in very high temperatures and moves towards solid species in low temperatures, but most of the potassium content exists always in slag. In addition, it was observed that the amounts of KCl formed depend exclusively on the Cl content of the fuel. The highest the K content, primarily, and also the Si content of the fuel are, the biggest amounts of slag are produced. Therefore the amounts of slag for TS were higher than for WP and also TS has much higher slagging potential than WP. Finally kaolinite was shown to reduce the slag and also lead Cl out of KCl.

The experimental results showed that the input of additive does not disturb the stable conditions of the combustion. It was clear that the additive does have an influence on Cl behaviour, which can be seen in the changes of HCl concentrations. The response on the HCl concentrations was fast when the additive was varied or when it was stopped. As the additive entering the system increased, so did HCl, until it reached a certain level close to the maximum theoretical value. This consequently meant that also the respective amount of Cl got out of KCl. Furthermore, it was shown that the molar ratio of K/(Al+Si) influences the percentage of total Cl content that forms into HCl, This molar ratio has to be less than 0.5 in order to have positive results. In addition, the effects of the two additives seem follow a similar trend. However, bentonite showed to have slightly higher effect for lower feeding rates. Finally, the ash sampling tests confirmed that with the presence of additive, chlorine is restrained from KCl and thus is restricted from going to ash.

The equilibrium and experimental results are comparable in the entire range of additive variation, but converge more with increased additive input, where the reaction mechanism between the aluminosilicates and the KCl is more dominant. Both conclude that the use of additive takes Cl out of KCl and forms it into gaseous HCl.

In order to understand more clearly the interaction of additives with KCl, the investigation of the HCl and additive relation with the help of HCl measurements inside the furnace is proposed, since at temperatures over 1000 °C, the sulfation mechanism does not have an impact on HCl formation.

6 References

[1] Unitated States Enviromental Protection Agency. Climate Change: Basic Information. [May 08, 2015]; Available from: http://www.epa.gov/climatechange/basics/.

[2] Netherlands Environmental Assessment Agency PBL. IPCC WGI AR5 Chapter Template.

[3] International Energy Agency. World Energy Outlook 2014, Executive Summary.

[4] gsr2014_full report_low res 2014.

[5] Markus Broström. Aspects of alkali chloride chemistry on deposit formation and high temperature corrosion in biomass and waste fired boilers 2010.

[6] Boström D, Skoglund N, Grimm A, Boman C, Öhman M, Broström M et al. Ash Transformation Chemistry during Combustion of Biomass. Energy Fuels 2012;26(1):85–93.

[7] Manoj Paneru, Selahattin Babat, Jörg Maier, Günter Scheffknecht. Role of potassium in deposit formation during wood pellets combustion. 25th Impacts of Fuel Quality on Power Production Conference 2014.

[8] Ivarsson E. Smälttemperaturen hos halmaskor med respektive utan tillsatsmedel: Laboratoriestudier och dataanalyser = Smelting temperatures of straw ashes with and without additives laboratory tests and computer analyses. Lund: Sveriges lantbruksuniversitet, Institutionen för lantbrukets byggnadsteknik, Avdelningen för jordbrukets byggnads- och klimatteknik; 1988.

[9] Wang L, Hustad JE, Skreiberg Ø, Skjevrak G, Grønli M. A Critical Review on Additives to Reduce Ash Related Operation Problems in Biomass Combustion Applications. Energy Procedia 2012;20:20–9.

[10] Öhman M, Nordin A. The Role of Kaolin in Prevention of Bed Agglomeration during Fluidized Bed Combustion of Biomass Fuels. Energy Fuels 2000;14(3):618–24.

[11] Chandrasekaran SR, Hopke PK, Rector L, Allen G, Lin L. Chemical Composition of Wood Chips and Wood Pellets. Energy Fuels 2012;26(8):4932–7.

[12] Miller SF, Miller BG. The occurrence of inorganic elements in various biofuels and its effect on ash chemistry and behavior and use in combustion products. Fuel Processing Technology 2007;88(11-12):1155–64.

[13] Grammelis Panagiotis. Solid biofuels for energy: A Lower Greenhouse Gas Alternative: Springer-Verlag London Limited 2011; 2011.

[14] van der Stelt M, Gerhauser H, Kiel J, Ptasinski KJ. Biomass upgrading by torrefaction for the production of biofuels: A review. Biomass and Bioenergy 2011.

[15] BERGMAN. Torrefaction for biomass co-firing in existing coal-fired power stations ECN-I--05-000 2005.

[16] D. Tito Ferro, V. Vigouroux A. Grimm and R. Zanzi. Torrefaction of agricultural and forest residues.

[17] Himmel M, Vinzant T, Bower S, Jechura J. BSCL Use Plan: Solving Biomass Recalcitrance; 2005.

[18] Analysis LT. Simultaneous Thermal Analysis; Available from: http://www.linseis.com/en/our-products/simultaneous-thermogravimetry/.

[19] Stelios Arvelakis, Peter Arendt Jensen, Kim Dam-Johansen. Simultaneous Thermal Analysis (STA) on Ash from High-Alkali Biomass 2004.

[20] Arvelakis S, Folkedahl B, Dam-Johansen K, Hurley J. Studying the Melting Behavior of Coal, Biomass, and Coal/Biomass Ash Using Viscosity and Heated Stage XRD Data. Energy Fuels 2006;20(3):1329–40.

[21] High Temperature Viscometers.

[22] Werkelin J, Skrifvars B, Zevenhoven M, Holmbom B, Hupa M. Chemical forms of ash-forming elements in woody biomass fuels. Fuel 2010;89(2):481–93.

[23] van Lith SC, Alonso-Ramírez V, Jensen PA, Frandsen FJ, Glarborg P. Release to the Gas Phase of Inorganic Elements during Wood Combustion. Part 1: Development and Evaluation of Quantification Methods: Energy & Fuels. Energy Fuels 2006;20(3):964–78.

[24] Frandsen FJ, van Lith SC, Korbee R, Yrjas P, Backman R, Obernberger I et al. Quantification of the release of inorganic elements from biofuels. Fuel Processing Technology 2007;88(11-12):1118–28.

[25] Turn S. The fate of inorganic constituents of biomass in fluidized bed gasification. Fuel 1998;77(3):135–46.

[26] Olsson JG, Jäglid U, Pettersson JBC, Hald P. Alkali Metal Emission during Pyrolysis of Biomass. Energy Fuels 1997;11(4):779–84.

[27] Kowalski T, Ludwig C, Wokaun A. Qualitative Evaluation of Alkali Release during the Pyrolysis of Biomass. Energy Fuels 2007;21(5):3017–22.

[28] Shao Y, Wang J, Preto F, Zhu J, Xu C. Ash Deposition in Biomass Combustion or Co-Firing for Power/Heat Generation. Energies 2012;5(12):5171–89.

[29] Kassman H, Broström M, Berg M, Åmand L. Measures to reduce chlorine in deposits: Application in a large-scale circulating fluidised bed boiler firing biomass. Fuel 2011;90(4):1325–34.

[30] van Sjaak Loo JK. The Handbook of Biomass Combustion and Co-firing. [May 11, 2015]; Available from: https://books.google.de/books?id=KE565zmFumQC&pg=PA36&lpg=PA36&dq=residual+ash+biomass&source=bl&ots=wJu7De3nio&sig=S9SStjtOLf0w-OU_fO5DBU-yymE&hl=el&sa=X&ei=ITg-

VZWoIpbdauXPgO-AB&ved=0CCoQ6AEwAQ#v=onepage&q=residual%20ash%20biomass&f=false.

[31] Nussbaumer T. Aerosols from biomass combustion. Zürich: Verenum; addresses for orders: Verenum [etc.]; op. 2001.

[32] Friedrich Biedermann IO. Ash-related Problems during Biomass Combustion and Possibilities for a Sustainable Ash Utilisation.

[33] Valmari T. Potassium behaviour during combustion of wood in circulating fluidised bed power plants. Espoo [Finland]: Technical Research Centre of Finland; 2000.

[34] Lokare SS, Dunaway JD, Moulton D, Rogers D, Tree DR, Baxter LL. Investigation of Ash Deposition Rates for a Suite of Biomass Fuels and Fuel Blends. Energy Fuels 2006;20(3):1008–14.

[35] Peter Arendt Jensen, Muhammad Shafique Bashir, Stig Wedel, Flemming Frandsen, Johan Wadenbäck, Søren Thaaning Pedersen, Kim Dam-Johansen. Final report: Characterization and quantification of deposits build up and removal in straw suspension fired boilers 2013.

[36] Andersen KH, Frandsen FJ, Hansen PFB, Wieck-Hansen K, Rasmussen I, Overgaard P et al. Deposit Formation in a 150 MW e Utility PF-Boiler during Co-combustion of Coal and Straw. Energy Fuels 2000;14(4):765–80.

[37] B.M. Jenkins, L.L. Baxter, T.R. Miles Jr. T.R. Miles. Combustion properties of biomass 1998.

[38] Jensen PA, Stenholm M, Hald P. Deposition Investigation in Straw-Fired Boilers. Energy Fuels 1997;11(5):1048–55.

[39] Zbogar A, Frandsen F, Jensen PA, Glarborg P. Shedding of ash deposits. Progress in Energy and Combustion Science 2009;35(1):31–56.

[40] Tobiasen L, Skytte R, Pedersen LS, Pedersen ST, Lindberg MA. Deposit characteristic after injection of additives to a Danish straw-fired suspension boiler. Fuel Processing Technology 2007;88(11-12):1108–17.

[41] Steenari B, Lundberg A, Pettersson H, Wilewska-Bien M, Andersson D. Investigation of Ash Sintering during Combustion of Agricultural Residues and the Effect of Additives. Energy Fuels 2009;23(11):5655–62.

[42] Xiong S, Burvall J, Örberg H, Kalen G, Thyrel M, Öhman M et al. Slagging Characteristics during Combustion of Corn Stovers with and without Kaolin and Calcite. Energy Fuels 2008;22(5):3465–70.

[43] Wu H, Glarborg P, Frandsen FJ, Dam-Johansen K, Jensen PA. Dust-Firing of Straw and Additives: Ash Chemistry and Deposition Behavior. Energy Fuels 2011;25(7):2862–73.

[44] C.W. Bale, P. Chartrand, S.A. Degterov, G. Eriksson, K. Hack,R. Ben Mahfoud, J. Melanqon, A.D. Pelton and S. Petersen. FactSage Thermochemical Software and Databases 2002.

[45] Bale CW, Bélisle E, Chartrand P, Decterov SA, Eriksson G, Hack K et al. FactSage thermochemical software and databases — recent developments. Calphad 2009;33(2):295–311.

[46] Lindberg D, Backman R, Chartrand P, Hupa M. Towards a comprehensive thermodynamic database for ash-forming elements in biomass and waste combustion — Current situation and future developments. Fuel Processing Technology 2013;105:129–41.

[47] LI H, Yoshihiko N, DONG Z, ZHANG M. Application of the FactSage to Predict the Ash Melting Behavior in Reducing Conditions. Chinese Journal of Chemical Engineering 2006;14(6):784–9.

[48] Wang W, Liu X, Zheng Y. Quantitative chemical composition determination and thermal analysis for typical biomass ashes in China. Asia-Pac. J. Chem. Eng. 2014;9(5):751–8.

[49] Nutalapati D, Gupta R, Moghtaderi B, Wall TF. Assessing slagging and fouling during biomass combustion: A thermodynamic approach allowing for alkali/ash reactions. Fuel Processing Technology 2007;88(11-12):1044–52.

[50] Zevenhoven-Onderwater M, Blomquist J, Skrifvars B, Backman R, Hupa M. The prediction of behaviour of ashes from five different solid fuels in fluidised bed combustion. Fuel 2000;79(11):1353–61.

[51] Zevenhoven-Onderwater, M., Backman, R., Skrifvars, B.-J. and Hupa, M. The ash chemistry in fluidised bed gasification of biomass fuels. Part I predicting the chemistry of melting ash and ash-bed material interaction 2001.

[52] Broström M, Kassman H, Helgesson A, Berg M, Andersson C, Backman R et al. Sulfation of corrosive alkali chlorides by ammonium sulfate in a biomass fired CFB boiler. Fuel Processing Technology 2007;88(11-12):1171–7.

[53] Persson K, Broström M, Carlsson J, Nordin A, Backman R. High temperature corrosion in a 65 MW waste to energy plant. Fuel Processing Technology 2007;88(11-12):1178–82.

[54] Broström M, Enestam S, Backman R, Mäkelä K. Condensation in the KCl–NaCl system. Fuel Processing Technology 2013;105:142–8.

[55] Stine Broholm Hansen, Peter Arendt Jensen, Flemming Jappe Frandsen, Hao Wu, Bo Sander, Johan Wadenbäck, Peter Glarborg. DEPOSIT PROBE MEASUREMENTS IN DANISH GRATE AND PULVERIZED FUEL BIOMASS POWER BOILERS.

[56] Gasmet FTIR. [May 13, 2015]; Available from: http://www.gasmet.com/technology/ftir.

[57] Introduction to Fourier Transform Infrared Spectrometry.

[58] FT-IR Reference manual.

[59] CALCMET v4.3 Software Manual.

[60] kerstin. TOPAS SAG 410.

[61] Guanjun Z. Mineral matter behavior during co-gasification of coal and biomass 2014.

[62] B. Coda, M.K. Cieplik, J.M. Jacobs, J.H.A. Kiel. IMPACT OF BIOMASS CO-FIRING ON ASH FORMATION AND ASH BEHAV IOUR IN IGCC PLANTS.

[63] Shao Y. Investigation of Ash Deposition During Co-Firing Biomass/Peat with Coal in a Pilot-Scale Fluidized-Bed Reactor 2011.

[64] Nordgren D, Hedman H, Padban N, Boström D, Öhman M. Ash transformations in pulverised fuel co-combustion of straw and woody biomass. Fuel Processing Technology 2013;105:52–8.

[65] Aho M. Reduction of chlorine deposition in FB boilers with aluminium-containing additives. Fuel 2001;80(13):1943–51.

7 Appendix

7.1 Fact Sage

7.1.1 Torrefied straw product species in respect to λ

The diagrams in paragraph 4.1.2 show the changes of products for λ variation, but in order to make them more distinguishable and also to show how the molar ratios of different important species in products change with λ, we created species-λ diagrams for K, Ca, Fe and Si for the case of TS, at 1200 °C. With molar ratios of a species in products we mean the ratio of mole of a species inside one product to the whole molar amount of this species inside all the products.

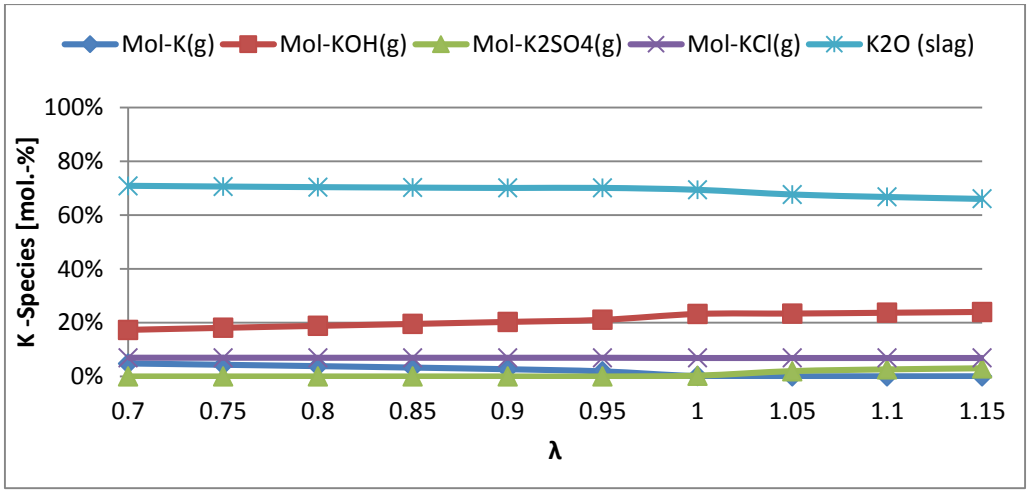

Figure 7.1: Molar ratio of K in respect to air-fuel ratio for Torrefied Straw at 1200 °C.

Above Figure 7.1 is observed that potassium species go under only small changes. With the increase of λ, the molar ratio of potassium in K-oxides (slag) and K(g) slightly decreases, while in KOH(g) and K_2SO_4(s) slightly increases. Interesting is the fact that the molar ratio of potassium in KCl(g) stays stable, which confirms the fact that potassium chloride formation is limited by Cl content.

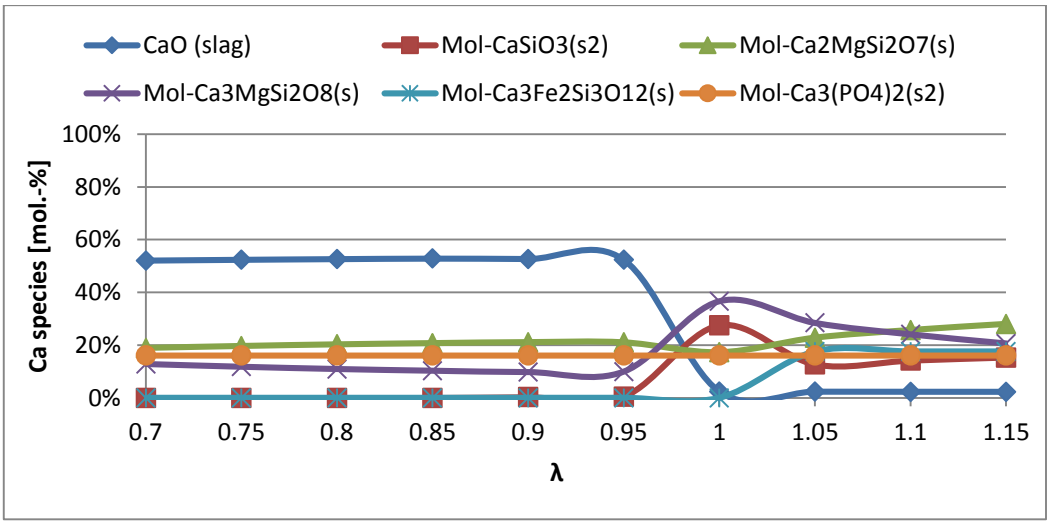

Figure 7.2: Molar ratio of Ca in respect to air-fuel ratio for Torrefied Straw at 1200 °C.

In Figure 7.2 is shown that the changes in the components' Ca molar ratios are greater. While the air-fuel ratio increases, the Ca leaves the slag and helps the formation or increase of solid species, like Ca-silicates, Ca-Fe-silicates and Ca-Mg-silicates. We also see here that phosphate formation is limited by P content.

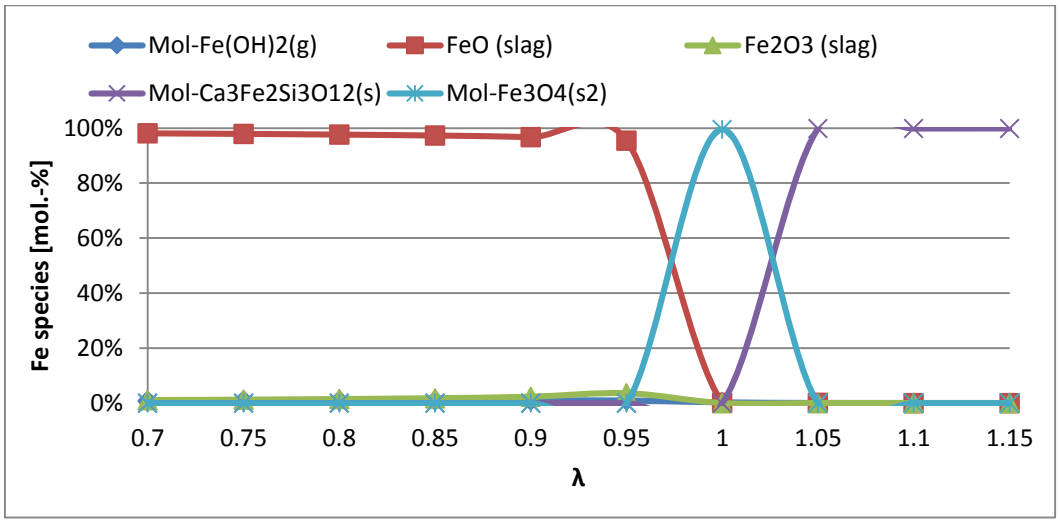

Figure 7.3: Molar ratio of Fe in respect to air-fuel ratio for Torrefied Straw at 1200 °C.

For the case of iron, from Figure 7.3 we see that, while λ increases, all the Fe leaves the slag sharply and contributes into forming solids. Only for λ=1 Fe_3O_4 is formed and for greater air-fuel ratios Fe exists only in Ca-Fe-silicates.

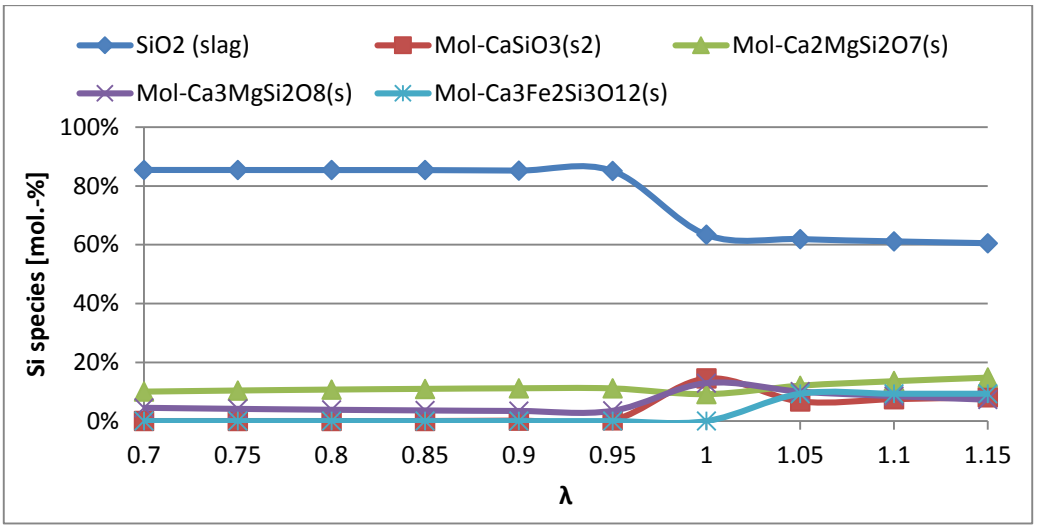

Figure 7.4: Molar ratio of Si in respect to air-fuel ratio for Torrefied Straw at 1200 °C.

Finally we see the changes in the silicon species in Figure 7.4. Silicon, as we see in all our results until now, plays a leading role in slag and solid formation, as it forms silicates with K, Ca, Fe and other components. Similarly to Ca, as the λ increases, silicon leaves the slag form and helps in the creation or increase of solid species like Ca-silicates, Ca-Mg-silicates and Ca-Fe-silicates.

All the above diagrams lead to the same conclusion, that it is preferable to have air-fuel ratio λ>1 because this way the formation of slag is reduced and instead we have more solids that are easier to handle.

7.1.2 Comparison between FT oxide-SLAGA and FT oxide-SLAGC databases.

FactSage gives the products of an equilibrium thermochemical calculation depending on the databases chosen to be used in this process. In this study FT Oxide-SLAGA and FT salt-SALTF have been used for defining the liquid phase. Instead of FT Oxide-SLAGA, another database could have been chosen that would give us similar results, but in the end the former databases were considered more suitable because of the previous existing experience from their use. Below (Figure 7.5, Figure 7.6) the differences in the results between the use of FT Oxide-SLAGA and FT Oxide-SLAGC in the presentation of the molar ratios of potassium inside different K products of TS, is shown. The air-fuel ratio is 1.15.

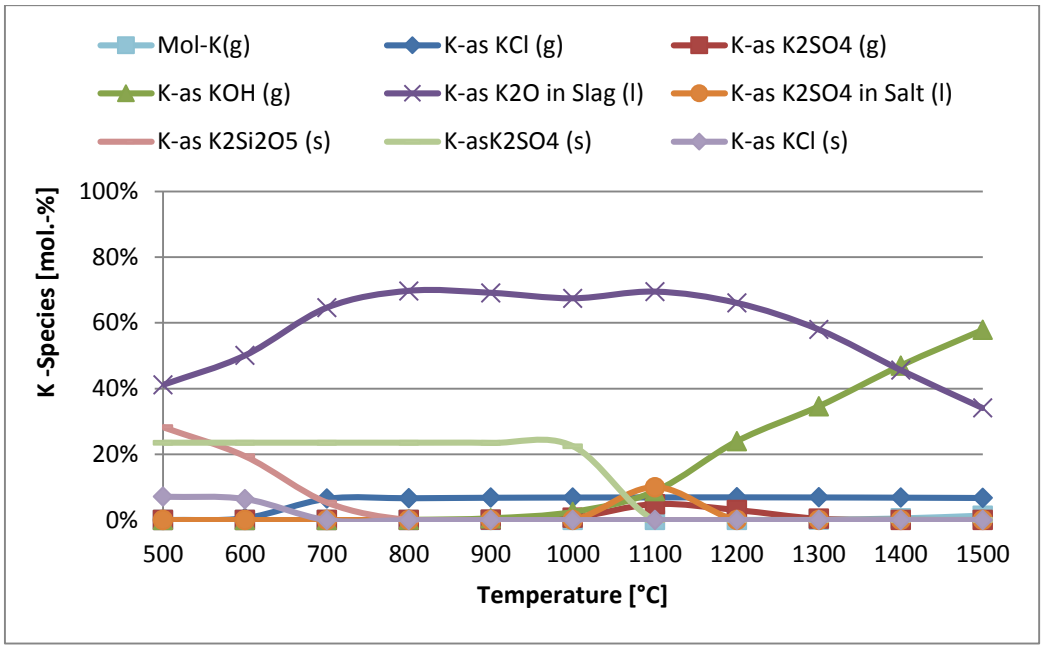

Figure 7.5: Molar ratio of potassium inside different K products of Torrefied Straw, FT oxide-SLAGA case.

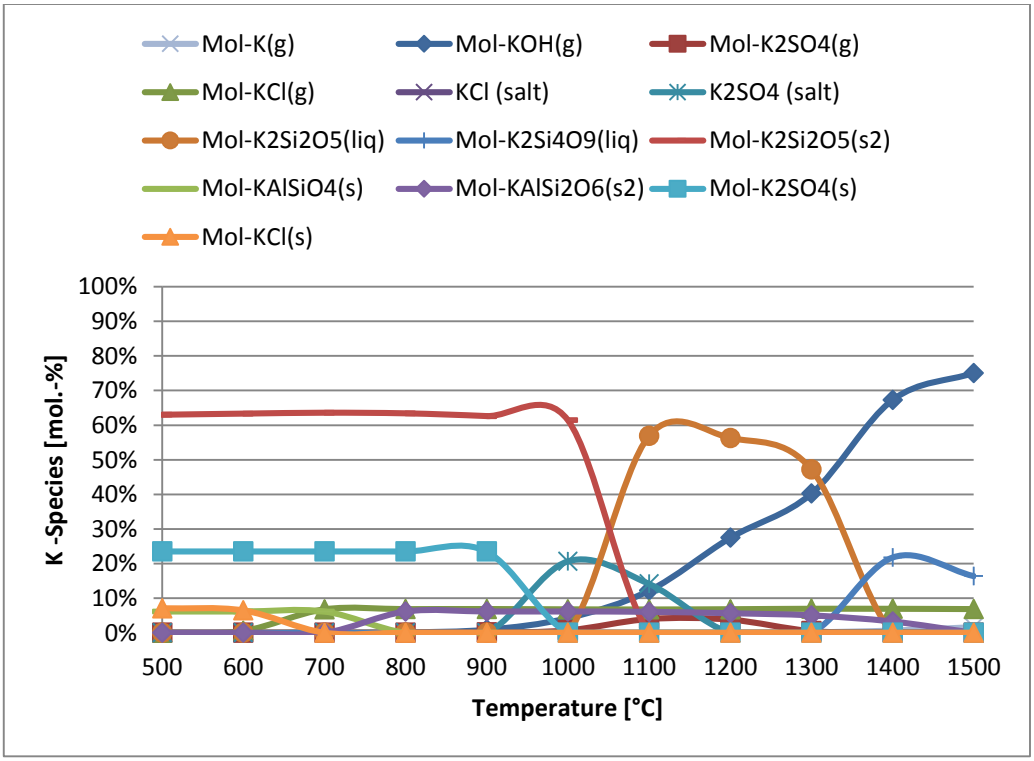

Figure 7.6: Molar ratio of potassium inside different K products of Torrefied Straw, FT oxide-SLAGC

Comparing the two diagrams it is shown that K, KOH, KCl, K_2SO_4 have similar behavior. What makes the difference of the databases obvious is that in the first case, molten potassium species appear as K_2O inside the slag, while in the second one they appear as K-

silicates inside the slag. Furthermore in the second case, some K is left for the production of K-Al-silicates.

7.1.3 Effect of variance of fuel components on K-species formation.

Investigation on how the variance of different fuel components influences the formation of the K-species was also of interest. For this reason calculations were made while varying SiO_2, CaO and Fe_2O_3 from zero to their maximum content. The variation took place while combusting torrefied straw, in the theoretical case that each one of these compounds could be extracted from the fuel and then fed together with the new "limp" fuel at will. The λ was set to 1.15 and three temperatures were chosen 900, 1100 and 1300 °C. This selection was made because each temperature seems to represent a different slagging behavior in Figure 4.2.

SiO_2 variation

The results calculated for SiO_2 variation in its full range 0-1.486 g, for the three temperatures are presented below in Figure 7.7 for 900°C, Figure 7.8 for 1100°C and Figure 7.9 for 1300°C.

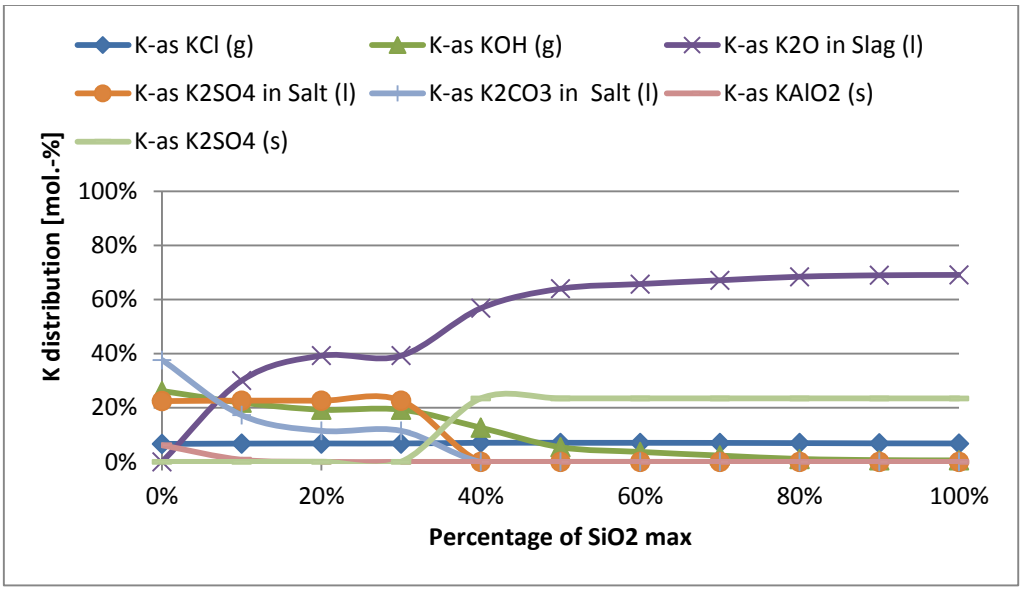

Figure 7.7: K distribution for SiO_2 variation at 900°C, Torrefied Straw.

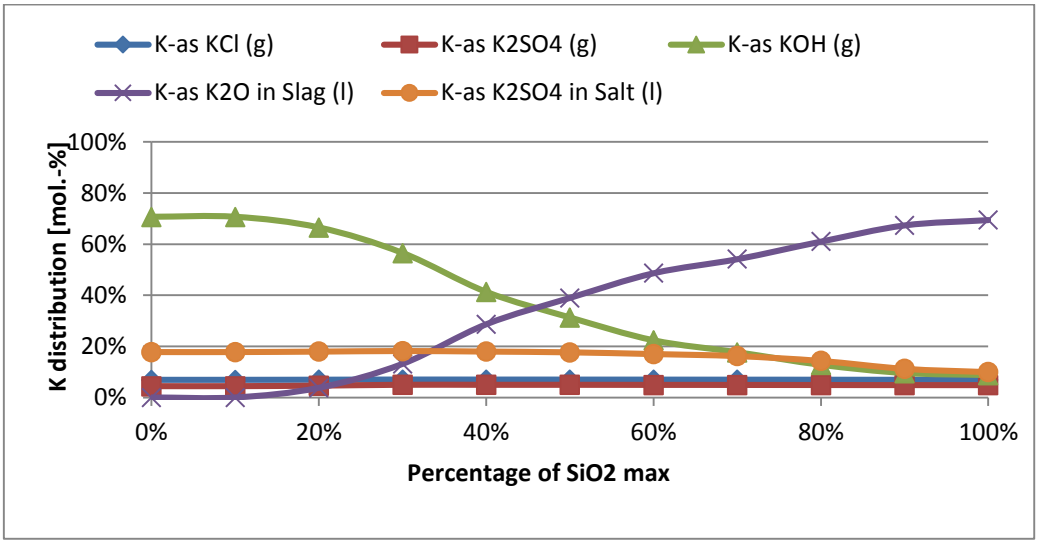

Figure 7.8: K distribution for SiO2 variation at 1100°C, Torrefied Straw.

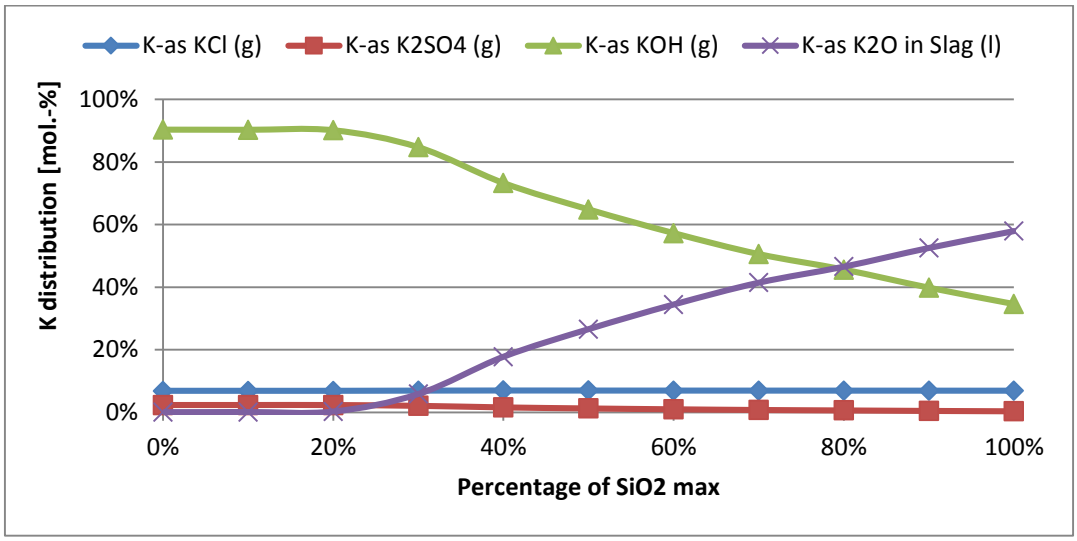

Figure 7.9: K distribution for SiO2 variation at 1300°C, Torrefied Straw.

From these diagrams some observations can be made:

- While SiO_2 increases, the K-gas species decrease but the K-species in slag phase increase
- In high temperatures there is no K_2SO_4 and when the temperature goes down first some K_2SO_4(g,l) form
- KCl is constant, which again confirms that KCl formation depends only on Cl levels
- Slag formation is higher for the lower temperatures of our case
- For 900 °C and low SiO_2 content there is some K available for K-carbonates formation

In Figure 7.10 below is presented where Si goes when SiO_2 is introduced together with the fuel. Also the major K-species behavior is presented in order to enable a possible relation.
It is clearly shown that as long as Si starts being inserted into the system, silicates are starting to form, i.e. Ca-silicates, K-silicates (not shown here because of chosen database). This means that almost all the Si content will exist into slag. Furthermore available KOH(g) starts quite early to react with SiO_2 in order to form different K-silicates with their own melting temperature ($K_2O.nSiO_2$). The reactions responsible for that have the general equation:

$$2KOH(g) + nSiO2(s) = K2O.nSiO2(l) + H2O \quad (7\text{-}1)$$

which has lower ΔG than the general equation:

$$CaO(s) + SiO2(s) = mCaO.nSiO2(s) \quad (7\text{-}2)$$

So (7-1) has priority to take place before (7-2). Also a reaction with its reactants and products like (g)+(s)→(l) is more probable than one with reactants and products like (s)+(s)→(s).

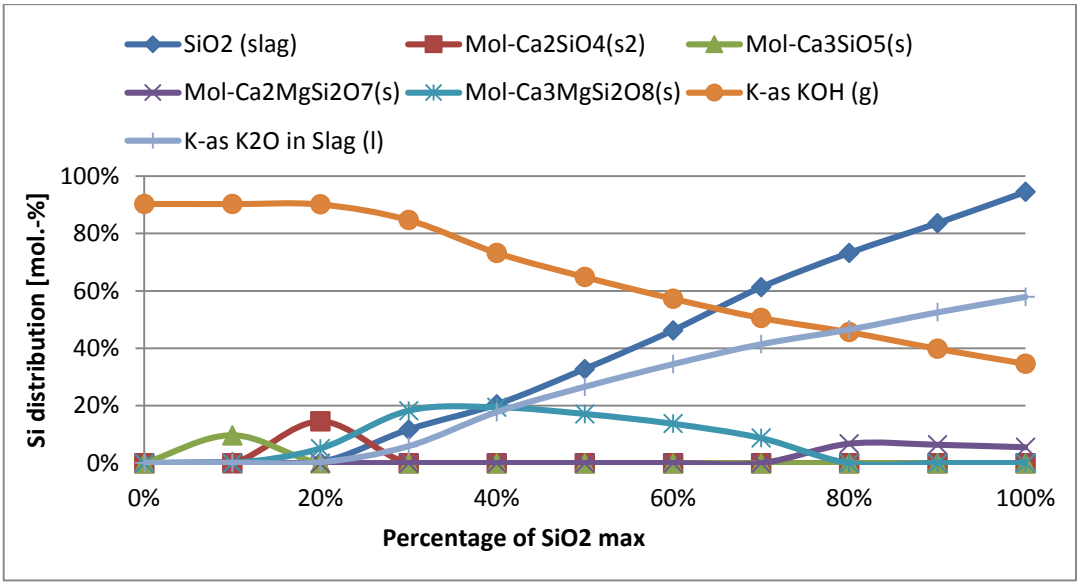

Figure 7.10: Si distribution and major K-species behavior for SiO2 variation at 1300°C, Torrefied Straw.

CaO variation

The results calculated for CaO variation in its full range 0-0.7331 g, for the three temperatures are presented below in Figure 7.11 for 900°C, Figure 7.12 for 1100°C and Figure 7.13 for 1300°C.

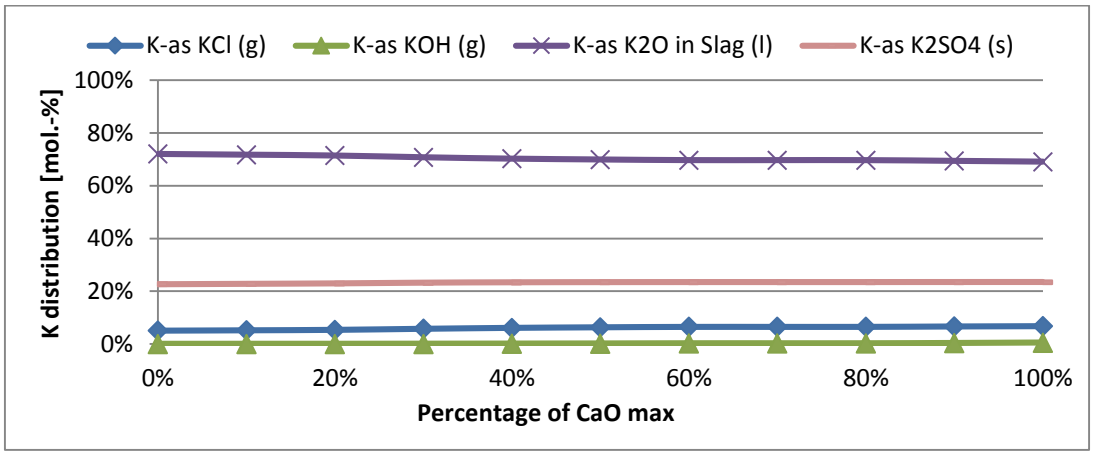

Figure 7.11: K distribution for CaO variation at 900°C, Torrefied Straw.

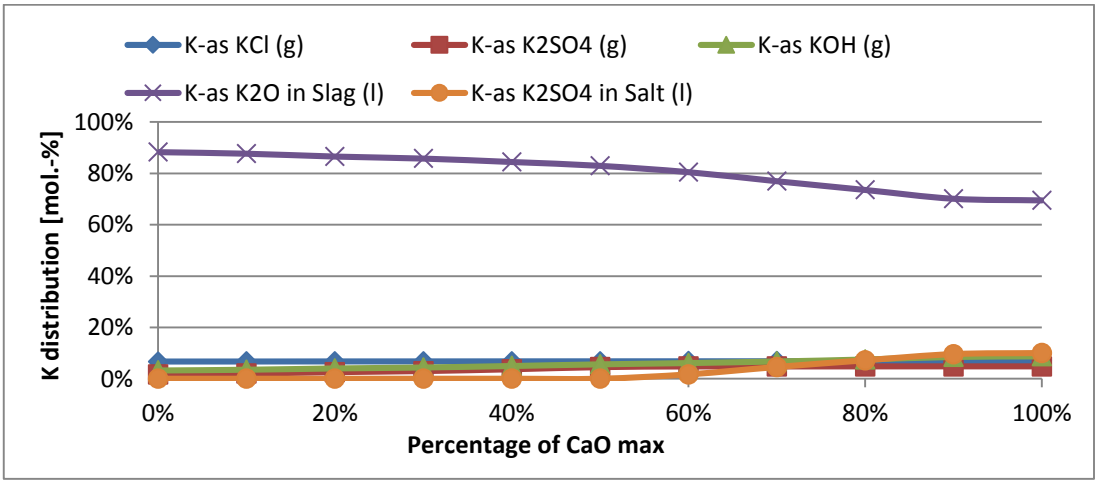

Figure 7.12: K distribution for CaO variation at 1100°C, Torrefied Straw.

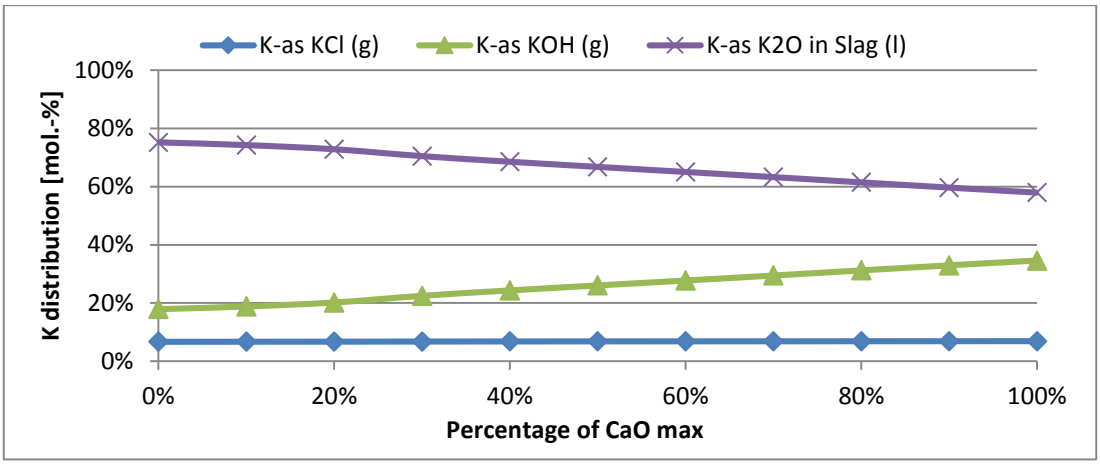

Figure 7.13: K distribution for CaO variation at 1300°C, Torrefied Straw.

From these diagrams can be seen that, while the temperature rises, K_2O in slag decreases and KOH(g) increases.

In Figure 7.10 below is presented where Si goes when SiO_2 is introduced together with the fuel. Also the major K-species behavior is presented in order to enable a possible relation. What is shown here is that while Ca content increases, K in slag decreases. This happens because Si not reacting exclusively with K to form K-silicates but also with Ca to form Ca-silicates. So obviously Ca content is slag increases as well.

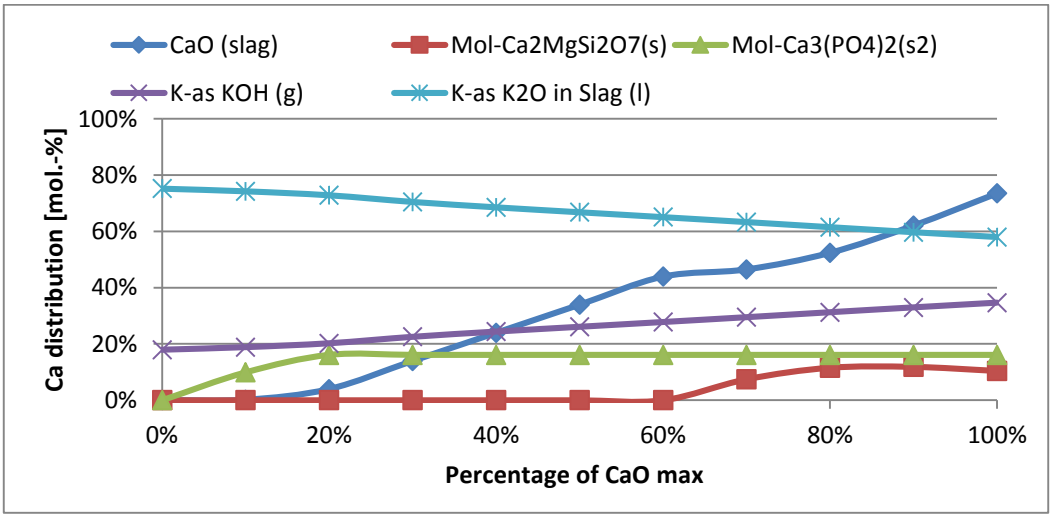

Figure 7.14: Ca distribution and major K-species behavior for CaO variation at 1300°C, Torrefied Straw.

Fe_2O_3 variation

The results calculated for Fe_2O_3 variation in its full range 0-0.1226 g, for the three temperatures are presented below in Figure 7.15 for 900°C,Figure 7.16 for 1100°C and Figure 7.17 for 1300°C.

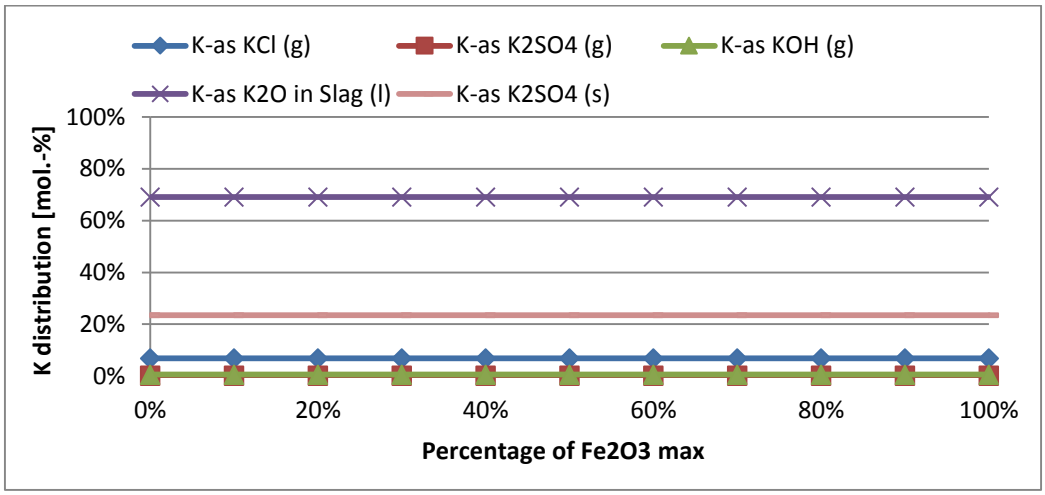

Figure 7.15: K distribution for Fe2O3 variation at 900°C, Torrefied Straw.

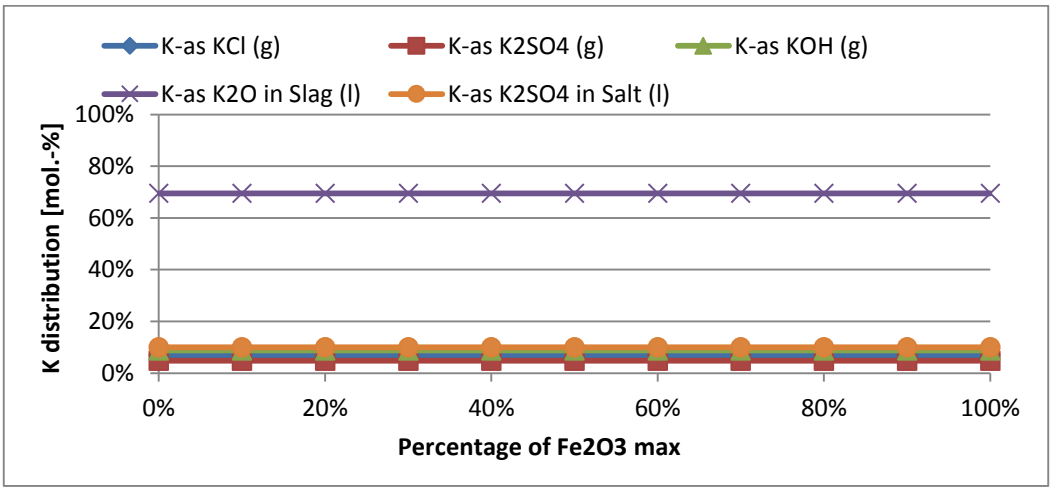

Figure 7.16: K distribution for Fe2O3 variation at 1100°C, Torrefied Straw.

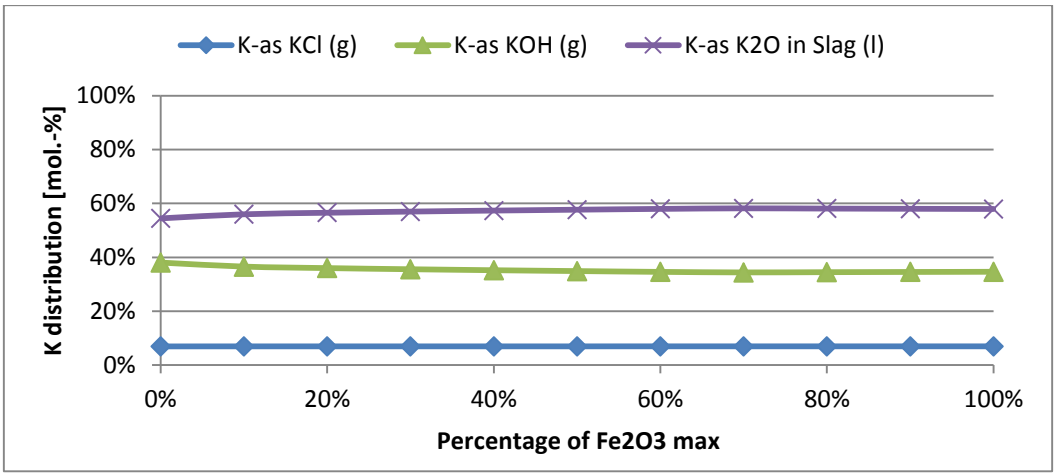

Figure 7.17: K distribution for Fe2O3 variation at 1300°C, Torrefied Straw.

The above diagrams do not show any important changes, except for a small one when starting to introduce Fe_2O_3 into the system at 1300 °C. There are no significant differences probably because the variation of Fe_2O_3 is small. So we decided to follow the same procedure again for Fe_2O_3 but this time with the variation range of SiO_2, i.e. 0-1.486 g. The new results calculated for the new Fe_2O_3 variation range, for the three temperatures are presented below in Figure 7.18 for 900°C, Figure 7.19 for 1100°C and Figure 7.20 for 1300°C.

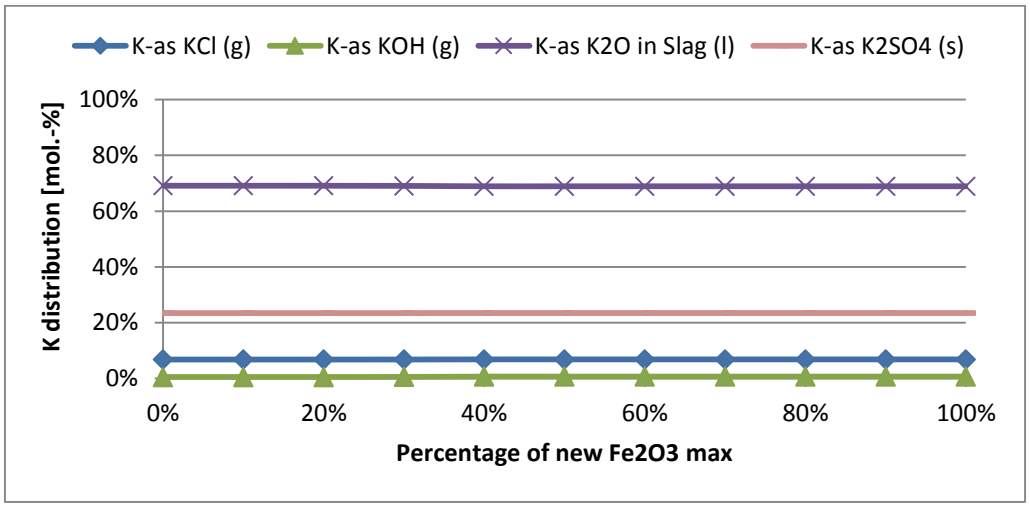

Figure 7.18: K distribution for new Fe2O3 variation at 900°C, Torrefied Straw.

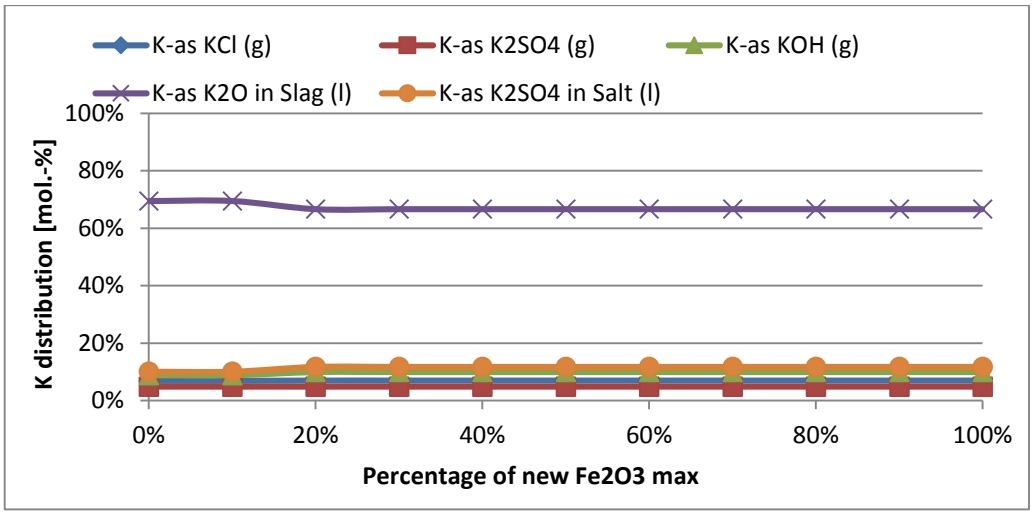

Figure 7.19: K distribution for new Fe2O3 variation at 1100°C, Torrefied Straw.

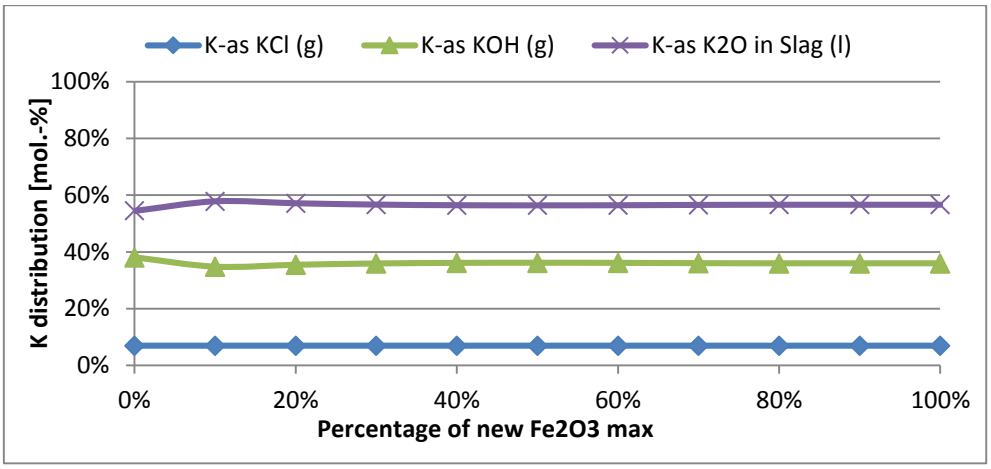

Figure 7.20: K distribution for new Fe2O3 variation at 1300°C, Torrefied Straw.

Once again in this case we don't see any important changes apart from small differences when starting to introduce Fe_2O_3 into the system for 1100 and 1300 °C.

After seeing also these diagrams, the conclusion is that iron plays a minor role in K-species formation when combusting TS.

Below in Figure 7.21, it is shown where iron goes when it is introduced into the system. It is obvious that all of it goes to iron slag species formation but it seems that there is no relation with K-species.

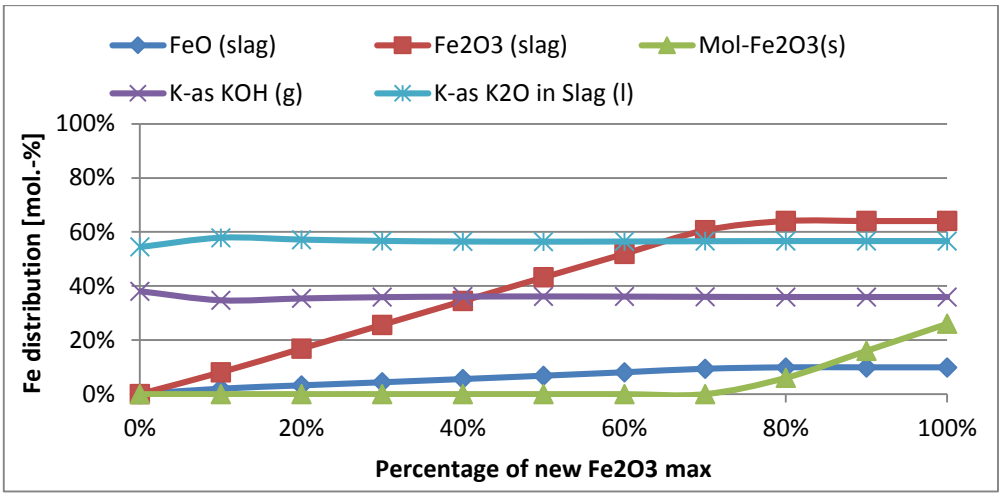

Figure 7.21: Fe distribution and major K-species behavior for CaO variation at 1300°C, Torrefied Straw.

After receiving and examining all these results there is one significant observation. With the used database FT oxide-SLAGA we get K-species in slag but in K_2O form and not as potassium silicates that would be more convenient for us. So a repetition of the important processes with FT oxide-SLAGC as a database would be of interest, in order to make clear which database is more suitable for this study.

7.2 Experimental results

7.2.1 Additive feeding

In Figure 7.22 the feeding rates of the additives, for different belt speeds (rotating speed 3), are presented. The image includes the additive feeding rates for the important sessions of the study. In Figure 7.23 and Figure 7.24 the range of feeding of the disperser for different belt speed (rotating speed 3) is presented. Big fluctuations are observed, probably because of small differences in the ejector nozzle adjustment. In Figure 7.25 the influence that of the rotating speed, of the stirring part inside the reservoir of the disperser, on the additive feeding rates is presented. Sometimes increasing the R.S. increases the feeding, some other times it decreases it.

From these diagrams and the experience obtained from the use of the disperser during the experimental campaign, occurs the conclusion that the feeding through this device depends on different factors. The nature of the additive, the usual cleaning of the device, the right choice of operational settings and an experienced operator, are all necessary for achieving the optimum feeding process.

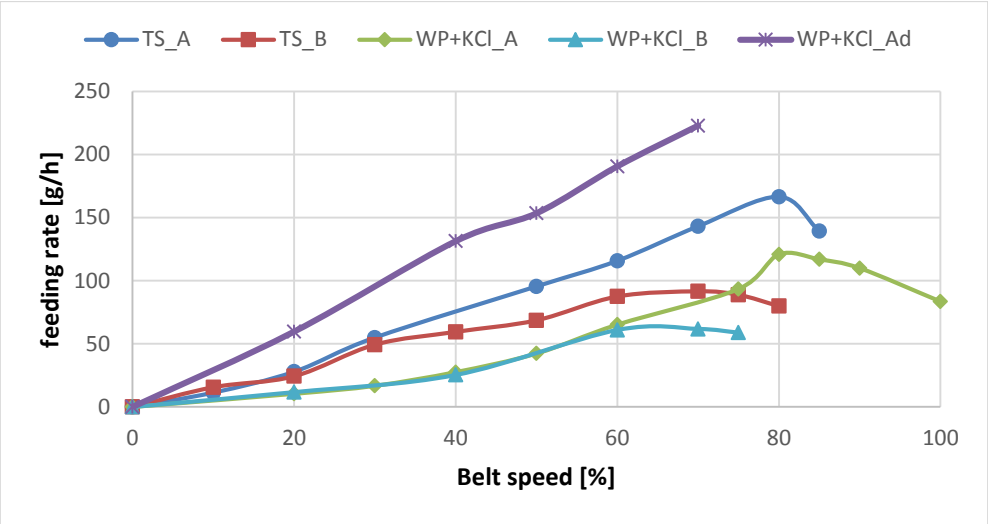

Figure 7.22: Additive feeding rates calculated for different cases.

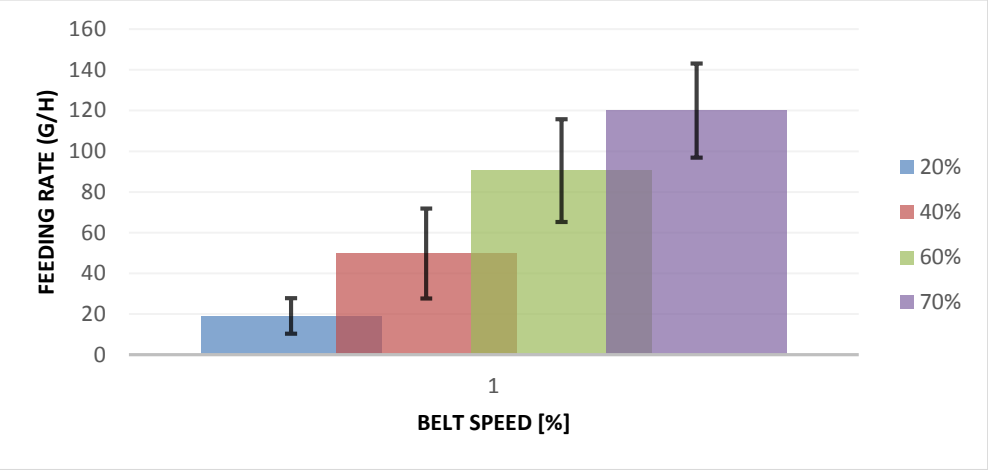

Figure 7.23: The feeding capability of the disperser for Aurora, for different belt speeds.

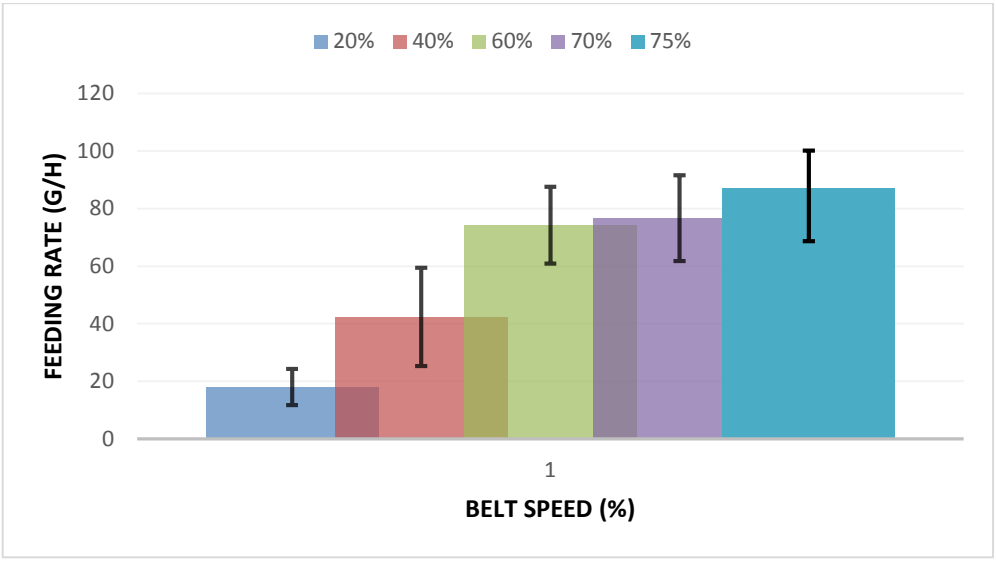

Figure 7.24: The feeding capability of the disperser for Bentonite, for different belt speeds.

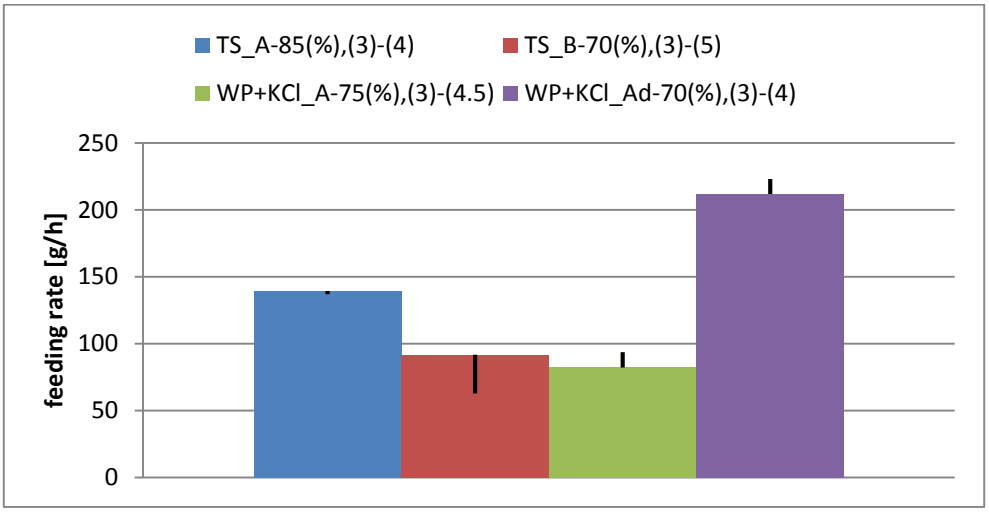

Figure 7.25: Influence of the stirring part's rotating speed of the disperser in feeding.

7.2.2 Whole experimental sessions

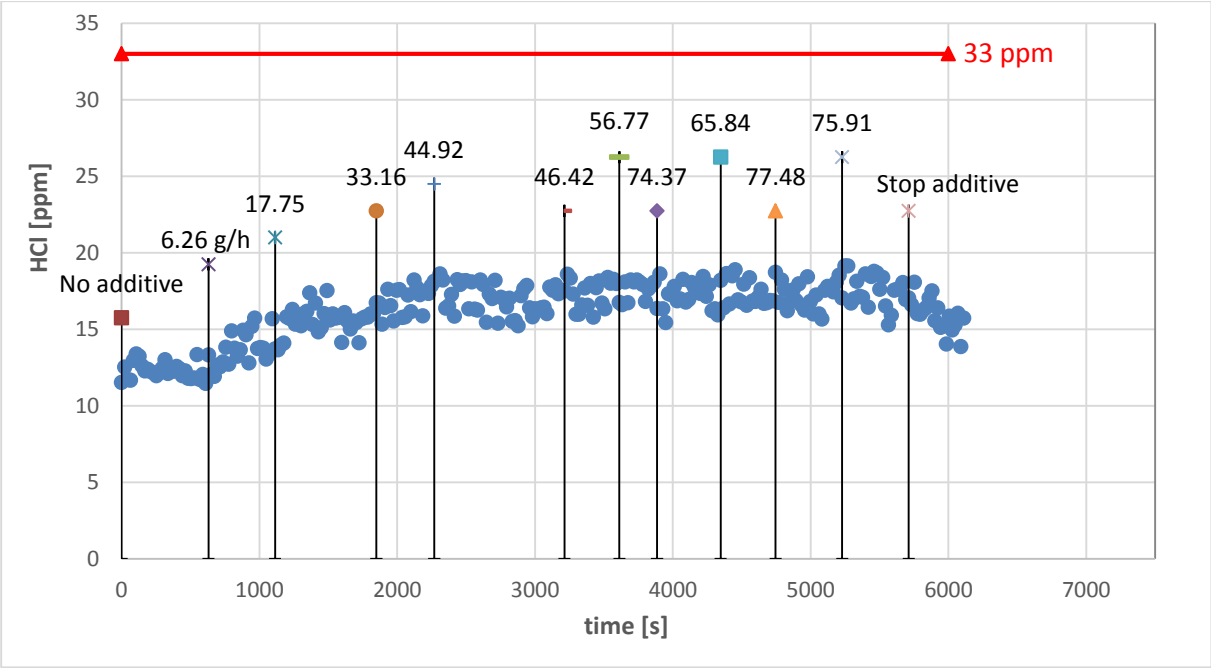

Figure 7.26: Whole WP - Bentonite session.

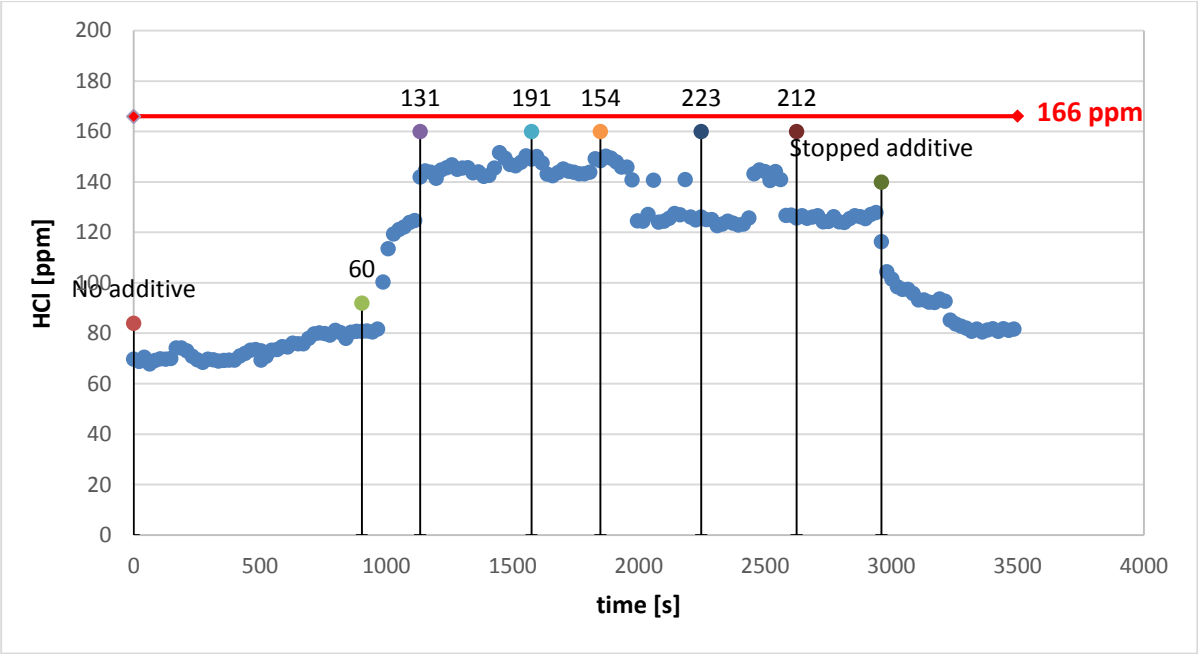

Figure 7.27: Whole WP+KCl - dried Aurora sub-session

7.2.3 HCl-feeding rate for WP+KCl-Aurora dry case

In Figure 7.28 the mean HCl values for WP+KCl fuel and the feeding of dried Aurora is presented. It is shown also in this diagram that for this case the highest HCl values were

achieved and the highest additive feeding rates. Nevertheless after some certain point, the HCl values did not move higher, even for more additive input into the system.

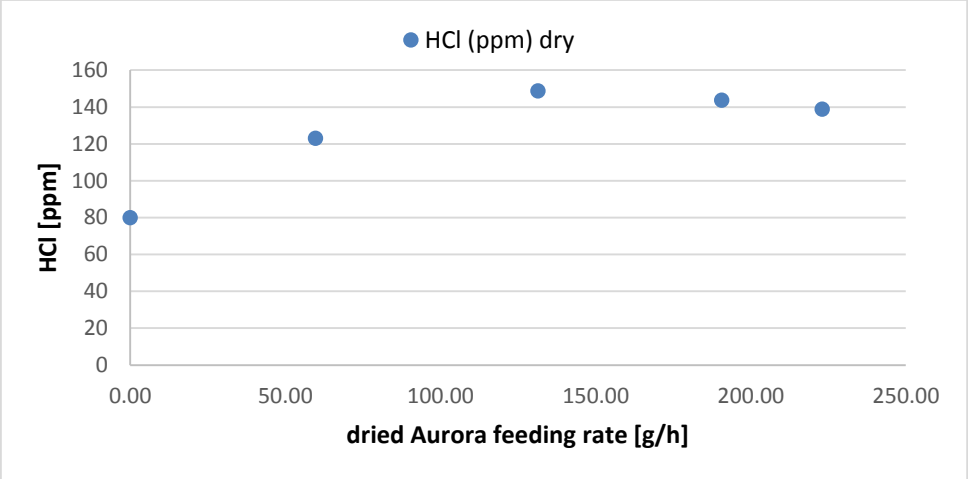

Figure 7.28: HCl mean values for their corresponding additive feeding rates. WP+KCl and Aurora dry case.

7.2.4 Chlorine as HCl in respect to K/(Si+Al)

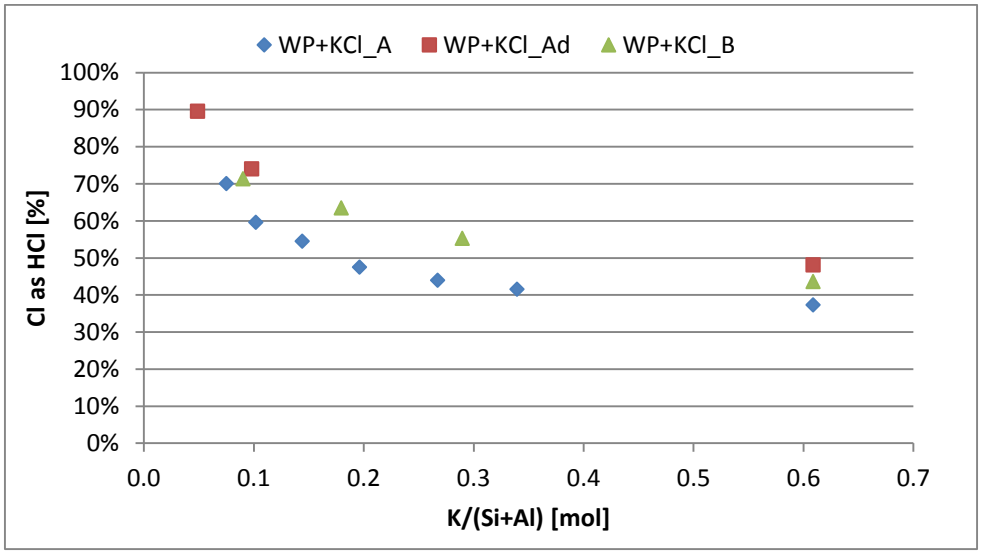

Figure 7.29: Percentage of fuel Cl that transforms into HCl in respect to K/(Si+Al) ratios, for WP+KCl.

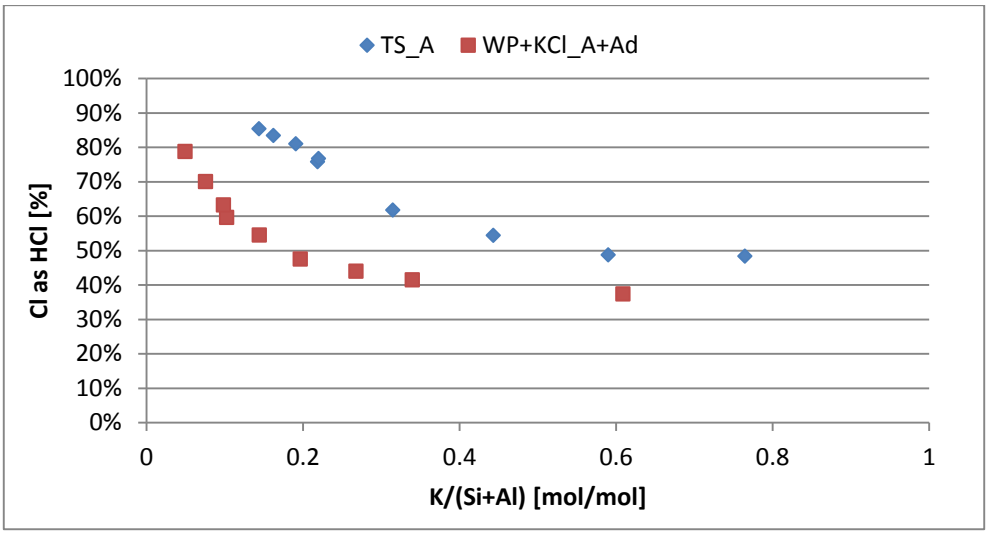

Figure 7.30: Effect of Aurora for Torrefied Straw and Wood Pellets+KCl.

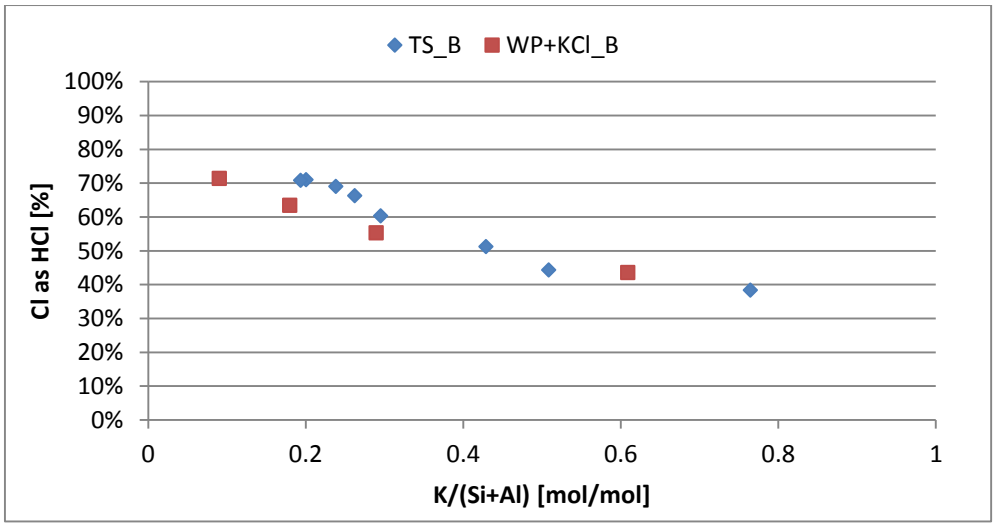

Figure 7.31: Effect of Bentonite for Torefied Straw and Wood Pellets+KCl.

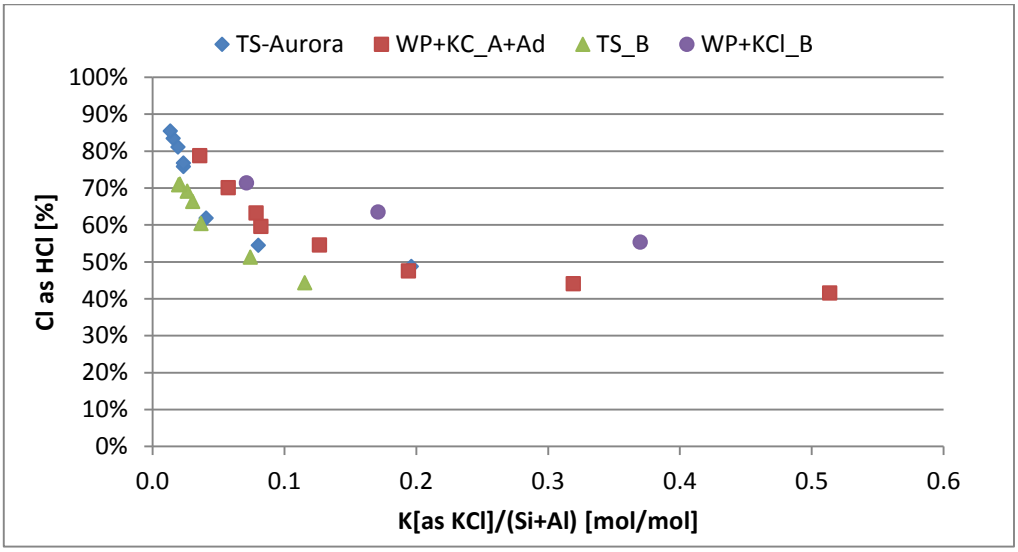

Figure 7.32: Relation of K in KCl with the formation of Cl into HCl. All cases.

7.2.5 HCl increase all cases

A different kind comparison is shown in Figure 7.33 and Figure 7.34. The values in these diagrams were calculated with the help of the formula:

$$HCl\ increase(\%) = \frac{HCli - HClpf}{HClpf} \qquad (7\text{-}3)$$

Where *HCli* is the calculated HCl value for the current additive feeding rate and *HClpf* is the HCl value which was calculated for pure fuel for the corresponding additive. Again though, this comparison is not absolutely accurate since the HClpf values are different between the the different cases.

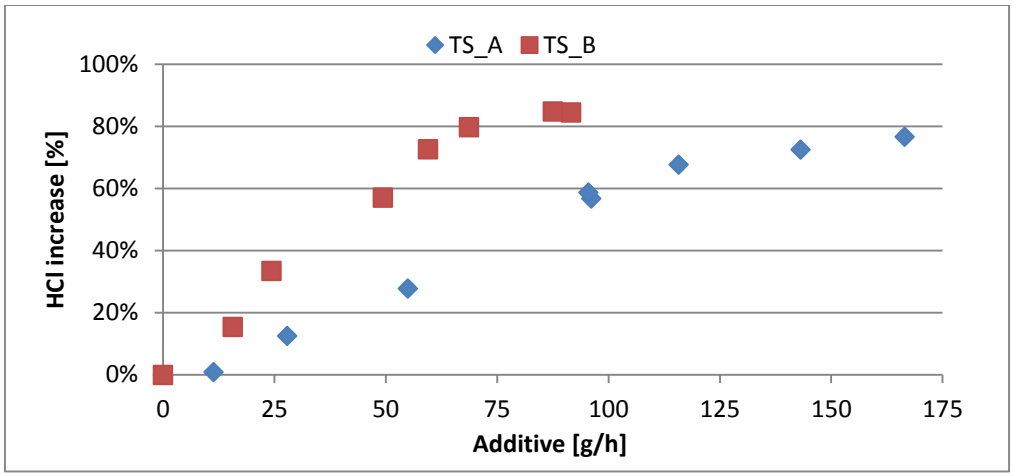

Figure 7.33: HCl increase in % for different additive feeding rates, for Torrefied Straw.

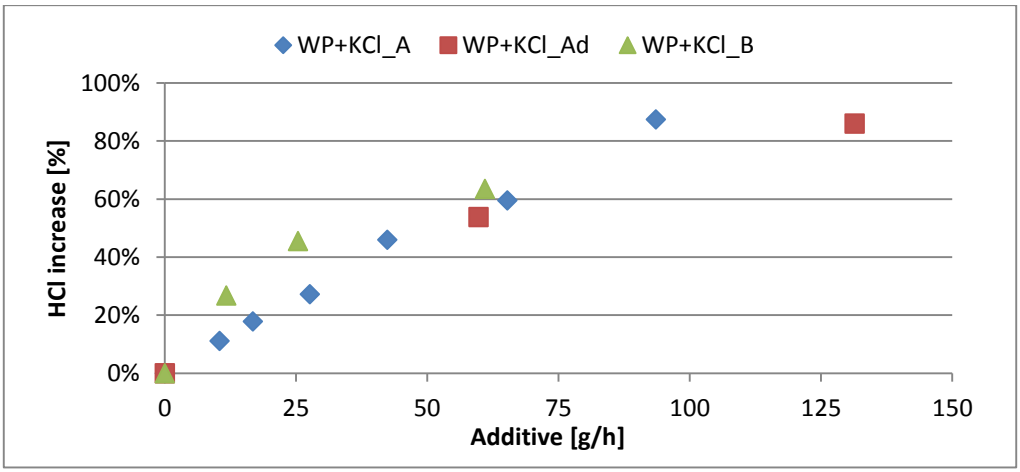

Figure 7.34: HCl increase in % for different additive feeding rates, for WP+KCl.

Stable cases

In some of the experimental sessions, the goal was not to see how the variation of additives influences the HCl emissions, but how the each HCl measurements vary for stable conditions and also if changes in oxygen influence HCl.

The fluctuation of HCl measurements is presented in Figure 7.35. This image's fluctuation ranges contain every single measurement for a continues period of time and differ from **Error! Reference source not found.** that takes into account as fluctuation range the mean HCl values of different sessions.

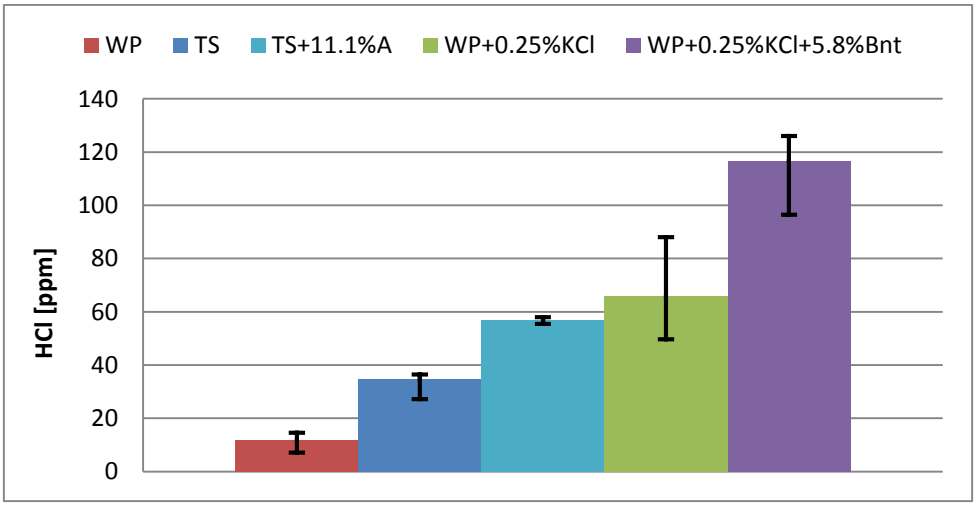

Figure 7.35: Fluctuation of HCl for stable conditions.

The mean, maximum, minimum and most frequent HCl values measured for these sessions are also presented in Figure 7.36, Figure 7.37, Figure 7.38 and Figure 7.39.

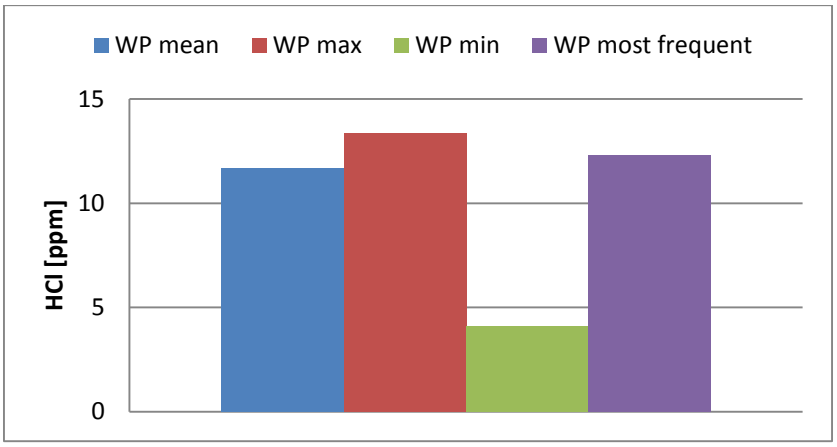

Figure 7.36: HCl measurement information about Wood Pellets.

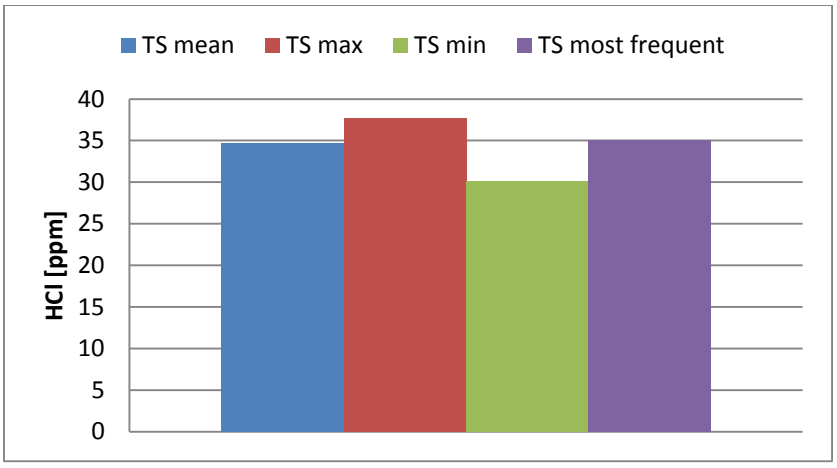

Figure 7.37: HCl measurement information about Torrefied Straw.

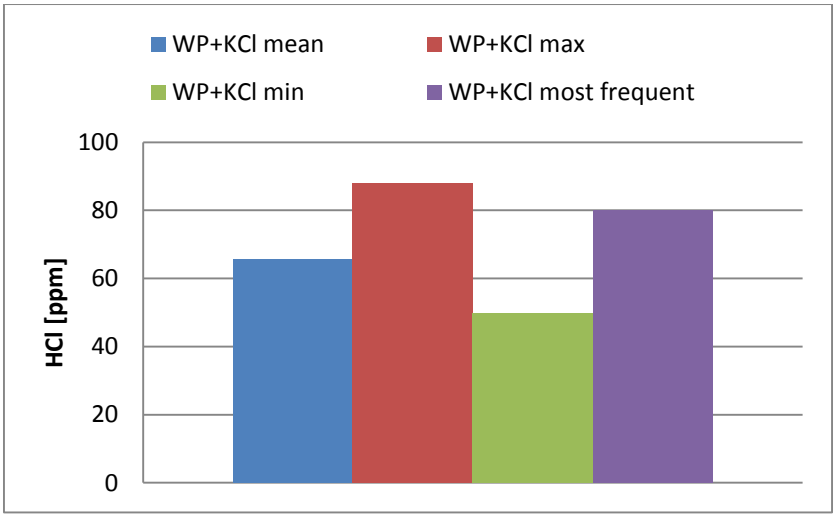

Figure 7.38: HCl measurement information about WP+0.25%KCl.

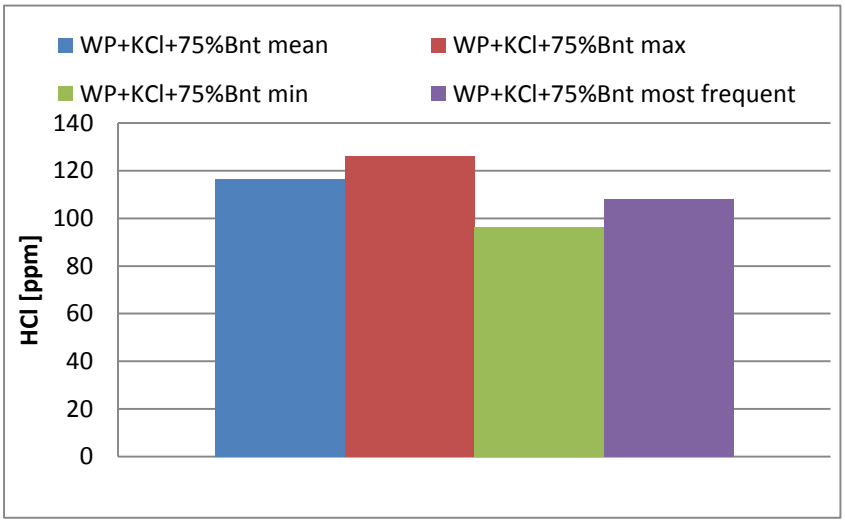

Figure 7.39: HCl measurement information about WP+0.25%KCl+5.8%Bentonite.

The relation of excess O_2 with HCl levels is presented in Figure 7.40, Figure 7.41 and Figure 7.42 for the pure TS, pure WP+KCl and WP+KCl+Bentonite. From these diagrams, changes in excess oxygen do not seem to influence the HCl emissions.

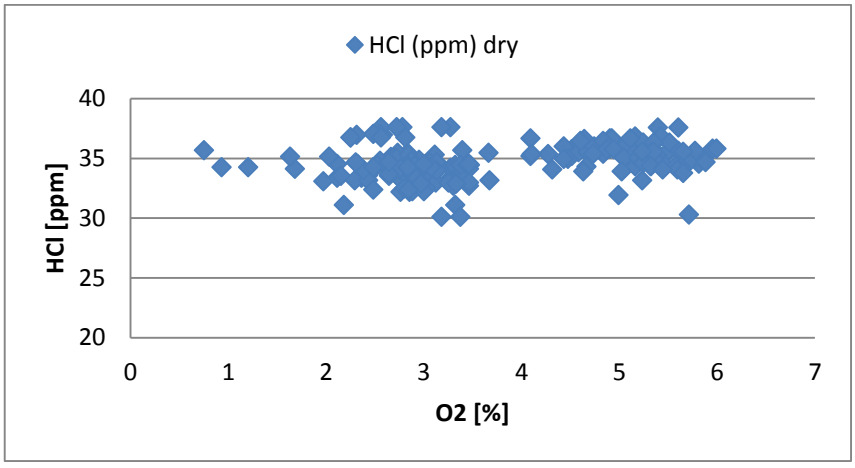

Figure 7.40: Relation between excess oxygen and HCl concentrations, in stable Torrefied Straw case.

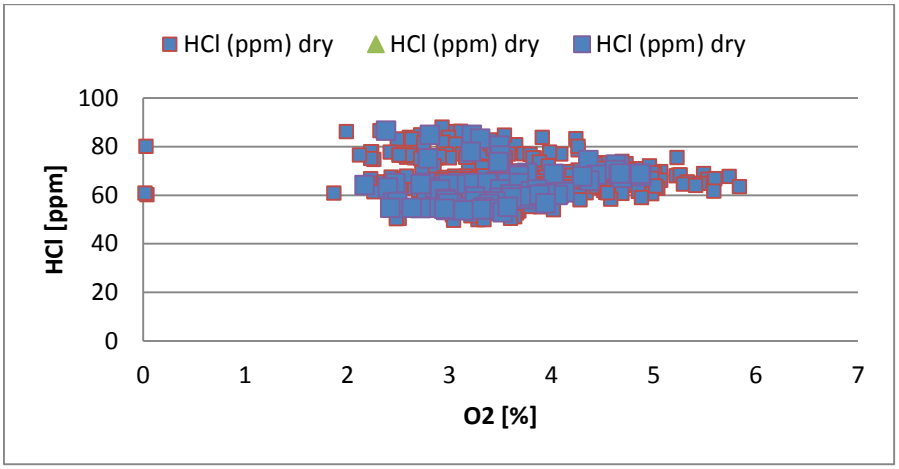

Figure 7.41: Relation between excess oxygen and HCl concentrations, in stable WP+0.25%KCl case.

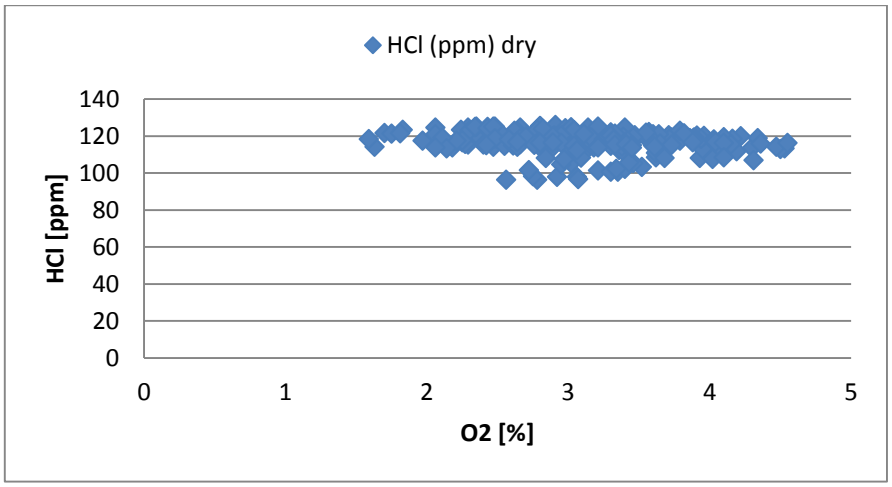

Figure 7.42: Relation between excess oxygen and HCl concentrations, in stable WP+0.25%KCl+5.8%Bentonite case.

8 Ελληνικό Τμήμα

Ιωάννης Πολυζώης

Θερμοδυναμικος υπολογισμός σε κατάσταση ισορροπίας για την αξιολόγηση της επίδρασης των πρόσθετων Πυριτικού Αργιλίου στην τάση προς δημιουργία επικαθίσεων και θρόμβωσης της βιομάζας

8.1 Εισαγωγή

Ένα από τα πιο σημαντικά αέρια του φαινομένου θερμοκηπίου είναι το CO_2 το οποίο επηρεάζει σημαντικά τη μέση θέρμανση τη επιφάνειας της γης. Το μεγαλύτερο μέρος των αερίων του θερμοκηπίου προέρχεται από την παραγωγή ενέργειας μέσω της καύσης στερεών καυσίμων σε εργοστάσια παραγωγής ηλεκτρικής ενέργειας. Η παγκόσμια ενεργειακή ζήτηση αναμένεται να αυξηθεί κατά 37% μέχρι το 2040, κάτι το οποίο θα οδηγούσε σε μεγαλύτερες σχετικές εκπομπές αερίων και σε σοβαρό αντίκτυπο για τους ανθρώπους και το οικοσύστημα. Παρ' όλα αυτά, οι ανανεώσιμες πηγές ενέργειας με τις χαμηλές εκπομπές άνθρακα κερδίζουν έδαφος, ενώ το μερίδιο τους στην παραγωγή ενέργειας αναμένεται να είναι το ένα τρίτο μέχρι το 2040. Εντός του 2012 το μερίδιο της παραδοσιακής βιομάζας ήταν το 9% της παγκόσμιας ενεργειακής κατανάλωσης (Figure 1.1), ενώ μέχρι το τέλος του 2013 το μερίδιο της βιομάζας στην παραγωγή της παγκόσμιας ηλεκτρικής ενέργειας ήταν 1.8%. Ομοίως με τις σύγχρονες ανανεώσιμες, η βιομάζα μπορεί να παρέχει αξιόλογο μερίδιο της συνολικής ηλεκρικής ενέργειας σε περιοχές όπου είναι οικονομικά ανταγωνιστική και σημαντικοί της πόροι είναι διαθέσιμοι.

Παρ' όλα αυτά, τα καύσιμα βιομάζας, τα οποία θεωρούνται πως έχουν ουδέτερο ανθρακικό αποτύπωμα, έχουν διαφορετική σύσταση από τα ορυκτά καύσιμα. Έχουν υψηλά ποσοστά αλκαλίων και χλωρίου κάτι το οποίο αλλάζει την συμπεριφορά των στοιχείων δημιουργίας τέφρας κι ως εκ τούτου και τα χαρακτηριστικά δημιουργίας αποθέσεων. Με αυτό τον τρόπο προκαλούνται συχνά σοβαρά προβλήματα λειτουργίας σχετιζόμενα με την τέφρα, όπως η δημιουργία επικαθίσεων, η θρόμβωση και η διάβρωση υψηλών θερμοκρασιών. Τα πιο σημαντικά στοιχεία δημιουργίας τέφρας στην βιομάζα είναι τα Si, Al, Fe, Ca, Mg, Mn, K, Na, P, S και Cl. Όσον αφορά την ξυλώδη βιομάζα, το πυρίτιο (Si), τα μέταλλα αλκαλικών γαιών (Ca, Mg), τα αλκαλικά μέταλλα (K, Na), το θείο (S) και το χλώριο (Cl) πάιζουν καθοριστικό ρόλο την δημιουργία επικαθίσεων, την θρόμβωση και την διάβρωση. Όσον αφορά την αγροτική βιομάζα, ο φώσφορος (P) έχει πρωτεύον ρόλο στις αντιδράσεις μετασχηματισμού τέφρας.

Το κάλιο είναι το κυρίως υπεύθυνο για την δημιουργία αποθέσεων εντός ενός κλιβάνου. Σε λέβητες κονιορτοποιημένου καυσίμου όπου οι θερμοκρασίες είναι υψηλές, γύρω στους 1300 ˚C, το κάλιο αναμένεται να απελευθερωθεί σε αέρια φάση ως υδροξείδια, χλωρίδια και/ή θειικά. Το ποσό του χλωρίου μέσα στο καύσιμο βάζει όρια στην δημιουργία χλωριούχου καλίου και το λοιπό κάλιο μετατρέπεται σε KOH, ενώ το K_2SO_4 είναι πιο σταθερό σε συμπυκνωμένη φάση (στερεή, υγρή). Έπειτα, τα χλωριούχα αλκάλια και τα θειικά αλκάλια συμπυκνώνονται στις ψυχρές επιφάνιες του λέβητα προωθώντας την θρόμβωση και την διάβρωση. Η επερχόμενη αλληλεπίδραση των αλκαλικών ειδών με το πυρίτιο δημιουργεί

πυριτικά αλκάλια με χαμηλό σημείο τήξης, τα οποία ύστερα διευκολύνουν την δημιουργία συμπαγούς και ισχυρής κρυστάλλινης απόθεσης μέσω της ρευστοποίησης άλλων διερχόμενων στοιχείων τέφρας. Αυτά τα συμπυκνωμένα χλωρίδια/θειικά μαζί με τα πυριτικά αλκάλια χαμηλής τήξης μειώνουν την απόδοση και την διαθεσιμότητα του λέβητα.

Μία αποτελεσματική λύση σε αυτά τα προβλήματα τέφρας της βιομάζας είναι η προσθήκη αργιλοπυριτικών μεταλλικών στοιχείων (π.χ. καολινίτης) κατά την καύση της βιομάζας. Προηγούμενες έρευνες έχουν αποδείξει τα πλεονεκτήματα των πρόσθετων με βάση το πυριτικό αργίλιο και την ικανότητα τους να αιχμαλωτίζουν τα στοιχεία αερίου καλίου. Ο μηχανισμός που λαμβάνει χώρα είναι, αρχικά ο σχηματισμός ενός άμορφου πυριτικού αργιλίου με το όνομα μετα-καολίνη ($Al_2O_3.2SiO_2$) κατά την θερμική αποσύνθεση του καολινίτη. Στην συνέχεια, η μετα-καολίνη αιχμαλωτίζει τα αέρια στοιχεία αλκαλίου (KOH, KCl και λιγότερο αποτελεσματικά το K_2SO_4) δημιουργώντας συστατικά με υψηλότερη θερμοκρασία τήξης. Με αυτό τον τρόπο ο σχηματισμός τηγμένων αποθέσεων, όπως και η υγροποίηση των χλωριούχων/θειικών αλκαλίων, στις ψυχρές επιφάνιες του λέβητα αναμένεται να μειωθούν. Επίσης, το πρόσθετο αντιδρά με το αέριο χλωριούχο κάλιο και μέσω αυτού απελευθερώνεται υδροχλωρικό οξύ, κάτι που με την σειρά του μειώνει τον κίνδυνο συμπύκνωσης των διαβρωτικών χλωριούχων αλκαλίων.

Ο στόχος αυτής της εργασίας είναι να αξιολογήσει την επίδραση των πρόσθετων με βάση το πυριτικό αργίλιο στον σχηματισμό τηγμένων αποθέσεων και συμπύκνωσης των αλκαλικών αλάτων στις ψυχρές επιφάνειες του λέβητα. Αυτός ο στόχος θα προσεγγιστεί με δύο ξεχωριστά βήματα. Το πρώτο είναι η προσομείωση με τη βοήθεια του Fact Sage της συμπεριφοράς της τέφρας δύο καυσίμων βιομάζας (ξηραμένο άχυρο και πελλέτες ξύλου) ανεμιγμένα με κυμαινόμενη ποσότητα πρόσθετων με βάση το πυριτικό αργίλιο. Το δεύτερο βήμα είναι η πειραματική αξιολόγηση της επίδρασης κυμαινόμενων ποσών πρόσθετων για το ξηραμένο άχυρο και τις πελλέτες ξύλου. Η πειραματική εργασία εστίασε στην αξιολόγηση της συμπεριφοράς του χλωρίου μέσω της μέτρησης του υδροχλωρικού οξέως.

8.2 Πειραματική Εγκατάσταση & Μεθόδος

8.2.1 Πειραματική Εγκατάσταση

Όλη η πειραματική διαδικασία έλαβε χωρα μέσα στον ατμοσφαιρικό κλίβανο κάθετης φλόγας (BTS-VR) θερμικής ισχύος 20kW στις εγκαταστάσεις του IFK (Ινστιτούτο Καύσης και Τεχνολογίας Λεβήτων) (Figure 3.1). Ο καυστήρας αποτελείται από ένα ηλεκτρικά θερμαινόμενο κεραμικό σωλήνα (θάλαμο), μήκους 2500 mm και διαμέτρου 200 mm. Μέσα στο σωλήνα μπορεί να επιτευχθεί ένα συγκεκριμένο θερμοκρασιακό προφίλ, μέσω θέρμανσης σε 5 διαφορετικές τοποθεσίες. Ο χρόνος διαμονής των σωματιδίων μέσα στο

θάλαμο ειναι 5-6 s. Τα καύσιμα εισάγωνταν σε ένα κωνικό σιλό πάνω από τον καυστήρα και από εκέι τρωφοδοτούνταν μέσω ενός ατέρμονα κοχλία μέσα σε ένα σωλήνα που οδηγούσε στην κορυφή του καυστήρα. Η συσκευή τροφοδότησης των πρόσθετων βρισκόταν δίπλα στην τροφοδοσία καυσίμου. Η εκτένης περιγραφή των δύο συστημάτων τροφοδοσίας παρουσιάζεται στην ενότητα 3.1.2. Ο κομιστής αέρας περνούσε διαμέσω της συσκευής τροφοδοσίας πρόσθετου και εισερχώταν στον ίδιο σωλήνα με το καύσιμο. Με αυτό τον τρόπο το καύσιμο, ο κομιστής αέρας και το πρόσθετο (όταν χρησιμοποιείτο) εισέρχωνταν στο θάλαμο ταυτόχρονα (Figure 3.7). Ο αέρας καύσης (πρωτεύων και δευτερεύον) εισαγόταν κατευθείαν στον καυστήρα. Στο τέλος του κλιβάνου, στα 2.5 m από τον καυστήρα, μετρούνταν οι εκπομπές του καυσαερίου. Το NO [ppm] και το NOx [ppm] μετρήθηκαν με τη βοήθεια ενός Chemiluminescence analyser, το O_2 μετρήθηκε με τη βοήθεια ενός paramagnetic analyser, τα SO_2, CO_2 vol.-% και CO vol.-% με NDIR (Nondispersive infrared analyser) και το O_2 [ppm] και SO_2 [ppm] με NDIR. Το HCl [ppm] μετρήθηκε με τη βοήθεια ενός FTIR Analyzer (Fourier Transform Infrared), με τη δειγματοληψία να πέρνει χώρα στον αγωγό καυσαερίων, πριν το φίλτρο (205~365 ˚C).

Gasmet™ FTIR

Η συντομογραφία FTIR συμαίνει Fourier Transform Infrared Spectroscopy. Ένας αναλυτής FTIR έχει τη δύνατότητα να ανιχνεύει αέρια συστατικά από την απορροφητικότητα τους σε υπέρυθρη ακτινοβολία. Κάθε συστατικό παράγει ένα μοναδικό υπέρυθρο φάσμα επειδή η κάθε μοριακή δομή έχει ένα μοναδικό συνδυασμό ατόμων, κάτι που επιτρέπει την αναγνώρηση (Ποιοτική ανάληση) και την ανάληση (Ποσοτική μέτρηση) του αέριου συστατικού. Ο αναλυτής FTIR μπορεί να ανιχνεύσει σχεδόν όλα τα στοιχεία σε αέρια φάση (οργανικά και μη οργανικά) και έτσι ταυτόχρονα να μετρήσει πολλαπλά αναλυόμενα σε ένα σύνθετο πλέγμα αερίων.

Η συσκευή που χρησιμοποιείται σε αυτή τη μελέτη είναι ένας φορητός αναλυτής αερίων FTIR τύπου Gasmet DX4000. Ολόκληρο το σετ εξαρτημάτων αποτελείται από τη μετρητική συσκευή Gasmet DX4000, ένα φορητό σύστημα δειγματοληψίας (συσκευή, καθετήρας) θερμαινόμενοι αγωγοί και ένα λάπτοπ εξοπλισμένο με το λογισμικό Calcmet.

Συσκευή τροφοδότησης πρόσθετων TOPAS SAG 410

Η συσκευή που χρησιμοποιήθηκε για τον εφοδιασμό πρόσθετου στο σύστημα είναι ένας διασκορπηστής σκόνης (SAG-Solid Aerosol Generator) με τη βοήθεια μιας μονάδος ελέγχου. Η διαδικασία διασκορπισμού σκόνης αποτελείται από δύο βήματα, τον εφοδιασμό του υλικού και το διασκορπισμό του σαν αεροζολ. Για εκτενέστερη περιγραφή της συσκευής και της λειτουργίας της βλ. ενότητα 3.1.2.

Καύσιμα & Πρόσθετα

Τα καύσιμα και πρόσθετα που χρησιμοποιήθηκαν σε αυτή τη μελέτη φαίνονται στον πίνακα Table 3-1. Η ανάλυση κατά προσέγγιση, η στοιχειώδης ανάλυση και η ανάλυση οξειδίων των καυσίμων φαίνεται στους πίνακες Table 3-2, Table 3-3 και **Table 3-5** αντίστοιχα. Οι θερμοκρασίες σύντηξη τέφρας των καφσίμων φαίνεται στον πίνακα Table 3-4. Για το καύσιμο WP+KCl δύο δείγματα πάρθηκαν και η εργαστηριακή ανάλυση ήταν όμοια και για τα δύο. Έτσι εδώ παρουσιάζεται ο μέσος όρος των αποτελέσμάτων των δύο δειγμάτων. Η ιδέα και η διαδικασία προετοιμασίας για το WP+KCl (πελλέτες ξύλου προανεμιγμένες με χλωριούχο κάλιο) παρουσιάζεται στην ενότητα 3.2.2. Επιπλέον, το επιτευγμένο περιεχόμενο χλωρίου του WP+KCl ήταν 5.3 φορές το αρχικό περιεχόμενο χλωρίου του WP. Η ανάλυση οξειδίων των πρόσθετων παρουσιάζεται στον πίνακα Table 3-6.

8.2.2 Πειραματική μέθοδος

Συνθήκες

Οι συνθήκες καύσης ήταν σταθερές με θερμοκρασία 1300 ˚C στην κορηφή του κλιβάνου, 1200 ˚C στη μέση και 1100 ˚C στον πυθμένα, ενώ η πίεση μέσα ήταν 1 atm. Ο ρυθμός τροφοδότησης καυσίμου κρατήθηκε γύρω στα 1.5 kg/h και η περίσσεια οξυγόνου στο τέλος του κλιβάνου γύρω στο 3%, έτσι ώστε να επιτευχθεί λόγος αέρα καυσίμου λ=1.15. Επίσης τα επίπεδα CO_2 κρατήθηκαν γύρω στο 16.5 %. Ο συνολικός όγκος καυσαερίων ήταν 11.5 Nm^3/h.

Πειραματική διαδικασία

Η πειραματική καμπάνια διεξήχθη σε διάρκεια δύο εβδομάδων. Την πρώτη εβδομάδα χρησιμοποιήθηκε Ξηραμένο Άχυρο (TS) σαν καύσιμο ενώ τη δεύτερη εβδομάδα Πελλέτες Ξύλου και Πελλέτες Ξύλου (WP) προανεμιγμένες με χλωριούχο κάλιο (WP+0.25%KCl). Ο στόχος ήταν να εξεταστεί πώς άλλαζαν τα επίπεδα HCl με τη χρήση πρόσθετων, έτσι έλαβαν χώρα ξεχωριστές πειραματικές συνεδρίες για κάθε καύσιμο με κοιμενόμενα ποσά προσθέτων. Μια λίστα με τις πειραματικές συνεδρίες που έλαβαν χώρα φαίνεται στον πίνακα Table 3-7. Στον πίνακα φαίνονται καύσιμα που χρησιμοποιήθηκαν σε κάθε συνεδρία, καθώς και η διακύμανση του πρόσθετου αλλά και το είδος των μετρήσεων που έλαβαν χώρα.

Κάθε μέτρηση μέσω του μετρητικού εξοπλισμού γινόταν συνεχόμενα και επαναλαμβανόμενα κάθε 10 ή 20 δευτερόλεπτα, ανάλογα με τις ρυθμίσεις του εξοπλισμού. Κυρίως η ποσότητα του HCl σε ppm, αλλά και των CO σε ppm και O_2 σε vol.-% ήταν τα αντικείμενα παρακολούθησης. Κάθε συνεδρία ξεκινούσε με την καύση καθαρού καυσίμου. Όταν οι συγκεντρώσεις HCl αυξάνονταν και ύστερα σταθεροποιούνταν για το καθαρό καύσιμο, άρχιζε

η εισαγωγή του πρόσθετου στο σύστημα. Αυξήσεις στην ταχύτητα της ζώνης της συσκευής τροφοδότησης του πρόσθετου κατα 5, 10, ή 20% (ανάλογα με το πόσο μεγάλη ήταν η διαφορά από τις προηγούμενες μετρήσεις) γίνονταν διαδοχικά, κάθε φορά που οι τιμές του HCl παρατηρούνταν ότι αύξαναν από τις προηγούμενες τιμές και ύστερα σταθεροποιούνταν ξανά. Η ταχύτητα ανάδευσης του πρόσθετου μέσα στο ρεζερβουάρ της συσκευής τροφοδοτήσεως ήταν σταθερή και αύξανε η μειωνόταν όπου αυτό κρινόταν σκόπιμο και εξυπηρετούσε προς καύτερη τροφοδότηση του υλικού. Αν μετά από αλλαγές στις ρυθμίσεις τις συσκευής τα επίπεδα HCl εξακολουθούσαν να μην αυξάνονται, τότε αυτό σήμαινε ότι δεν ήταν δυνατή η επίτευξή μεγαλύτερου ρυθμού τροφοδότησης πρόσθετου στο σύστημα μας, ή ότι τα μέγιστα επίπεδα HCl είχαν επιτευχθεί. Στη συνέχεια η τροφοδότηση πρόσθετου τερματιζόταν και παρατηρείτο ο ρυθμός μείωσης της συγκέντρωσης του HCl, για μια περίοδο 5 έως 10 λεπτών.

Η ιδέα των πελλετών ξύλου προανεμιγμένων με χλωριούχο κάλιο (WP+KCl)

Στην περίπτωση του ξηραμένου άχυρου (TS), λόγω της υψηλής του περιεκτικότητας σε Cl, οι χαμηλότερες (στην περίπτωση κάυσης καθαρού καυσίμου) και υψηλότερες συγκεντρώσεις HCl ήταν αρκετά υψηλές ώστε να μπορούν να εξετασθούν και επίσης η διαφορά μεταξύ τους ήταν μεγάλη. Το ίδιο συνέβει και για την Aurora και το Bentonite ως πρόσθετα. Αντιθέτως, στην περίπτωση των πελλετών ξύλου (WP), λόγω της χαμηλότερης περιεκτικότητας του σε Cl, οι χαμηλότερες και οι υψηλότερες συγκεντρώσεις HCl ήταν χαμηλές, έτσι η επίδραση των πρόσθετων δε μπρορούσε να εξεταστεί ικανοποιητικά. Αυτό οδήγησε στην ιδέα της ανάμηξης WP με KCl ώστε να αυξηθεί η περιεκτικότητα Cl των πελλετών σε 6 φορές την αρχική. Με αυτό τον τρόπο επιτεύχθηκαν τα υψηλότερα επίπεδα HCl μεταξύ όλων των πειραματικών συνεδριών. Η διαδικασία ανάμηξης του καυσίμου με το KCl περιγράφεται στην ενότητα 3.2.2.

Θερμοχημική προσομοίωση

Μέρος αυτής της έρευνας είναι επίσης η θεωρητική εξέταση της επίδρασης των πρόσθετων μέσω της θερμοχημικής προσομοίωσης και η σύγκριση αυτών των αποτελεσμάτων με τα πραγματικά πειραματικά αποτελέσματα. Γι' αυτό το σκοπό χρησιμοποιήθηκε το θερμοχημικό λογισμικό και οι βάσεις δεδομένων 'FactSage software 6.3', ώστε να πραγματοποιήσει υπολογισμούς σε συνθήκες ισοροπίας, στο θερμοκρασιακό εύρος που συναντάται στο θάλαμο καύσης.

8.3 Αποτελέσματα

Σε αυτή την ενότητα παρουσιάζονται τα αποτελέσματα των πειραμάτων καθώς και της προσομείωσης, ξεχωριστά και με τη σειρά που διεκπαιρεώθηκαν. Συμπεριλαμβάνονται περιγραφή, συζήτηση και σχόλεια για καλύτερη επεξήγηση και κατανόηση των αποτελεσμάτων.

8.3.1 Αποτελέσματα πρσομοίωσης σε συνθήκες ισορροπίας

Οι υπολογισμοί έγιναν για ένα μεγάλο εύρος θερμοκρασιών από 500 έως 1500 °C και κυρίως για θερμοκρασίες μέσα στον κλίβανο (1100-1300 °C). Επίσης άλλοι παράμετροι κυμάνθηκαν σε ένα επιθυμητό εύρος ώστε να διερευνηθεί η επίδραση τους πάνω στα είδη τέφρας και στη δημιουργία αποθέσεων.

Λόγος ρευστού μίγματος

Ο λόγος ρευστού μίγματος SR (Slag Ratio) ορίζεται εδώ ως:

$$SR = \frac{liquids}{liquids + solids} \quad (8\text{-}1)$$

Όπου τα υγρά (liquids) είναι το άθροισμα όλων των υγρών συστατικών της τέφρας και στερεά (solids) το άθροισμα όλων των στερεών συστατικών της τέφρας που παράγονται σε αυτές τις θερμοκρασίες. Όλα τα συστατικά μετρούνται σε γραμμάρια. Ο λόγος ρευστού μίγματος χρησιμοποιείται για να εξετασθεί η τάση προς δημιουργία επικαθίσεων των δύο καυσιμων βιομάζας και να δειχθεί σε ποιά θερμοκρασία είναι πιο κρίσιμη. Ένας πρώτος υπολογισμός και μια πρώτη σύγκριση μεταξύ των λόγων δύο καυσίμων, για λ=1.15 και ένα μεγάλο θερμοκρασιακό εύρος (500-1500°) φαίνεται παρακάτω (Figure 8.1, Figure 8.2).

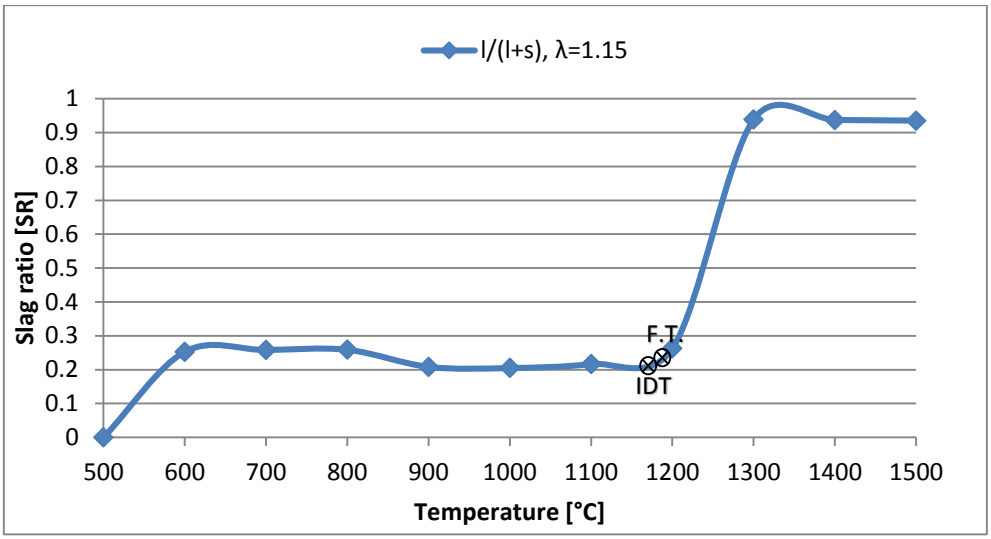

Figure 8.1: Λόγος ρευστού μίγματος Πελλετών Ξύλου για εύρος θερμοκρασιών και λ=1.15

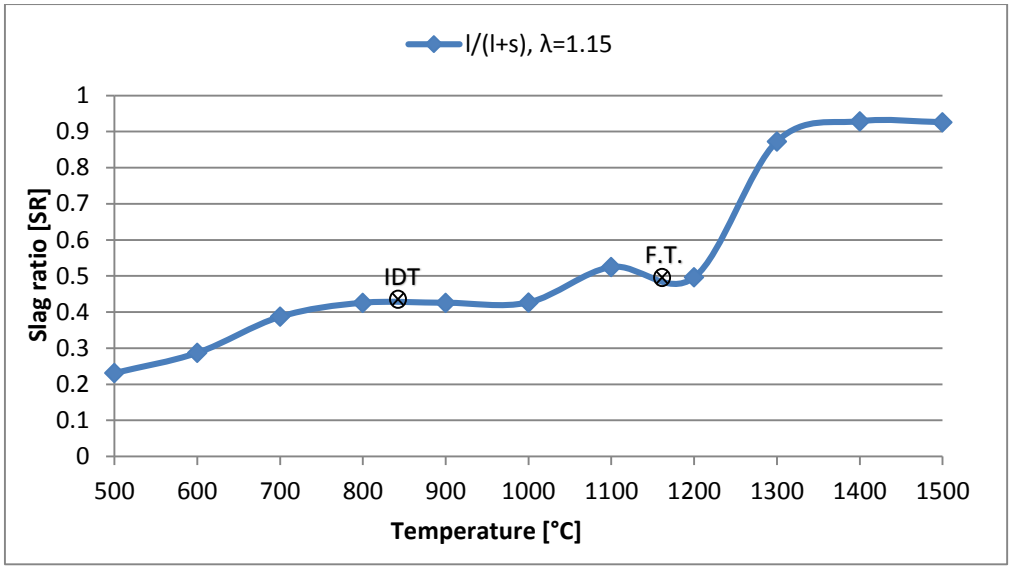

Figure 8.2: Λόγος ρευστού μίγματος ς Ξηραμένου Άχυρου για εύρος θερμοκρασιών και λ=1.15

Αρχικά τα παραπάνω αποτελέσματα δείχνουν ότι, καθώς η θερμοκρασία αυξάνεται το ίδιο συμβαινει και με τους λόγους ρευστού μίγματος. Αυτό συμβαίνει επειδή με την αύξηση της θερμοκρασίας τα στερεά συστατικά μειώνονται ενώ τα υγρά συστατικά αυξάνονται. Η σύγκριση μεταξύ των δύο καυσίμων βιομάζας δείχνει ότι το TS έχει υψηλότερους λόγους ρευστού μίγματος στο μεγαλύτερο εύρος των εξεταζόμενων θερμοκρασιών. Αυτό συμβαίνει επειδή η αρχική θερμοκρασία παραμόρφωση της τέφρας του TS είναι 840 °C η οποία είναι αρκετά χαμηλότερη από την αντίστοιχη θερμοκρασία του WP που είναι 1170 °C (Table 3-4). Έτσι τα συστατικά της τέφρας του TS ξεκινάνε να τήκωνται νωρίτερα από αυτά του WP. Παρόλα αυτά και στα δύο διαγράμματα (Figure 8.1, Figure 8.2) φαίνεται ότι οι θερμοκρασίες υγροποίησης της τέφρας των TS και WP είναι πολύ κοντά, στους 1160 και 1190 °C

αντίστοιχα. Μετά από αυτές τις κρίσιμες θερμοκρασίες, σχεδόν όλα τα συστατικά τέφρας μεταβαίνουν στην υγρή φάση. Έτσι οι λόγοι ρευστού μίγματος αυξάνουν ραγδαία πάνω από τους 1200 °C, και στους 1400 °C οι λόγοι και για τα δύο καύσιμα βρίσκονται ήδη πάνω από το 0.9. Αυτό μεταφράζεται σε πολύ υψηλό κίνδυνο αποθέσεων και διάβρωσης μέσα στο θάλαμο καύσης, όπου υπάρχουν τόσο υψηλές θερμοκρασίες. Η προσομοίωση της συμπεριφοράς της τέφρας με τη βοήθεια του FactSage έχει εξετασθεί από πολλούς συγγραφείς. Η αύξηση της ποσότητας επικαθίσεων με την αύξηση της θερμοκρασίας είναι ένα κοινό εύρημα.

Ο λόγος ρευστού μίγματος υπολογίστηκε επίσης για διφορετικά λ (λόγος αέρα καυσίμου). Υπολογισμοί για το θερμοκρασιακό εύρος 500-1500 °C και για λ=0.7-1.15 λάβαν χώρα και τα αποτελέσματα φαίνονται παρακάτω.

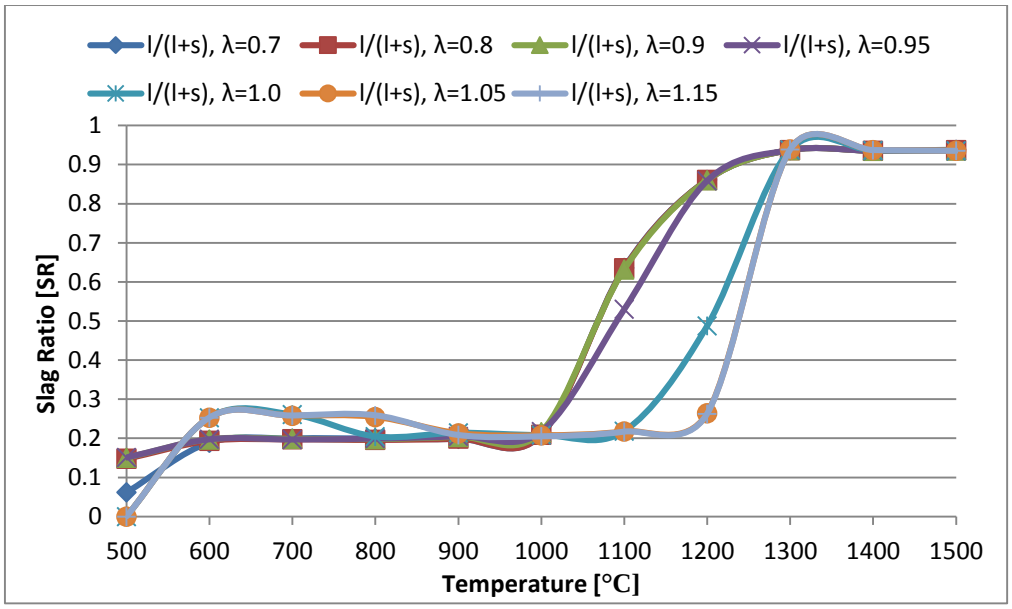

Figure 8.3: Λόγος ρευστού μίγματος των Πελλετών Ξύλου για κυμαινόμενη θερμοκρασία και λ.

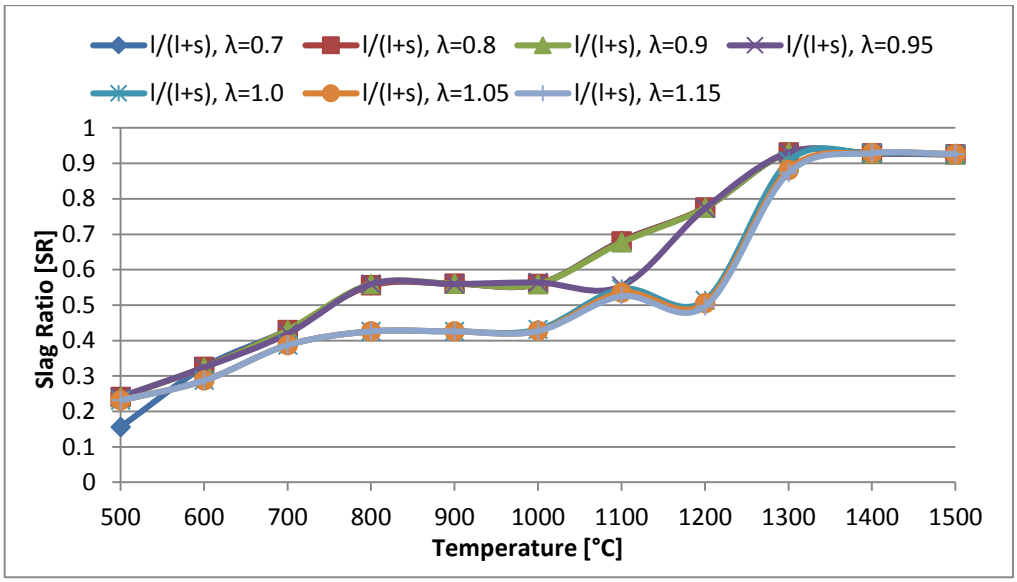

Figure 8.4: Λόγος ρευστού μίγματος του Ξυραμένου Άχυρου για κυμαινόμενη θερμοκρασία και λ.

Μια πρώτη ματιά δείχνει ότι το λ είναι ένας παράγοντας που επηρεάζει του λόγους ρευστού μίγματος. Στην περίπτωση του WP (Figure 8.3), μπορούν να διακριθούν δύο θερμοκρασιακές ζώνες όπου η συμπεριφορά σχηματισμού επικαθίσεων αλλάζει. Για τις χαμηλότερες θερμοκρασίες (600-900 °C), καθώς το λ αυξάνει, ο λόγος ρευστού μίγματος αυξάνει επίσης. Όμως για υψηλότερες θερμοκρασίες (1000-1300 °C), καθώς το λ αυξάνει, ο λόγος ρευστού μίγματος μειώνεται. Ακόμα αυτή η συμπεριφορά μπορεί να χωριστεί σε σχέση με το λ σε 3 ομάδες. Μία για υποστοιχειομετρική καύση (λ<1), μία για στοιχειομετρική (λ=1) και μια για υπερστοιχειομετρικη (λ>1).

Στην περίπτωση του TS (Figure 8.4), παντού μεταξύ 700 και 1300 °C η συμπεριφορά των λόγων ρευστού μίγματος είναι παρόμοια, δηλαδή καθώς το λ αυξάνει ο λόγος ρευστού μίγματος μειώνεται. Σε σχέση με το λ μπορούμε να χωρίσουμε αυτή τη συμπεριφορα σε 2 ομάδες. Μία για λ<1 και μία για λ≥1. Συνεπώς, σε υψηλές θερμοκρασίες όπου η κάυση λαμβάνει χώρα, όπως μέσα στον κλίβανο, είναι προτιμέτερο να υπάρχει λόγος αέρα καύσης μεγαλύτερος του 1 ώστε ο λόγος ρευστού μίγματος να μειώνεται σημαντικά, όπως φαίνεται στις Figure 8.3 και Figure 8.4.

Σχηματισμός συστατικών σε σχέση με το λ

Όπως φαίνεται παραπάνω, ο λόγος ρευστού μίγματος τείνει να ελαττωθεί όταν ο λόγος αέρα καυσίμου μειώνεται σε υψηλές θερμοκρασίες. Εδώ παρουσιάζονται λεπτομερώς οι αλλαγές στα παραγόμενα συστατικά για τη θερμοκρασία των 1200 °C και για διακύμανση του λ, καθώς επίσης επεξηγείται πως επηρεάζεται ο λόγος ρευστού μίγματος. Η θερμοκρασία επιλέχθηκε σαν αντιπροσωπευτική για συνθήκες στο μέσο του λέβητα.

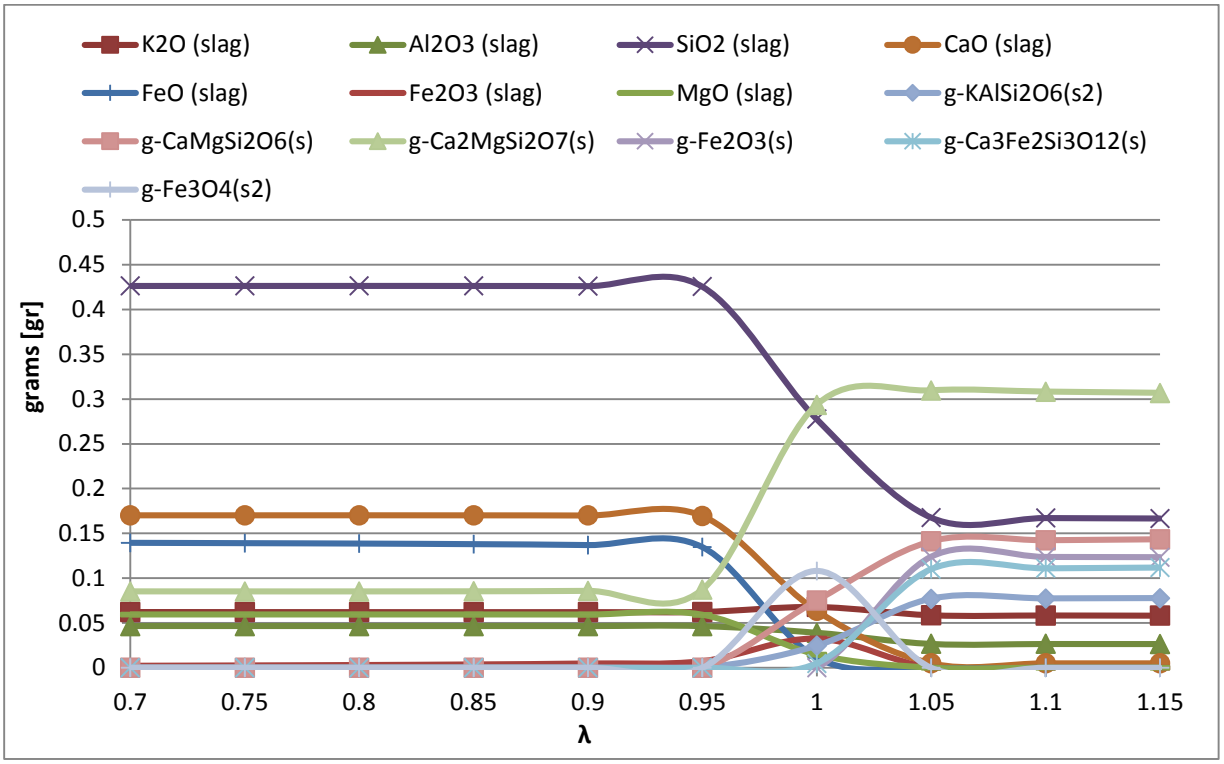

Figure 8.5: Διακύμανση των προιόντων καύσης Πελλετών Ξύλου για κύμανση του λ, 1200 °C.

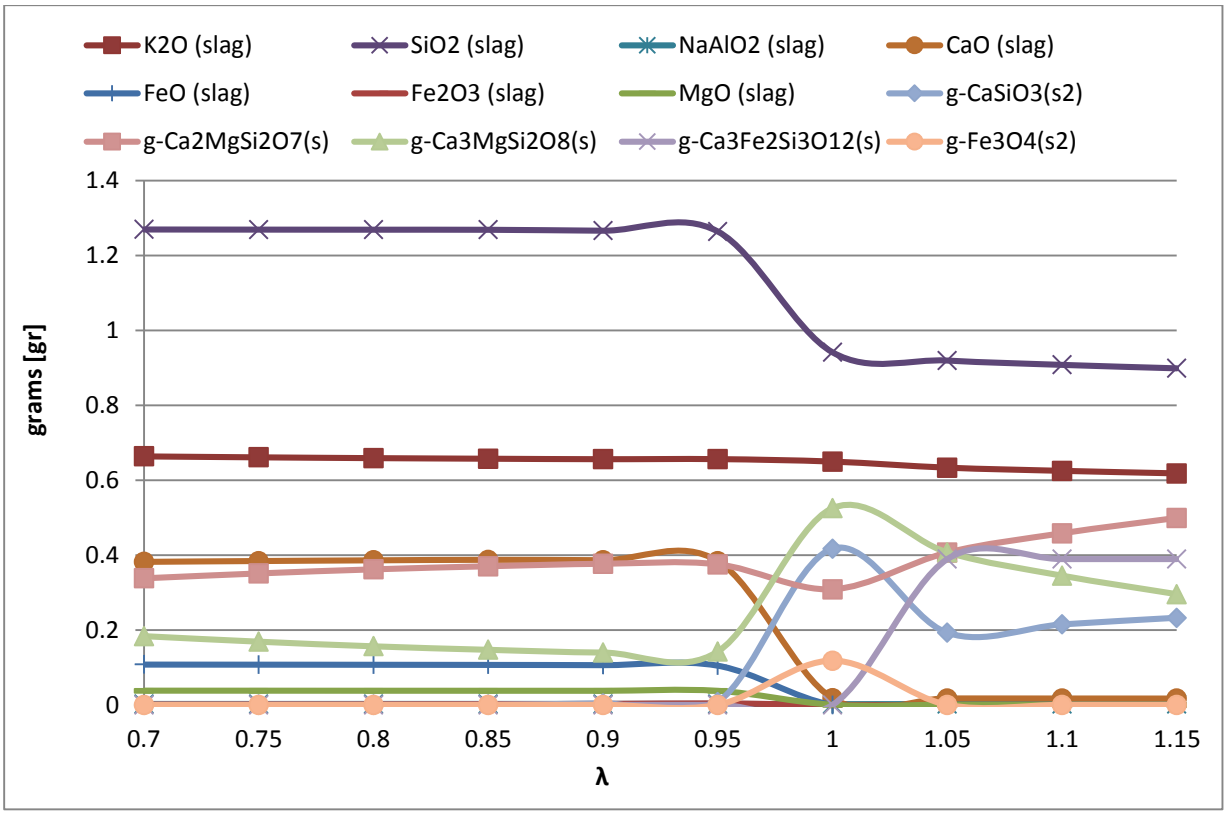

Figure 8.6: Διακύμανση των προιόντων καύσης Ξηραμένου Άχυρου για κύμανση του λ, 1200 °C.

Για το WP (Figure 8.5) και TS (Figure 8.6) η συμπεριφορά των παραγόμενων στοιχείων είναι παρόμοια. Για χαμηλότερες τιμές λ (0.7-0.95) σχηματίζεται κυρίως ρευστό μίγμα (**slag**), ενώ τα στερεά είναι λιγότερα ή δεν υπάρχουν καθόλου. Για 0.95≤λ≤1.05 υπάρχει μια περιοχή όπου οι φάσεις και οι ποσότητες των συστατικών αλλάζουν. Έτσι, καθώς το λ αυξάνει σ'αυτή την περιοχή, το ρευστό μίγμα μειώνεται ενώ τα στερεά αυξάνονται. Τέλος, για υψηλότερα λ (1.5-1.15), τα ρευστά είναι λιγότερα, ενώ τα στερεά είναι υψηλότερα ή αρχίζουν να σχηματίζονται. Γενικά το εύρος 0.95≤λ≤1.05 είναι μια μεταβατική περιοχή, ενώ για λ<0.95 και λ>1.05, τα συστατικά τείνουν να είναι πιο σταθερά.

Κάλιο στα προϊόντα των WP και TS σε σχέση με τη θερμοκρασία

Οι υψηλοί λόγοι ρευστού μίγματος που παρατηρήθηκαν στις Figure 8.1 και Figure 8.2, προκαλούνται κυρίως από τα διάφορα είδη καλίου. Γιαυτό το λόγο αυτό το κομμάτι των αποτελεσμάτων εστιάζει κυρίως στη συμπεριφορά του K των προϊόντων της καύσης. Στις εικόνες Figure 8.7 και Figure 8.8 παρουσιάζεται πως το κάλιο (K) κινείται μεταξύ διαφόρετικών προϊόντων εξαρτόμενο από ένα μεγάλο θερμοκρασιακό εύρος, για λόγο αέρα καυσίμου 1.15.

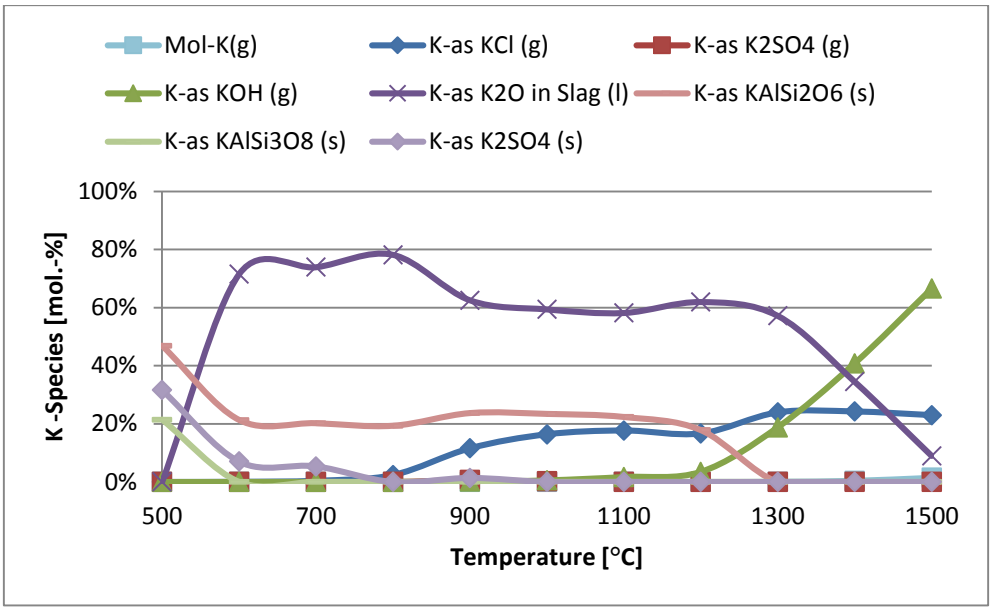

Figure 8.7: Μοριακός λόγος του καλίου στα διάφορα είδη καλίου του WP, λ=1.15.

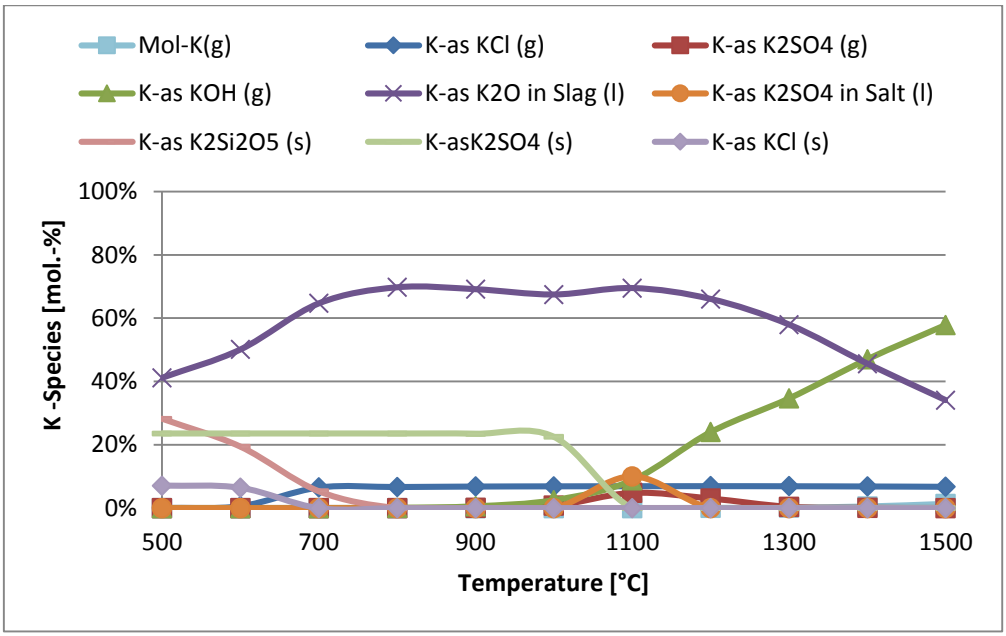

Figure 8.8: Μοριακός λόγος του καλίου στα διάφορα είδη καλίου του TS, λ=1.15.

Στις περιπτώσεις και των δύο καυσίμων φαίνεται μια γενική τάση του καλίου να υπάρχει, στο μεγαλυτερο μέρος αυτού του θερμοκρασιακού εύρους, κυρίως μέσα σε ρευστό μίγμα.

Ξεκινώντας από την υψηλότερη θερμοκρασία, είναι φανερό ότι το κάλιο υπάρχει κυρίως σε αέρια συστατικά, όπως το KOH(g) και το KCl(g) (συν ένα μικρό ποσοστό K(g)) και λιγότερο σε ρευστό μίγμα. Καθώς η θερμοκρασία μειώνεται, το ποσοστό του K μέσα ο ρευστό μίγμα αυξάνεται, ενώ η μεγάλη διαθεσιμότητα του KOH οδηγεί προς το σχηματισμό πυριτικών καλίων και πυριτικών αργιλιοκαλίων. Επιπλέον, η ύπαρξη SO_2 σε συσδυασμό με τα

υπάρχοντα χλωρίδια και υδροξείδια οδηγεί στην παραγωγή θειικών. Ακόμα, είναι φανερό πως για το TS, το ίδιο ποσοστό αερίου KCl μετατρέπεται απευθείας σε στερεό KCl. Αυτό σημαίνει ότι η ποσότητα KCl εξαρτάται αποκελιστικά από το περιεχόμενο ποσοστό Cl του καυσίμου. Επίσης, καθώς η θερμοκρασία μειώνεται, η αντίστοιχη μοριακή ποσότητα καλίου, δε περνάει από την υγρή φάση, επειδή αν αιχμαλωτιζόταν στο ρευστό μίγμα, τότε το χλώριο θα απελευθερωνόταν σαν αέριο HCl, κάτι που είναι μια μη αναστρέψιμη αντίδραση και ύστερα το KCl(s) δε θα σχοιματιζοταν. Παρόλα αυτά, για το WP, καθώς ο χρόνος περνάει, το αέριο KCl αντιδρά ξανά με το SO_2 και παράγεται K_2SO_4(s). Υγρό K_2SO_4 φαίνεται να σχηματίζεται μόνο στην περίπτωση του TS, για 1100°C.

Άλλη συμαντικη παρατήρηση στην περίπτωση του TS, είναι ότι το κάλιο που υπάρχει μέσα στο ρευστό μίγμα, μένει σε υψηλά επίπεδα ακόμα και στις υψηλότερες και στις χαμηλότερες θερμοκρασίες του εύρους. Το περιεχόμενο κάλιο στο καύσιμο είναι τόσο πολύ που δε μπορεί να αιχμαλωτιστεί όλο από άλλα συστατικά, όπως τα Si, Al ή SO_4 (θειωποίηση).

Και οι δύο περιπτώσεις καυσίμων βοηθούν προς την κατανόηση του ότι, επειδή ρευστό μίγμα εμφανίζεται ήδη στις χαμηλές θερμοκρασίες, χρειάζεται να χρησιμοποιηθούν μέσα για την αύξηση της θερμοκρασίας τήξης των στοιχείων καλίου της τέφρας, ώστε να μειωθούν τα προβλήματα αποθέσεων σε θερμοκρασίες λειτουργίας σχετικές με την καύση κονιορτοποιημένου καυσίμου.

Διακύμανση Καολινίτη

Σε αυτό το στάδιο παρουσιάζεται στην εικόνα Figure 8.9 η προσθήκη Καολινίτη και η επίδραση του στη συμπεριφορά των ειδών καλίου. Η επιλογή του Καολινίτη έγινε επειδή αυτό είναι το βασικό συστατικό των πρόσθετων με βάση το πυριτικό αργίλιο, τα οποία έχουν την ικανότητα να ανεβάζουν τη θερμοκρασία τήξης των ειδών της τέφρας. Η διακύμανση έγινε από 0 έως 6.17 γραμμάρια ή από 0 έως 100% αντιστοίχως, και αυτό το ποσό επιλέχθηκε μετά από μια πληθώρα υπολόγισμών έτσι ώστε να επιτευχθούν τα καλύτερα αποτελέσματα, εννοώντας τον περιορισμό του K στο ρευστό μίγμα. Ο λόγος αέρα καυσίμου ορίστηκε σε λ=1.15 και η θερμοκρασία στους 1200 °C, επειδή μπορεί να βρεθεί μέσα στο θάλαμο καύσης και επειδή, οπώς φλέπουμε στην Figure 8.2, μετά από αυτή τη θερμοκρασία οι λόγοι ρευστού μίγματος αυξάνονται ραγδέως.

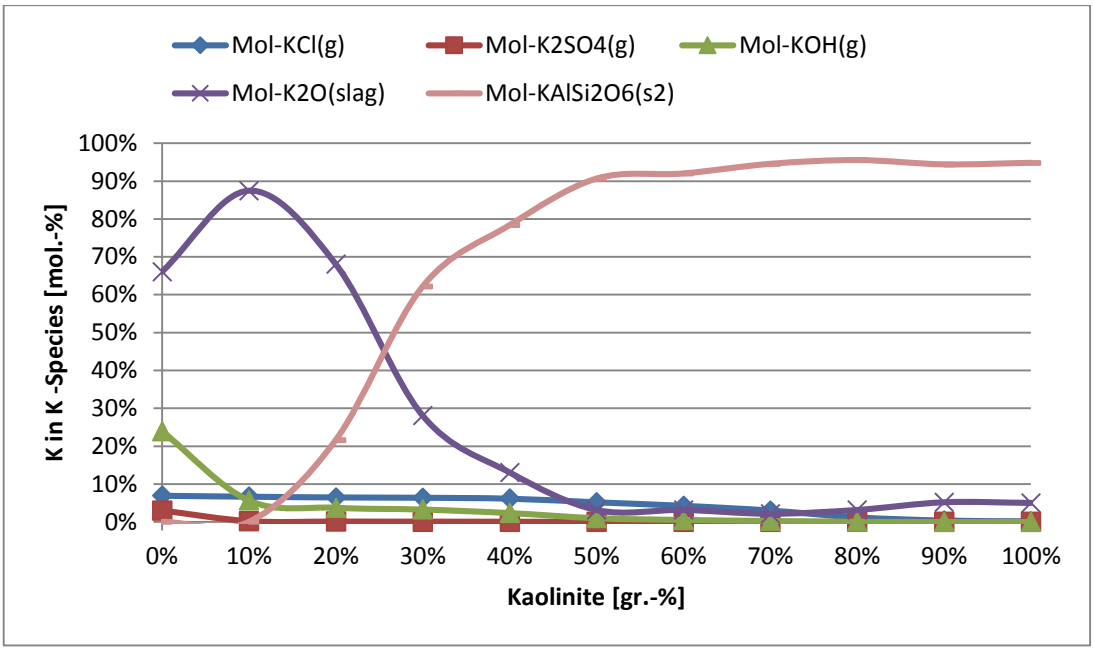

Figure 8.9: Επίδραση της διακύμανσης Καολινίτη στην κατανομή καλίου. Ξηραμένο Άχυρο, 1200 °C, λ=1.15

Για 0-10% διακύμανση, καθώς ο πρόσθετο αυξάνεται, ο Καολινίτης αντιδρά με το λοιπό κάλιο στο αέριο (KOH, K_2SO_4) και σχεδόν όλο το κάλιο πηγαίνει προς το ρευστό μίγμα. Με ακόμα μεγαλύτερη εισαγωγή Καολινίτη στο σύστημα, αντιδρά με ότι περίσεψε από το λοιπό Κάλιο στο αέριο, με το KCl και κυρίως με το K στο ρευστό μίγμα και ως αποτέλεσμα αρχίζουν να σχηματίζονται πυριτικά αργιλιοκάλια και αυξάνονται αναλόγως. Τέλος, για 80-100% διακύμανση, το μεγαλύτερο μέρος του K υπάρχει μέσα στα πυριτικά αργιλιοκάλια. Είναι σημαντικό να παρατηρηθεί ότι το KCl αντιδρά ελαφρώς για μικρή διακύμανση Καολινίτη, ενώ αυτή η αντίδραση γίνεται σημαντική κοντά στο 50% της διακύμανσης, αφού το πρόσθετο έχει αντιδράσει με σχεδόν όλο το K στο ρευστό μίγμα. Φαίνεται λοιπόν ότι η αντίδραση των πυριτικών αργιλίων με το KCl δεν προηγείται.

Το επόμενο βήμα είναι να εξετασθέι πως συμπεριφέρεται το Cl όταν το πρόσθετο εισάγεται στο σύστημα. Η προσομοίωση πραγματοποιήθηκε για τις ίδιες συνθήκες και παραμέτρους Τα αποτελέσματα φαίνοντα στην εικόνα Figure 8.10.

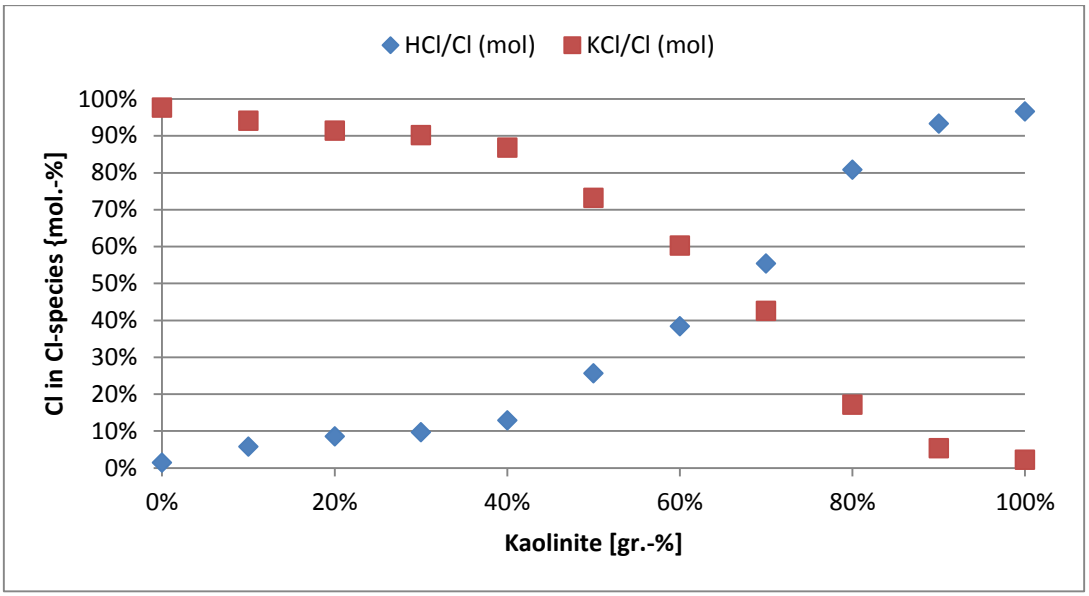

Figure 8.10: Επίδραση της διακύμανσης Καολινίτη στην κατανομή χλωρίου. Ξηραμένο Άχυρο, 1200 °C, λ=1.15

Μια πρώτη όψη δείχνει ότι το Cl υπάρχει αποκλειστικά μέσα στα δύο συστατικά, KCl και HCl. Οι συμπεριφορά τους είναι αντίθετη καθώς η εισάγωγή του πρόσθετου στο σύστημα αυξάνεται, επειδή οι αντιδράσεις (2-14), (2-15) και (2-16) λαμβάνουν χώρα. Για χαμηλή διακύμανση Καολινίτη, όπως ειπώθηκε προηγουμένως, η αντίδραση με το KCl είναι περιορισμένη (επειδή το πρόσθετο αντιδρά πρώτα με τα άλλα συστατικα καλίου), πράγμα που οδηγεί σε μικρή αύξηση του HCl. Με μεγαλύτερη εισαγωγή Καολινίτη, ο ρυθμός αντίδρασης με το KCl αυξάνεται επειδή το πρόσθετο ξεκινά να αντιδρά περισσότερο με το KCl, και έτσι αυξάνεται επίσης ο ρυθμός σχηματισμού του HCl. Ειδικά μετά από διακύμανση 50%, ο Καολινίτης αντιδρά κυρίως με το KCl, και για μέγιστη εισαγωγή Καολινίτη στο σύστημα τα ποσά KCl είναι αμελητέα και όλο το περιεχόμενο Cl υπάρχει σαν αέριο HCl.

Σε αυτό το σημείο παρουσιάζεται μια σημαντική παρατήρηση για τις Figure 8.9 και Figure 8.10. Όταν το HCl είναι υψηλό σημαίνει πως το πρόσθετο έχει αντιδράσει με το KCl, αλλά προηγουμένως έχει αντιδράσει με το K στο ρευστό μίγμα, έτσι εκεί είναι χαμηλό. Επομένως οι υψηλές συγκεντρώσεις HCl μπορεί να συνεπάγονται ότι το κάλιο στο ρευστό μίγμα έχει αντιμετωπισθεί.

8.3.2 Πειραματικά Αποτελέσματα

Συμπεριφορά της καύσης

Για όλες τις πειραματικές συνεδρίες η περίσσεια οξυγόνου (O_2) εξόδου και το διοξείδιο του άνθρακα (CO_2) διατηρήθηκαν περί το 3 vol.-% και 16.5 vol.-% αντίστοιχα. Ακόμα, η συγκέντρωση του μονοξειδίου του άνθρακα (CO) είναι ενδεικτική για την απόδοση της

διδικασίας καύσης, επειδή υψηλότερα επίπεδα CO δείχνουν ατελή καύση, ενώ μεγάλες αυξομειώσεις CO μπορεί να σημαίνουν αστάθεια στην καύση. Στα παρούσα πειράματα οι τιμές CO ήταν σχετικά χαμηλές, κυρίως κάτω από 20 ppm.

Στην εικόνα Figure 8.11, δίνεται σαν παράδειγμα η περίπτωση του WP+KCl, όπου φαίνονται οι μετρήσεις των εκπομπών πριν και μετά τη χρήση πρόσθετου. Είναι φανερό πως για καύση διαρκείας μόνο του καυσίμου, όλα τα συστατικά των εκπομπών είναι μέσα σε όρια και οι διακυμάνσεις δεν είναι σημαντικές. Ακόμα, όταν το πρόσθετο εισέρχεται στο σύστημα, το εύρος των εκπομπών δεν αλλάζει. Αυτό σημαίνει όχι μόνο πως κάθε συνεδρία ξεχωριστά ήταν σταθερή, αλλά ακόμα ότι η εισαγωγή πρόσθετου δεν επηρεάζει την συμπεριφορά της καύσης. Όλες οι υπόλοιπες περιπτώσεις δείχνουν μία όμοια σταθερότητα και ποιότητα καύσης.

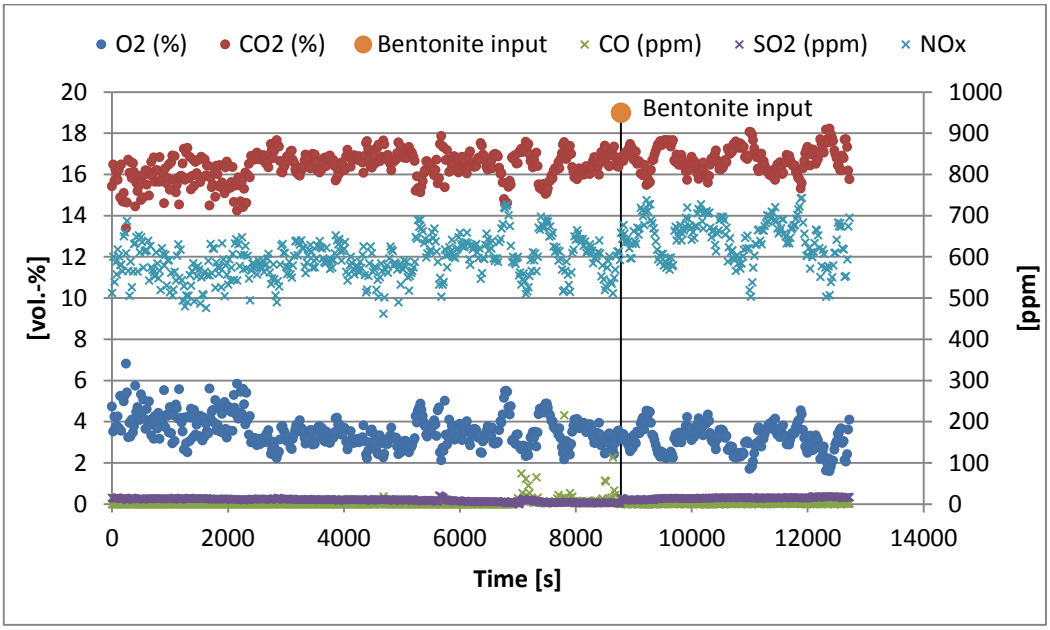

Figure 8.11: Εκπομπές καύσης για WP+0.25%KCl με και χωρίς προσθήκη Βεντονίτη.

Επίδραση της χρήσης πρόσθετου στην εκπομπή HCl

Η μέγιστη θεωρητική συγκέντρωση HCl στις εκπομπές που μπορεί να επιτευχθεί αν όλο το περιεχόμενο Cl του καυσίμου αντιδρούσε προς το σχηματισμό HCl υπολογίζεται με τη βοήθεια του τύπου:

$$C_{HCl_{max}} = \frac{\frac{\gamma_{Cl}}{M_{Cl}} * \frac{M_{HCl}}{V_{mol}} * 10^6}{(\frac{\gamma_S}{M_S} + \frac{\gamma_C}{M_C} + \frac{\gamma_N}{2M_N} + \frac{0.79}{0.21}\left(\frac{\gamma_S}{M_S} + \frac{\gamma_C}{M_C} + \frac{\gamma_H}{4M_H} - \frac{\gamma_O}{2M_O}\right)) \frac{21}{21 - y_{O_2}}} \quad (8\text{-}2)$$

σε mg/m^3 όπως φαίνεται στην ενότητα 4.2.1.

Για να συγκρίνουμε αυτή την τιμή με τις μετρήσεις μας, η (4-2) μετατρέπεται έτσι ώστε τα αποτελέσματα να έιναι σε ppm, στον καινούργιο τύπο:

$$HClmax = C_{HCl_{max}} * \frac{V_{mol}}{M_{HCl}} \quad (8\text{-}3)$$

Πλήρεις πειραματικές συνεδρίες

Οι πλήρεις πειραματικές συνεδρίες για τα TS και WP+KCl και τα πρόσθετα παρουσιάζεται στις εικόνες Figure 8.12, Figure 8.13, Figure 8.14, Figure 8.15 και Figure 8.16. Σε κάθε διάγραμμα φαίνεται η επίδραση του πρόσθετου που χρησιμοποιείται, με την παρουσίαση κάθε μοναδικής συγκεντρωσης HCl στην πορεία του χρόνου. Οι αριθμοί πάνω απο τα διαγράμματα υποδεικνύουν τους ρυθμούς τροφοδότησης του πρόσθετου σε gr/h, οι οποίοι προσαρμόστηκαν κατά τη συνεδρία εκείνη τη χρονική στιγμή. Ακόμα, οι μέγιστη θεωρητική συγκέντρωση HCl εικονίζεται ως το άνω όριο για κάθε καύσιμο.

Από δω και στο εξής, όταν αναφερόμαστε σε τιμές συγκέντρωσης HCl, η λέξη συγκέντρωση μπορεί να παραλείπεται για χάριν ευκολίας.

Ξηραμένο Άχυρο

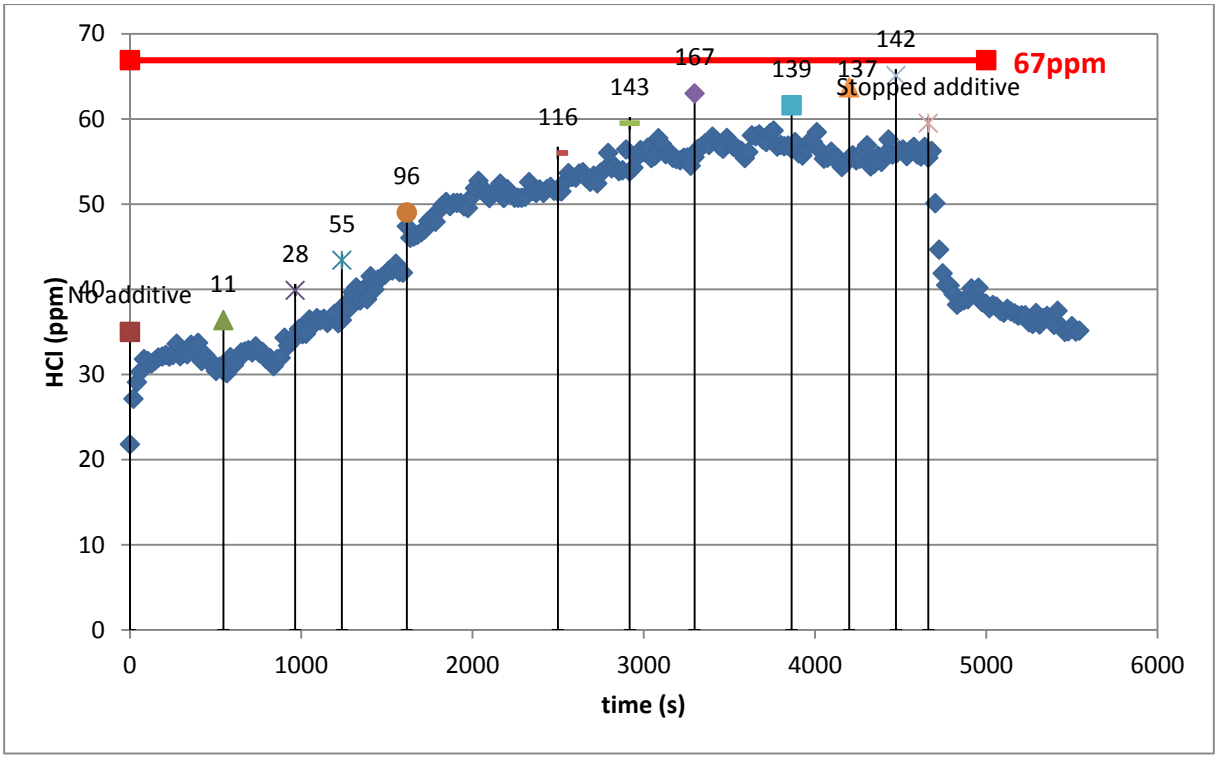

Figure 8.12: Πλήρης συνεδρία Ξηραμένου Άχυρου με Αρόρα

Στην εικόνα Figure 8.12, παρουσιάζεται η πλήρης πειραματική συνεδρία καύσης Ξηραμένοου Άχυρου (TS) με προσθήκη Αρόρας (Aurora). Η μέγιστη θεωρητική τιμή HCl για το TS υπολογίστηκε στα 67 ppm. Μια γενική όψη της εικόνας δείχνει πως οι εκπομπές HCl για καθαρό TS ξεκινούν με χαμηλές τιμές και ανεβαίνουν καθώς η τροφοδότηση της Aurora ξεκινά και ύστερα αυξάνεται. Ξεκινούν από 32 ppm, το οποίο σημαίνει πως για καθαρό καύσιμο, το 48% του Cl υπάρχει στο HCl(g). Ύστερα το πρόσθετο εισάγεται στο σύστημα ακολουθώντας τη διαδοχικη διαδικασία που περιγράφεται στο 8.2.2. Τελικά το HCl φτάνει τη μεγαλύτερη τιμή του γύρω στα 57 ppm που είναι κοντά στη μέγιστη θεωρητική (67 ppm), όπου επίσης επιτυγχάνεται και ο μεγαλύτερος ρυθμός τροφοδότησης Aurora στα 166.5 g/h. Σε αυτό το σημείο περίπου 85% της χλωρίνης απελευθερώνεται σαν αέριο HCl.

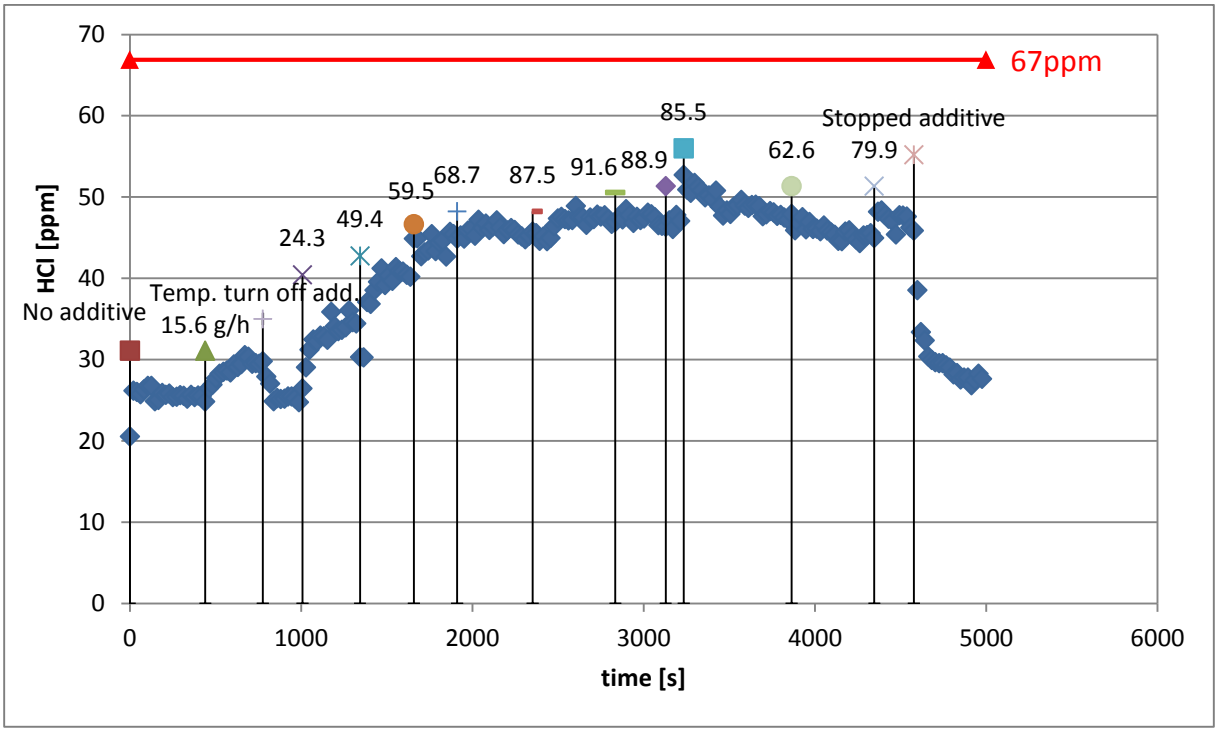

Figure 8.13: Πλήρης συνεδρία Ξηραμένου Άχυρου με Βεντονίτη

Στην εικόνα Figure 8.13 παρουσιάζεται η πλήρης πειραματική συνεδρία του TS με προσθήκη Βεντονίτη (Bentonite). Όμοια με την περίπτωση της Αρόρα, η γενική εντύπωση που δίνει η εικόνα είναι πως για καθαρό καύσιμο, οι εκπομπές HCl είναι χαμηλές και αυξάνονται με την εισαγωγή Βεντονίτη στο σύστημα. Σε αυτή τη συνεδρία τα αρχικά επίπεδα HCl για το καθαρό καύσιμο ήταν περίπου 26 ppm (~38% του Cl ως HCl). Η μεγαλύτερη μετρημένη τιμή HCl ήταν κοντα στα 48 ppm (~71% του Cl ως HCl), όταν επίσης παρατηρήθηκε και ο μεγαλύτερος ρυθμός τροφοδότησης Βεντονίτη, στα 91.6 g/h. Αυτές οι τιμές είανι ερκετά κοντά στη μέγιστη θεωρητική τιμή HCl του TS, αλλά όχι τόσο κοντά όπως όταν χρησιμοποιήθηκε Αρόρα. Αυτή η διαφορά θα συζητηθεί παρακάτω.

Πελλέτες Ξύλου+KCl

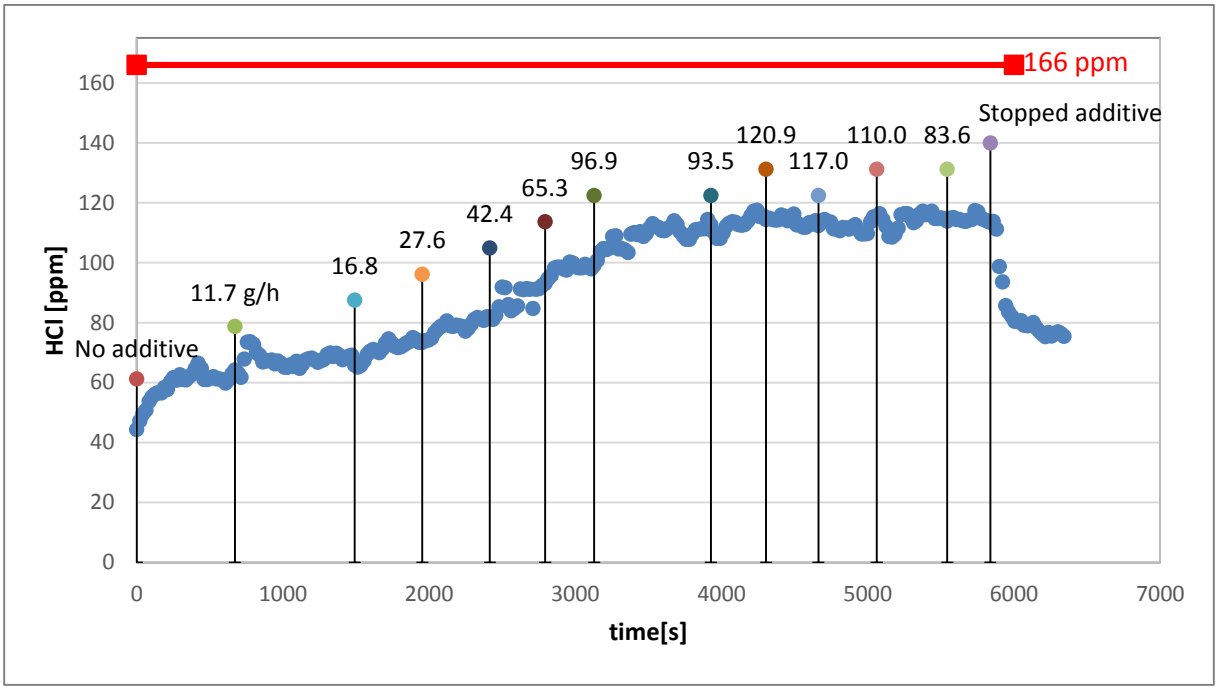

Figure 8.14: Πλήρης συνεδρία Πελλετών Ξύλου+KCl με Αρόρα

Στην εικόνα Figure 8.14, παρουσιάζεται η πλήρης πειραματική συνεδρία καύσης Πελλετών Ξύλου προανεμιγμένων με Χλωριούχο Κάλιο (WP+0.25%KCl) με την προσθήκη Αρόρας (Aurora). Όμοια με τις προηγούμενες περιπτώσεις, είναι φανερό πως καθώς αλλάζει ο ρυθμός τροφοδότησης του πρόσθετου, το ίδιο συμβαίνει και με τις εκπομπές HCl. Για το καθαρό καύσιμο οι συγκεντρώσεις HCl ήταν περίπου 62 ppm (~37% του Cl ως HCl) και οι μεγαλύτρες τιμές HCl περίπου 116 ppm (~70% του Cl ως HCl), για τροφοδότηση 93.5 g/h Αρόρας.

Γενικά η συμπεριφορά του WP+KCl με τη συντροφοδότηση της Aurora φαίνεται όμοια με τη περίπτωση TS-Aurora. Παρόλα αυτά οι μέγιστες τιμές HCl δεν είναι κοντά στη μέγιστη θεωρητικά για το WP+0.25%KCl, που είναι 166 ppm.

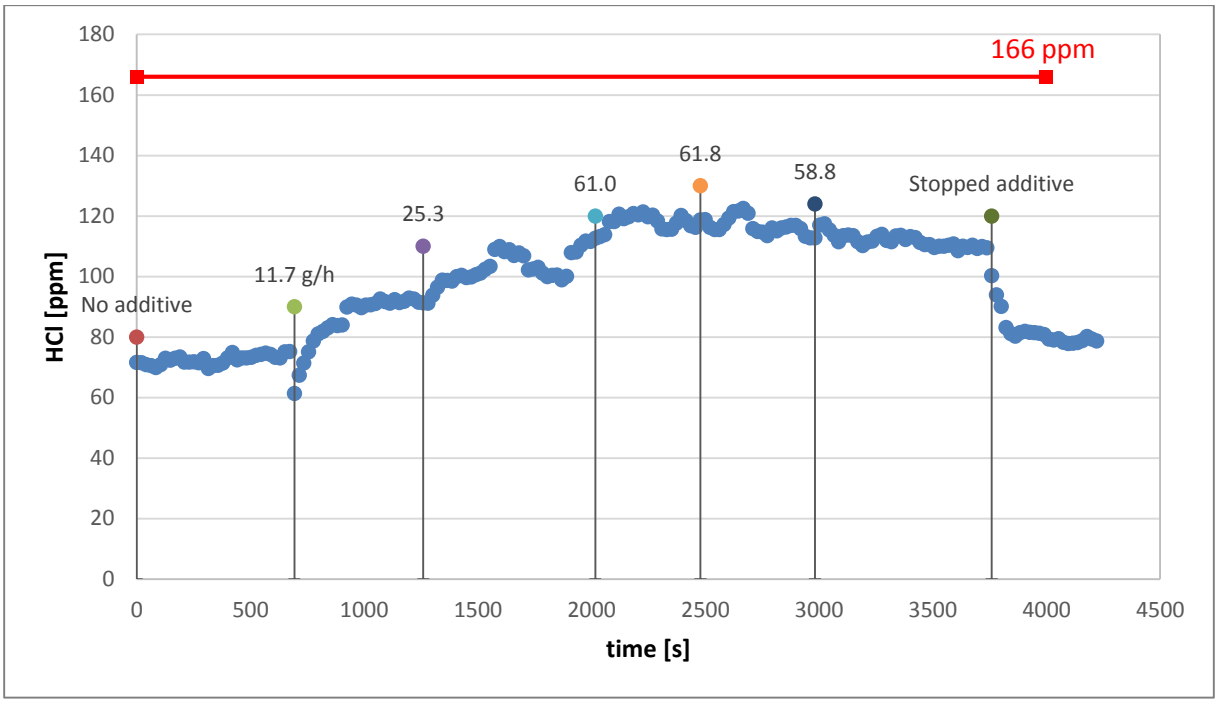

Figure 8.15: Πλήρης συνεδρία Πελλετών Ξύλου+KCl με Βεντονίτη

Στην εικόνα Figure 8.15 φαίνεται η πλήρης συνεδρία του WP+KCl με Βεντονίτη ως πρόσθετο. Μια πρώτη όψη δείχνει πως γενικά το καύσιμο ανταποκρίθηκε στην χρήση πρόσθετου και τα επίπεδα HCl αυξήθηκαν σχετικά. Οι τιμές HCl για καθαρό καύσιμο ήταν γύρω στα 75 ppm (~44% του Cl ως HCl). Οι υψηλότερες τιμές HCl μετρήθηκαν γύρω στα 119 ppm (~71% του Cl ως HCl) για την προσθήκη Βεντονίτη στα 61 g/h. Τα αποτελέσματα δείχνουν πως οι υψηλότερες τιμές HCl που μετρήθηκαν δεν ήταν κοντά στη μέγιστη θεωρητική τιμή HCl, που είναι 166 ppm για το WP+0.25%KCl.

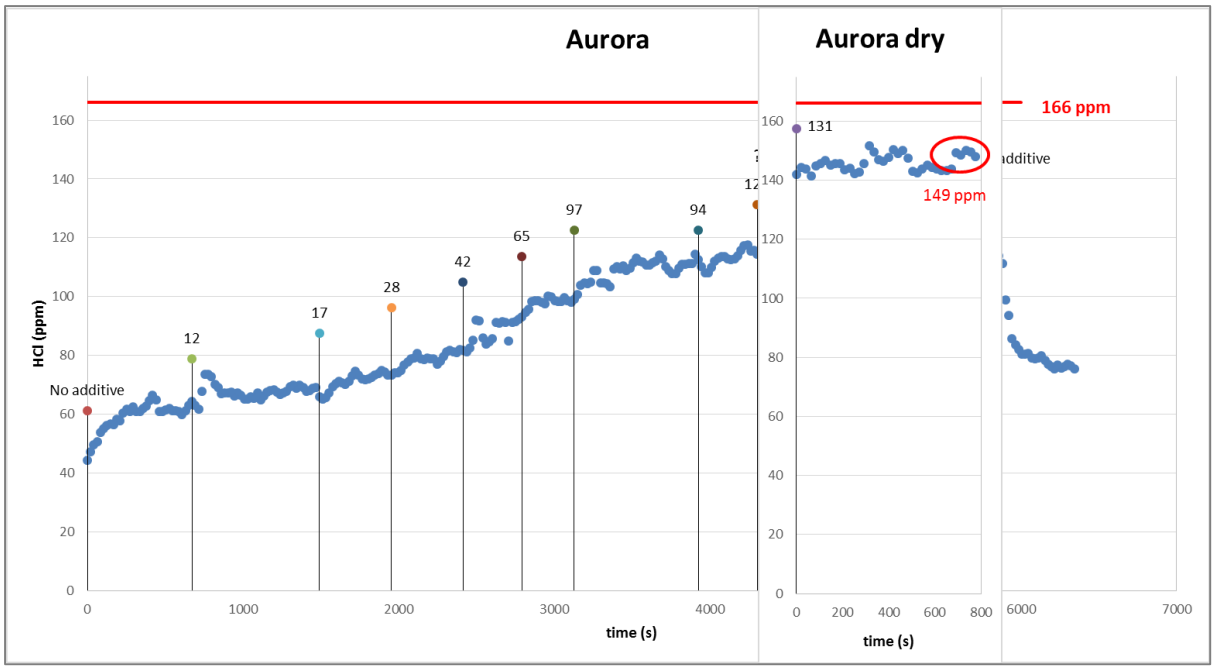

Figure 8.16: Πλήρης συνεδρία Πελλετών Ξύλου με ξηραμένη Αρόρα

Επιπλέον, για να τροφοδοτηθεί περισσότερο πρόσθετο στο σύστημα και να επιτευχθούν μεγαλύτερες συγκεντρώσεις HCl από την καύση WP+KCl, έλαβε χώρα η διαδικασία για την ξήρανση Αρόρας που περιγράφεται στο 8.2.2. Η απόπειρα ήταν επιτυχής. Όπως φαίνεται στην εικόνα Figure 8.16, με το που ξηράνθηκε η Αρόρα είχε μεγάλο αντίκτυπο στο σύστημα. Το νέο πρόσθετο πέτυχε υψηλότεους ρυθμούς τροφοδότησης και είχε ταχύτερη ανταπόκριση, ίσως λόγω της πολύ λεπτής και ξηρής του φύσης, το οποίο οδηγεί σε μεγαλύτερη ειδική επιφάνεια και λιγότερους περιορισμούς στη μεταφορά του. Οι μεγαλύτερες τιμές HCl που παρατηρήθηκαν ήταν γύρω στα 149 ppm (~90% του Cl ως HCl) για την τροφοδότηση πρόσθετου στα 131.4 g/h. Αυτές οι τιμές είναι κοντά στη μέγιστη θεωρητική τιμή HCl για το WP+0.25%KCl (166 ppm) και επίσης είναι η μεγαλύτερες συγκεντρώσεις HCl που παρατηρήθηκαν μεταξύ όλων των συνεδριών.

Επιπλέον, η πειραματική συνεδρία για καύση Πελλέτων Ξύλου (WP χωρίς KCl) με την προσθήκη Βεντονίτη έλαβε χώρα και τα αποτελέσματα φαίνονται στην εικόνα Figure 7.26. Όπως αναμενόταν, τα καυσαέρια των WP φαίνονται να έχουν χαμηλότερες συγκεντρώσεις HCl συγκριτικά με το TS, λόγω της χαμηλότερης περιεκτικότητας τους σε Cl.

Σε ορισμένες από τις παραπάνω περιπτώσεις δεν ήταν δυνατό να αυξηθεί η τροφοδότηση του πρόσθετου μετά από κάποιο σημείο, έτσι δεν αποκλείεται η πιθανότητα να επιτευχθούν μεγαλύτερες τιμές HCl με αυτά τα καύσιμα και πρόσθετα. Σε κάποιες άλλες περιπτώσεις, η μετρηθείσες συγκεντρώσεις HCl δεν αυξήθηκαν, ακόμα και όταν ο ρυθμός τροφοδότησης του

πρόσθετου φαινόταν να αυξάνει. Αυτό μπορεί να σημαίνει ότι η επίδραση του πρόσθετου περιορίζεται μετά από ένα ρυθμό εισαγωγής του στο σύστημα, ή ότι ο χρόνος παραμονής των σωματιδίων μέσα στο θάλαμο (5-6 s) δεν είναι αρκετός για να συμβεί η αντίδραση για όλο το ποσό KCl(g), ή ότι κάποιοι ρυθμοί τροφοδότησης που μετρήθηκαν σε υψηλές ταχύτητες της συσκευής δεν ήταν ακριβής.

Αφού παρουσιάσθηκαν όλες οι περιπτώσεις, μπορεί να ειπωθεί πως η πορεία των συνεδριών πήγε όπως αναμενώταν. Δεν παρατηρήθηκαν σημαντικές διακυμάνεις και οι αποκρίσεις του συστήματος τόσο στην Αρόρα όσο και στον Βεντονίτη ήταν γρήγορες, συλλογιζόμενοι μακράς διάρκειας συνεδρίες καύσης. Επιπλέον, ήταν δυνατό να δειχθεί πως η χρήση των πρόσθετων κατά της καύση βιομάζας έχει αντίκτυπο στις συγκεντρώσεις HCl. Η επίδραση των πρόσθετων ήταν μεγάλη, αφού για το TS και το WP+KCl οι υψηλότερες συγκεντρώσεις HCl μου μετρήθηκαν πλησίασαν τη μέγιστη θεωρητική τιμή για το κάθε καυσιμο. Αυτό συνέβει κατα κανόνα για το μέγιστο ρυθμό τροφοδότησης που επιτεύχθηκε.

Οι υψηλές συγκεντρώσεις HCl μεταφράζονται σε αντιμετώπιση του καλίου στο ρευστό μίγμα και ακόμα αποτροπή της κατάληξης του Cl στην τέφρα. Αυτά τα πειραματικά δεδομένα συμφωνούν με τα αποτελέσματα της προσομοίωσης που παρουσιάσθηκαν πριν, αφού η εισαγωγή του πρόσθετου στο σύστημα αυξάνει τις συγκεντρώσεις HCl. Επίσης, τα ευρήματα αυτά έρχονται να επαληθεύσουν τις υποθέσεις που έγιναν σε προηγούμενες έρευνες, οι οποίες λένε πως το χλώριο πιθανότατα απελευθερώθηκε σαν αέριο υδροχλωρικό οξύ, επειδή μετά της προσθήκη πυριτικών αργιλίων το χλώριο που βρέθηκε στην τέφρα της βιομάζας ήταν πολύ χαμηλότερο από την περίπτωση μη προσθήκης.

Μέσες τιμές HCl για τους αντίστοιχους ρυθμούς τροφοδότησης πρόσθετου

Στην εικόνα Figure 8.17 παρουσιάζονται τα αποτελέσματα από τέσσερεις διαφορετικές συνεδρίες. Χρησιμοποιήθηκαν TS και WP+0.25%KCl ως καύσιμα με την προσθήκη Aurora και Bentonite για το καθένα. Αυτή η εικόνα είναι μια σύνοψη των πλήρων πειραματικών συνεδριών. Οι ξεχωριστές τιμές συγκεντρώσεως HCl (ppm) μαζεύονται εδώ σε μέσες τιμές συγκεντρώσεως HCl (ppm). Οι μέσες τιμές HCl (ppm) είναι ένας μέσος όρος για ένα εύρος δεδομένων. Αυτό το εύρος επιλέχθηκε για τιμές HCl (ppm) που φαίνονταν να έχουν σταθεροποιηθεί μετά από τον ορισμό ενό ρυθμού τροφοδότησης πρόσθετου (g/h) και πριν αλλαχθεί σε νεό ρυθμό τροφοδότησης. Κάθε μέση τιμή συγκεντρώσεων HCl (ppm) αντιστοιχεί στο προηγούμενο ρυθμό τροφοδότησης (g/h) που εικονίζεται. Οι τιμές ρυθμού τροφοδότησης παρουσιάζονγται εδώ αφού υπολογίστηκαν σαν ξηρές. Έτσι η σύγκριση μεταξύ των πρόσθετων γίνεται χωρίς υγρασία και λαμβάνεται υπόψην μόνο το πραγματικά

δραστικό τους μέρος. Οι μέσες τιμές HCl παρουσιάζονται μόνο εως τη μεγαλύτερη τιμή που υπολογίστηκε. Ακόμα, η μέγιστη θεωρητική τιμή HCl εικονίζεται ως το ανώτατο όριο για κάθε καύσιμο.

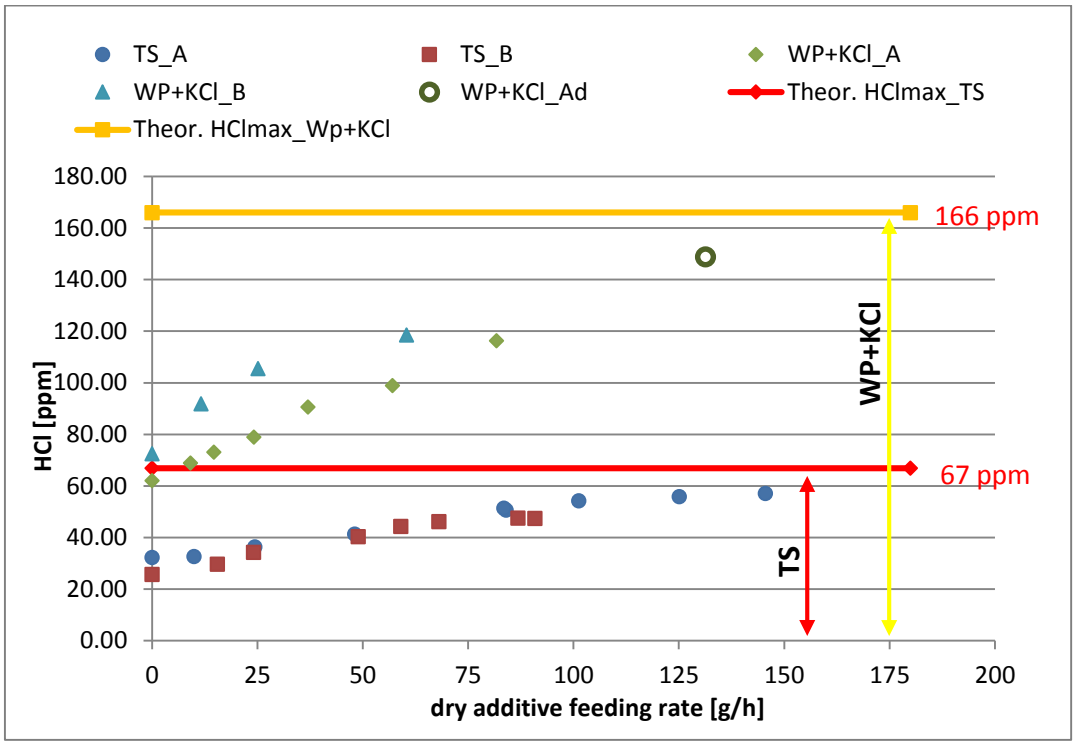

Figure 8.17: Μέσες τιμές HCl για τους αντίστοιχους ρυθμούς τροφοδότησης πρόσθετου – Περιπτώσεις TS και WP+KCl

Αυτή η εικόνα κάνει πιο εμφανές πως η διακύμανση πρόσθετων επηρεάζει τις συγκεντρώσεις HCl. Καθώς οι ρυθμοί τροφοδότησεις αυξάνουν διαδοχικά, το ίδιο συμβαίνει με τις συγκεντρώσεις HCl σε όλες τις περιπτώσεις. Έτσι μπορούν να επιτευχθούν διαφορετικά αποτελέσματα με διαφορετική εισαγωγή πρόσθετου στο σύστημα.

Επίσης είναι φανερό, πως οι περιοχές με τιμές HCl για κάθε καύσιμο (και τις περιπτώσεις τους A και B) δεν συναντιούνται. Οι αρχικές τιμές HCl για καθαρό καύσιμο (πρόσθετο 0 g/h) και οι υψηλότερες τιμές HCl, μεταξύ των δύο καυσίμων έχουν μεγάλες διαφορές. Αυτό συμβαίνει φυσικά λόγω του διαφορετικού περιεχόμενου χλωρίου των δύο καυσίμων (το χλώριο στο WP+0.25%KCl είναι υπερδιπλάσιο από του TS).

Η επίδραση και των δύο πρόσθετων φαίνεται να είναι όμοια για τα δύο καύσιμα όσων αφορά το HCl. Παρόλα αυτά υπάρχουν μερικές μικρές διαφορές. Αρχικά δείχνεται πως η Aurora μπόρεσε να τροφοδοτηθεί μέχρι μεγαλύτερους ρυθμούς από το Bentonite (το Ad σημαίνει dried Aurora – ξηραμένη Αρόρα και είναι η επέκταση της περίπτωσης WP+KCl_A). Η τροφοδότηση υψηλότερων ποσοτήτων προσθέτου έδωσε πλεονέκτημα και οδήγησε σε μεγαλύτερη επίδραση και υψηλότερες τιμές HCl. Στην περίπτωση του TS, οι δύο σειρές από

τιμές HCl φαλινονται να ακολουθούν την ίδια γραμμή. Όμως στην περίπτωση WP+KCl, για τους ίδιους ρυθμούς τροφοδότησης, η αύξηση HCl φαίνεται να συμβαίνει πιο απότομα με το Bentonite παρά με την Aurora. Αυτές οι διαφορές μεταξύ της επίδρασης των πρόσθετων μπορεί να συνδέεται με τα φυσικά τους χαρακτηριστικά και την κινητική των επιφανειακών αντιδράσεων.

Παρόλα αυτά, φαίνεται πως υπάρχει διακύμαση στις μετρήσεις του FTIR. Οι μετρήσεις για τα καθαρά καύσιμα, μεταξύ των συνεδριων για τα δύο πρόσθετα, δε δίνουν τις ίδιες μέσες τιμές HCl. Από την μια πλευρά, στην περίπτωση του TS, οι τιμές HCl για το καθαρό καύσιμο είναι μεγαλύτερες στην συνεδρία για την Aurora. Από την άλλη πλευρά, στις περιπτώσεις WP+KCl, οι πρώτες μετρήσεις για καθαρό καύσιμο δίνουν επίσης διαφορετικές μέσες τιμές HCl, αλλά αυτή τη φορά, είναι υψηλότερες για την περίπτωση της ξηραμένης Αρόρας (που δεν παρουσιάζεται παραπάνω αλλά στο Annex). Αυτό το εύρος διακυμάνσεων των μετρήσεων που παρατηρείται για το FTIR παρουσιάζται στην εικόνα Figure 8.18. Η προανάμιξη WP με KCl μπορεί να είναι υπεύθυνη για τις μεγαλύτερες διαφορές στην περίπτωση του WP+KCl, αφού η ομοιογένοια του δεν είναι γνωστή. Θεωρείται πιθανό πως αυτό το εύρος διαφοράς σε τιμές HCl για το καθαρό καύσιμο να είναι το ίδιο για τις επόμενες τιμές HCl, μεταξύ των περιπτώσεων των δύο πρόσθετων, για τους ίδιους ρυθμούς τροφοδότησης πρόσθετου. Το γεγονός ότι αυτά τα εύρη μετρήσεων υπάρχουν είναι σημαντικό και θα χρησιμοποιηθούν στη συνέχεια.

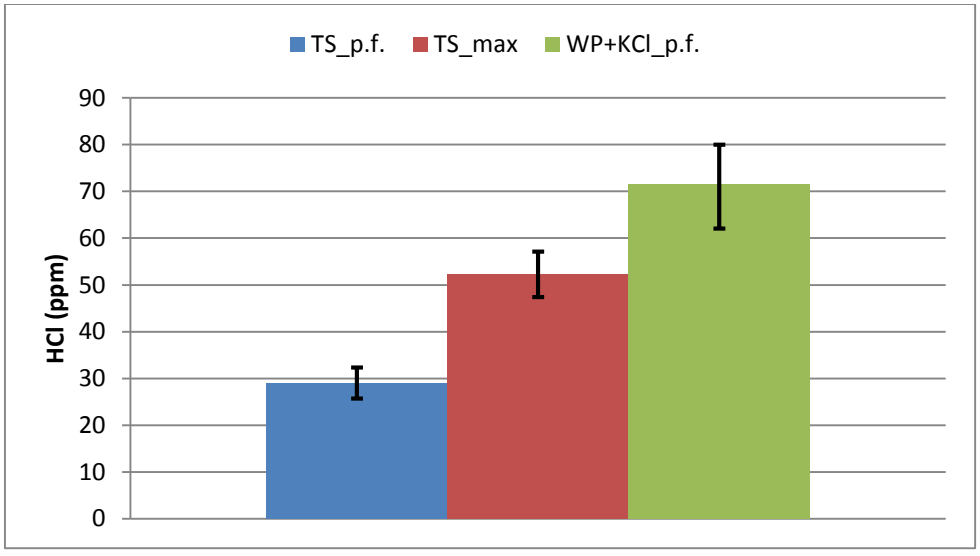

Figure 8.18: Εύρος διακυμάνσεων για τις μετρήσεις FTIR.

Χλώριο ως HCl σε σχέση με το K/(Si+Al)

Τα συστατικά που αντιδρουν με το κάλιο του καυσίμου και οδηγούν στην απελευθέρωση του HCl είναι το πυρίτιο και το αργίλιο, τα οποία υπάρχουν στο εισερχόμενο πρόσθετο, αλλά και ως ένα ορισμένο σημείο μέσα στο καύσιμο. Γι'αυτό το λόγο, ο μοριακός λόγος του καλίου μέσα στο καύσιμο προς το αργίλο και το πυρίτιο μέσα στο καύσιμο και το πρόσθετο είναι μεγάλης σημασίας. Ο μοριακοί λόγοι K/(Si+Al) για τα ξηρά συστατικά που αναφέρθηκαν παραπάνω, υπολογίστηκαν για ρυθμούς τροφοδότησης ξηραμένου πρόσθετου (ξηραμένου στους 105°C) και παρουσιάζονται στην εικόνα Figure 8.19 (το σύμβολο * στο WP+KCl_A* σημαίνει πως τα δεδομένα για την Aurora και την dried Aurora συγχωνεύτηκαν για τα αποτελέσματα που παρουσιάζονται). Αυτή η εικόνα δείχνει πως ο λόγος συμπεριφέρεται για διαφορετικά ποσά πρόσθετων, όμως επίσης δείχνει και τη σύγκριση μεταξύ των δύο πρόσθετων.

Φαίνεται πως καθώς αυξάνεται ο ρυθμός τροφοδότησης του πρόσθετου, ο μοριακός λόγος K/(Si+Al) μειώνεται. Επιπρόσθετα, είναι φανερό πως για κάθε καύσιμο, οι περιπτώσεις για Aurora και Bentonite έχουν τους ίδιους μοριακούς λόγους K/(Si+Al) για τους ίδιους ρυθμούς τροφοδότησης πρόσθετου, το οποίο οφείλεται στην παρόμοια ξηρή τους σύσταση.

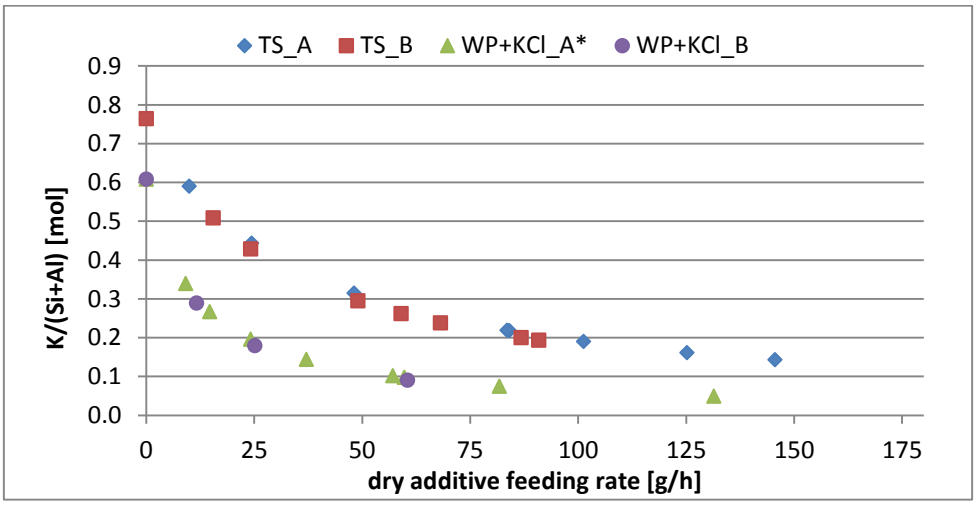

Figure 8.19: Λόγοι K/(Si+Al) για διφορετικούς ρυθμούς τροφοδότησης. Περιπτώσεις TS και WP+KCl

Είναι ενδιαφέρον να εξετασθεί τι μέρος του συνολικού περιεχόμενου στο καύσιμο χλωρίου πηγαίνει προς το σχηματισμό HCl όταν εισάγωνται πρόσθετα. Αυτό μπορεί να μεταφραστεί σε, λόγο του πραγματικού HCl που σχηματίστηκε, προς τη μέγιστη θεωρητική τιμή HCl που μπορεί να επιτευχθεί.

Ξηραμένο Άχυρο

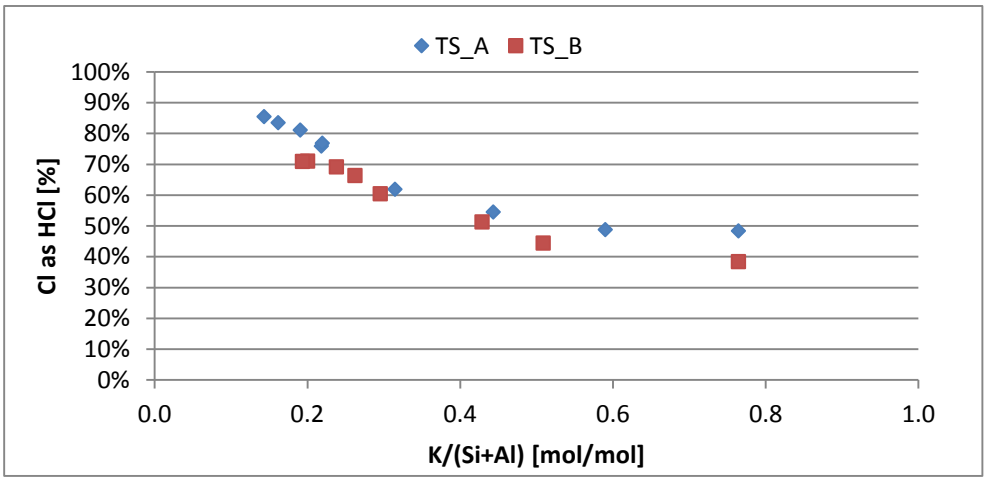

Figure 8.20: Ποσοστό χλωρίου του καυσίμου που μετατρέπεται σε HCl σε σχέση με το λόγο K/(Si+Al), για το TS.

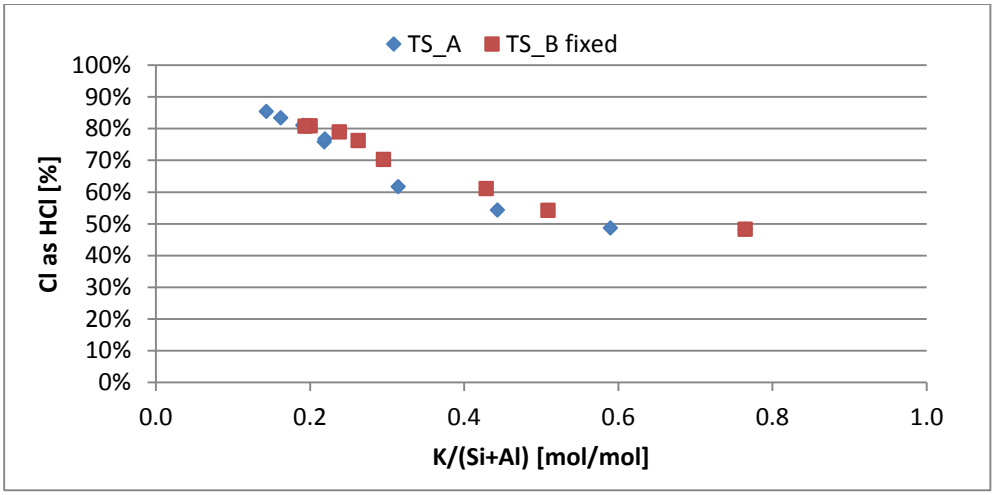

Figure 8.21: Προσαρμοσμένο ποσοστό χλωρίου του καυσίμου που μετατρέπεται σε HCl σε σχέση με το λόγο K/(Si+Al), για το TS.

Για τις περιπτώσεις TS οι λόγοι HCl/HClmax (Cl ως HCl) υπολογίστηκα για τους αντίστοιχους μοριακούς λόγους K/(Si+Al) που παρουσιάζονται στην εικόνα Figure 8.19 και τα αποτελέσματα εικονίζονται στην εικόνα Figure 8.20. Φαίνεται πως για τους ίδιους λόγους K/(Si+Al) η ύπαρξη του Cl στο HCl είναι όμοιο και για τα δύο πρόσθετα. Όμως αυτή η

σύγκριση δε μπορεί να είναι τελείως ακριβής αφού τα αρχικά επίπεδα HCl για καθαρό καύσιμο, όπως φαίνονται στην εικόνα Figure 8.18, είναι διαφορετικά.

Γι' αυτό το λόγο δημιουργήθηκε επίσης η εικόνα Figure 8.21, που απεικονιζει τα ίδια διαγράμματα όπως η προηγούμενη, αλλά αυτή τη φορά στην περίπτωση του Bentonite (αναφέρεται ως fixed) όλες οι υπολογισμένες τιμές HCl έχουν αυξηθεί ίσα με το εύρος διαφοράς για καθαρό καύσιμο όπως φαίνεται στην εικόνα Figure 8.18. Με αυτό τον τρόπο, η σύγκριση μεταξύ των δύο πρόσθετων ξεκινά από την ίδια βάση.

Πελλέτες Ξύλου + KCl

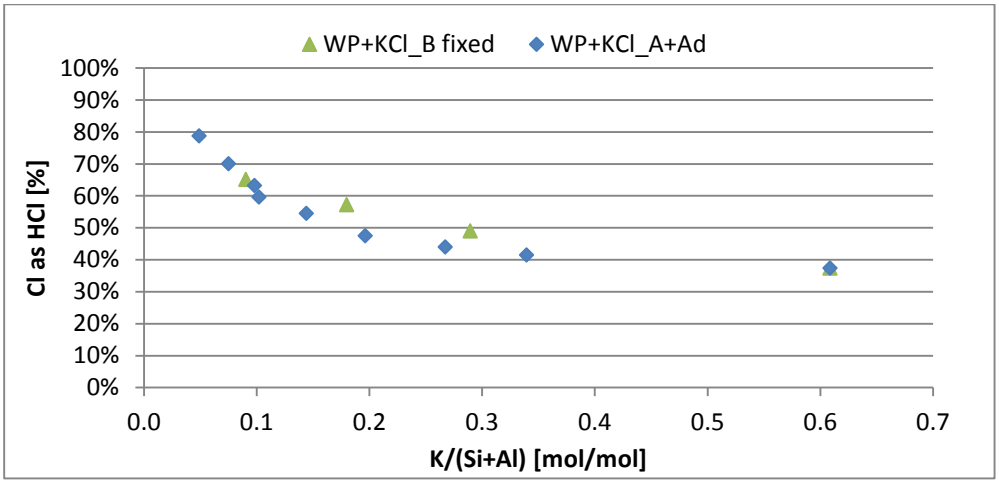

Figure 8.22: Προσαρμοσμένο ποσοστό χλωρίου του καυσίμου που μετατρέπεται σε HCl σε σχέση με το λόγο K/(Si+Al), για το WP+KCl.

Για τις περιπτώσεις WP+KCl οι λόγοι HCl/HClmax υπολογίστηκαν για τους αντλιστοιχους λόγους K/(Si+Al) που παρουσιάζονται Figure 8.19 και τα αποτελέσματα παρουσιάζονται στην εικόνα Figure 7.29. Η σύγκριση από αυτή την εικόνα δεν μπορεί να είναι απολύτως ακριβής αφού τα αρχικά επίπεδα HCl καθαρού καυσίμου για τις δύο περιπτώσεις είναι διαφορετικά, όπως φαίνεται στην εικονα Figure 8.18.

Έτσι, δημιουργήθηκαν επίσης τροποποιημένα διαγράμματα (fixed) για τις περιπτώσεις WP+KCl και παρουσιάζονται στην εικόνα Figure 8.22. Αυτή τη φορά αλλάχθηκαν τα δεδομένα των συνεδριών Bentonite και dried Aurora (αναφέρεται ως fixed). Όλες υπολογισμένες τιμές HCl μειώθηκαν σύμφωνα με το εύρος διαφοράς καθαρού καυσίμου που εικονίζεται στην εικόνα Figure 8.18. Ακόμα τα δεδομένα και των δύο περιπτώσεων Αρόρας συγχωνεύτηκαν μαζί, αφού η παρουσίαση αποτελεσμάτων εδώ είναι για ξηρά καύσιμα.

Αφού λήφθηκαν υπόψιν οι διακυμάνσης μετρήσεων του FTIR και παρατηρήθηκαν οι εικόνες Figure 8.21 και Figure 8.22, η σύγκριση μεταξύ της Αρόρας και του Βεντονίτη γίνεται ευκολότερη. Από αυτές τις εικόνες παρατηρείται ότι και για τα δύο καύσιμα, η επίδραση των

δύο πρόσθετων και οι διαφορές τους είναι παρόμοιες. Η χρήση του Βεντονίτη, οδηγεί περισσότερο περιεχόμενο χλώριο προς τη δημιουργία HCl παρά με την Αρόρα, για το μεγαλυτερο μέρος του εύρους K/(Si+Al) που τα δύο πρόσθετα έχουν κοινό. Παρόλα αυτά, επειδή η Αρόρα τελικά τροφοδοτήθηκε σε μεγαλύτερους ρυθμούς, για τους μικρότερους λόγους καλίου προς πυριτικού αργιλίου κατάφερε να οδηγήσει περισσότερο χλώριο προς τη δημιουργία HCl. Αυτό είναι επειδή τα σημεία των περιπτώσεων Βεντονίτη μοιάζουν να ακολουθούν μια πιο ευθεία γραμμή, όταν οι περιπτώσεις Αρόρας ακολουθούν μια καμπύλη γραμμή (φαίνονται καλυτερα στις εικόνες Figure 7.30, Figure 7.31).

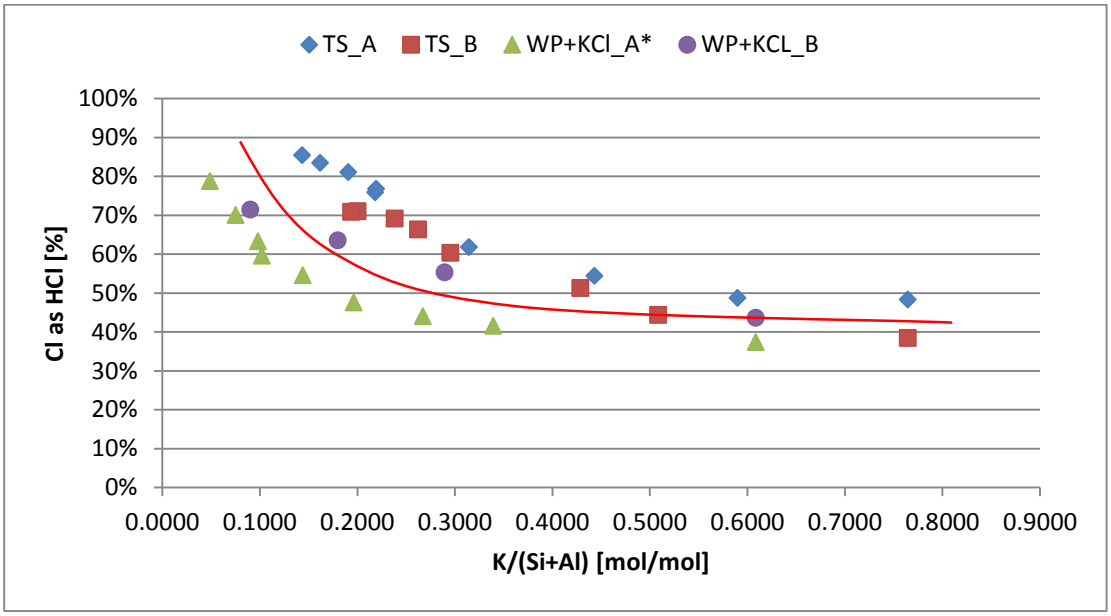

Figure 8.23: Ποσοστό χλωρίου του καυσίμου που μετατρέπεται σε HCl σε σχέση με το λόγο K/(Si+Al), για τα TS και WP+KCl.

Στην εικόνα Figure 8.23 παρουσιάζονται τα αποτελέσματα του Cl ως HCl σε σχέση με τους μοριακούς λόγους K/(Si+Al), για τις περιπτώσεις TS και WP+KCl. Είναι ξεκάθαρο πως καθώς ο λόγος K/(Si+Al) μειώνεται, το Cl ως HCl αυξάνεται. Αυτό σημαίνει ότι όσο περισσότερο πρόσθετο εισέρχεται στο σύστημα, τόσο περισσότερο Cl απελευθερώνεται ως αέριο HCl.
Επιπλέον, αν παραβλευθούν οι μικρές διαφορές, τα πρόσθετα φαίνονται να έχουν μια παρόμοια δράση η οποία ακολουθεί μια γενική τάση. Αυτή η τάση εικονίζεται εδώ με μία γραμμή που περνάει ανάμεσα από τα σημεία. Από τη βιβλιογραφεία, η αντίδραση που λαμβάνει χώρα μεταξύ των πυριτικών αργιλίων και του KCl ώστε να απελευθερωθεί HCl είναι: $2\mathrm{KCl(g)} + \mathrm{Al_2Si_2O_7} + \mathrm{H_2O} = 2\mathrm{KAlSiO_4(s)} + 2\mathrm{HCl}$. Αυτό σημαίνει πως για αν συμβεί η αντίδραση πρέπει ο μοριακός λόγος K/(Si+Al) να είναι μικρότερος του 0.5. Βλέποντας την εικόνα Figure 8.23, για το K/(Si+Al) ακριβώς μικρότερο του 0.5, η αύξηση σε HCl/HClmax (Cl ως HCl) είναι πολύ μικρή. Αυτό συμβαίνει πιθανώς επειδή, όπως φάνηκε στους

υπολογισμούς των προσομοιώσεων ισορροπίας στην 8.3.1 (διακύμανση Καολινίτη), το πρόσθετο δεν είναι διαθέσιμο για αν αντιδράσει με το KCl, αλλά αρχικά φαίνεται να αντιδρά με το λοιπό κάλιο στο αέριο και το κάλιο στο ρευστό μίγμα. Η αντίδραση με το KCl χαμηλότερα από το λόγο 0.5 είναι πολύ μικρή και αφού αντιμετωπισθεί όλο το κάλιο στορευστό μίγμα, τότε η αντίδραση με το KCl γίνεται κυρίαρχη. Η αύξηση του Cl ως HCl γίνεται πιο ραγδαία όταν ο λόγος K/(Si+Al) είναι περί το 0.3 και γίνεται κυρίαρχη περί το 0.2. Έτσι, μπορεί να ειπωθεί πως για μοριακούς λόγους K/(Si+Al) μεγαλύτερους του 0.5, το πρόσθετο αντιδρά περισσότερο με το λοιπό κάλιο στο αέριο (KOH, K_2SO_4), για λόγους μεταξύ του 0.5 και 0.3 αντιδρά κυρίως με το κάλιο στο ρευστό μίγμα και για λόγους χαμηλότερους του 0.3 αντιδρά περισσότερο με το KCl(g).

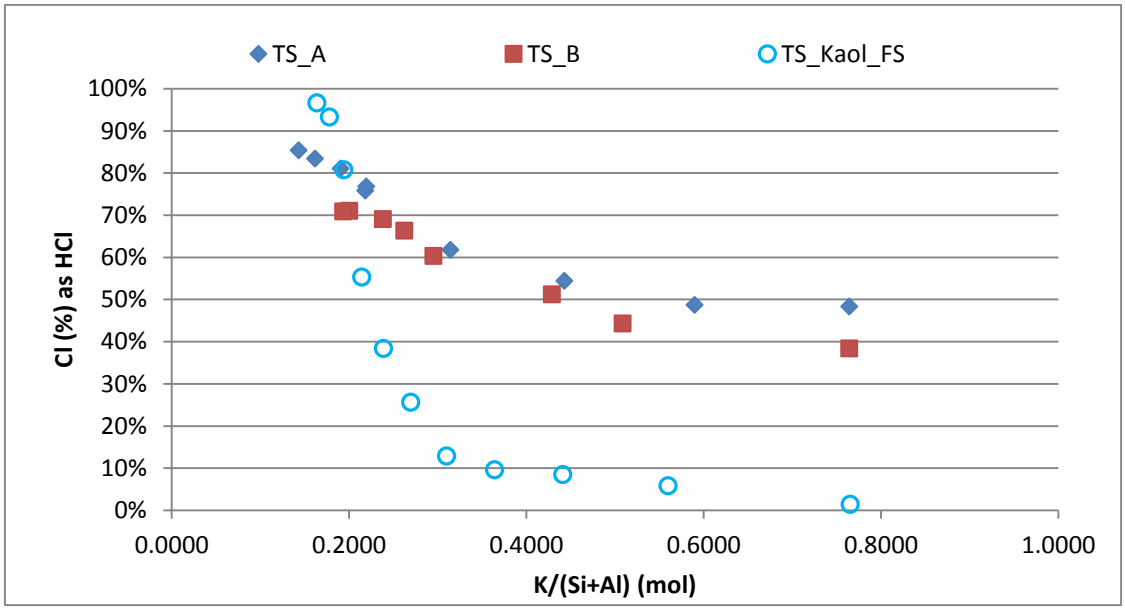

Figure 8.24: Ποσοστό χλωρίου του καυσίμου που μετατρέπεται σε HCl σε σχέση με το λόγο K/(Si+Al), σύγκριση πειραματικών αποτελεσμάτων και αποτελεσμάτων FactSage για το TS.

Η εικόνα Figure 8.24 παρουσιάζει τη σύγκριση του Cl ως HCl [%] για τα πειραματικά αποτελέσματα του TS και τα αποτελέσματα της προσομοίωσης σε συνθήκες ισορροπίας του TS. Πρέπει να σημειωθεί ότι οι μετρήσεις έλαβαν χώρα στους 200 °C, όταν τα αποτελέσματα του FactSage είναι προϊόντα καύσης σε συνθήκες ισορροπίας στους 1200 °C. Για υψηλούς μοριακούς λόγους K/(Si+Al) τα γραφήματα είναι συγκρίσιμα, αλλά οι διαφορές εξακολουθούν να είναι μεγάλες μεταξύ των πειραματικών και της προσομοίωσης αποτελεσμάτων. Αυτό συμβαίνει πιθανώς επειδή η θερμοκρασία στην τοποθεσία των μετρήσεων είναι στους 200°C και έτσι συνυπολογίζεται ο μηχανισμός θειοποίησης για τη δημιουργία HCl (2-12). Από την άλλη μεριά, οι υπολογισμοί της προσομοίωσης στους 1200 °C δεν λαμβάνουν υπόψιν αυτό το μηχανισμό, αφού συμβαίνει σε χαμηλότερες θερμοκρασίες (2.6). Παρόλα αυτά, η

αλληλεπίδραση μεταξύ των αλκαλικών ειδών και των πυριτικών αργιλίων αναμένεται να λάβει χώρα σε θερμοκρασίες οπως μέσα στο θάλαμο καύσης. Έτσι χρησιμοποιούνται οι 1200 °C στους υπολογισμούς σε συνθήκες ισορροπίας. Σε μοριακούς λόγους K/(Si+Al) μικρότερους του 0.3, εισέρχεται στο σύστημα πολύ περισσότερο πρόσθετο και ξεκινά να αντιδρά επίσης περισσότερο με το KCl. Έτσι το Cl ως HCl [%] αυξάνεται. Σε αυτή την περιοχή, τα αποτελέσματα των πειραμάτων και της προσομοίωσης έρχονται πιο κοντά, πιθανώς επειδή η αύξηση σε HCl επηρεάζεται κυρίως απο την αύξηση του πρόσθετου.

8.4 Συμπεράσματα

Ο στόχος αυτής της έρευνας ήταν να αξιολογήσει την επίδραση των πρόσθετων με βάση το πυριτικό αργίλιο στο σχηματισμό τηγμένων αποθέσεων και συμπυκνώσεων αλκαλικών αλάτων σε ψυχρές επιφάνειες του λέβητα. Η συμπεριφορά της τέφρας δύο καυσίμων βιομάζας (Ξηραμένο Άχυρο και Πελλέτες Ξύλου) προσομοιόθηκε με τη βοήθεια του θερμοχημικού λογισμικού και βάσης δεδομένων ‘FactSage 6.3’, με και χωρίς τη διακύμανση πρόσθετου. Πειράματα καύσης διεξήχθησαν στον ατμοσφαιρικό κλίβανο κάθετης φλόγας (BTS), θερμικής ισχύος 20kW, των εγκαταστάσεων του IFK, με την καύση Ξηραμένου Άχυρου, Πελλετών Ξύλου και Ενισχυμένων Πελλετών Ξύλου με χλώριο (με προανάμειξη KCl) και τη διακύμανση Αρόρας και Βεντονίτη ως πρόσθετα. Τα πειράματα εστιάζονταν στην αξιολόγηση της συμπεριφοράς του χλωρίου.

Τα αποτελέσματα από τους υπολόγισμούς σε προσομοίωση συνθηκών ισορροπίας δείχνουν ότι και για τα δύο καύσιμα ο λόγος ρευστού μίγματος αυξάνει με την αύξηση της θερμοκρασίας. Η αύξηση είναι πολύ ραγδαία για θερμοκρασίες μεγαλύτερες της θερμοκρασίας υγροποίησης της τέφρας, θερμοκρασίες που πάρθηκαν από δοκιμές τήξης της τέφρας. Επιπρόσθετα, ο ρυθμός επικάθισης επηρεάζεται από το λόγο αέρα καυσίμου. Γενικά καθώς το λ αυξάνει οι λόγοι επικάθισης μειώνονται. Επιπλέον, τα αποτελέσματα έδειξαν ότι η δημιουργία επικαθίσεων της βιομάζας οδηγείται πρωτίστως από το υψηλό της περιεχόμενο σε κάλιο. Το κάλιο υπάρχει σε αέρια είδη σε πολύ υψηλές θερμοκρασίες και κινείται προς στερεά είδη σε χαμηλές θερμοκρασίες, αλλά το μεγαλύτερο του μέρος υπάρχει πάντα στο ρευστό μίγμα. Ακόμη, παρατηρήθηκε ότι τα ποσά του KCl που σχηματίστηκαν εξαρτούνται αποκλειστικά από το περιεχόμενο Cl του καυσίμου. Όσο μεγαλύτερη είναι η περιεκτικότητα του καυσίμου σε K πρωτίστως, και επίσης σε Si, τόσο μεγαλύτερες ποσότητες επικαθίσεων δηιουργούνται. Γιαυτό το λόγο οι ποσότητες επικαθίσεων για το TS ήταν υψηλότερες από ότι για το WP και επίσης γι’αυτό το TS έχει μεγαλύτερο δυναμικό δημιουργίας επικαθίσεων από ότι το WP. Τελικά ο Καολινλιτης βρέθηκε να μειώνει τις επικαθίσεις και επίσης να οδηγεί το Cl έξω από το KCl.

Τα πειραματικά αποτελέσματα έδειξαν ότι η εισαγωγή των πρόσθετων δεν διαταράσει τις σταθερές συνθήκες της καύσης. Ήταν ξεκάθαρο ότι το πρόσθετο ασκεί επιρροή στη συμπεριφορά του Cl, κάτι που μπορεί να φανεί στις αλλαγές των συγκεντρώσεων HCl. Η απόκριση των συγκεντρώσεων HCl ήταν γρήγορη όταν κυμαινόταν το πρόσθετο ή όταν διακοβόταν η παροχή του. Καθώς αύξανε η εισαγωγή του πρόσθετου στο σύστημα, το ίδιο συνέβαινε και με το HCl, όσπου έφτανε ένα ορισμένο επίπεδο κοντα στη μέγιστη θεωρητική τιμή. Συμπερασματικά αυτό σήμαινε ότι το αντίστοιχο ποσό Cl έφυγε από το KCl. Επιπρόσθετα, δείχθηκε ότι ο μοριακός λόγος K/(Al+Si) επηρεάζει το ποσοστό του συνολικού περιεχόμενου Cl που σχηματιζόταν ως HCl. Αυτός ο μοριακός λόγος πρέπει να είναι μικρότερος του 0.5 ώστε να υπάρξουν θετικά αποτελέσματα. Ακόμα, η επίδραση των δύο πρόσθετων φαίνεται πως τείνει να ακολουθεί μια παρόμοια τάση. Παρόλα αυτά, ο Βεντονίτης φάνηκε να έχει ελαφρώς υψηλότερη επίδραση για χαμηλότερους ρυθμούς τροφοδότησης. Τελικά, τα τέστ δειγματοληψίας τέφρας επιβεβαίωσαν ότι με την παρουσία πρόσθετου το χλώριο συγκρατείται από το KCl και επομένως περιορίζεται η κατάληξη του στην τέφρα.

Τα αποτελέσματα από την προσομοίωση σε συνθήκες ισορροπίας και τα πειράματα ειναι συγκρίσιμα σε όλο το εύρος της διακύμανσης των πρόσθετων, αλλά συγκλίνουν περισσότερο για αυξημένη εισαγωγή πρόσθετου, όπου ο μηχανισμός αντίδρασης μεταξύ των πυριτικών αργιλίων και του KCl είναι κυρίαρχος. Και οι δύο πλευρές καταλήγουν, πως η χρηση πρόσθετου δεσμέυει το Cl από το KCl και το οδηγελι προς αέριο HCl.